



**The Abdus Salam
International Centre for Theoretical Physics**



2141-28

**Joint ICTP-IAEA Workshop on Nuclear Reaction Data for Advanced
Reactor Technologies**

3 - 14 May 2010

**Generalized Least-Squares Evaluation of Nuclear Data
Non-model evaluation of experimental data: system of codes GLUCS and GMA**

PROYAEV V.G.

*PPE
Obninsk
Russia*

Generalized Least-Squares Evaluation of Nuclear Data
 Lecture notes at the IAEA/ICTP Workshop on Nuclear Reaction Data
 for Advanced Reactor Technology
 ICTP, Trieste, 3 – 14 May 2010
 V.G. Pronyaev
 Institute of Physics and Power Engineering
 Obninsk, Russia

Lecture 1. Non-model evaluation of experimental data: system of codes GLUCS and GMA

Error Propagation Law

Error (uncertainty) propagation law follows from the definition of the average variance-covariance. Namely, if we have functional dependence (D , reduction function), which connect the primarily-measured quantities r_i with data obtained as the result of reduction $d_i=D(r_i)$, then in linear approximation, variation of data in the most general form is related with the variation of primary values as $\delta d_i=(\partial D_i/\partial r_k)\delta r_k$, where $\partial D_i/\partial r_k$ is a partial derivative and there is summation on k -index. Then the averaged value of the square of the variance-covariance of the reduced quantity, which presents the element of the covariance matrix can be written as:

$$\langle \delta d_i \delta d_j \rangle = \langle (\partial D_i / \partial r_k) \delta r_k \delta r_l (\partial D_j / \partial r_l) \rangle$$

where summation runs on the k and l indexes. Because the partial derivatives in this case are just numbers (usually called as sensitivity coefficients), they can be taken away of the averaging and averaged square of the variance-covariance can be written as:

$$\langle \delta d_i \delta d_j \rangle = (\partial D_i / \partial r_k) \langle \delta r_k \delta r_l \rangle (\partial D_j / \partial r_l)$$

Because $\langle \delta d_i \delta d_j \rangle$ and $\langle \delta r_k \delta r_l \rangle$ are the elements of variances-covariances, then if designate through d_{ij} and r_{ij} the elements of the covariance matrices of the uncertainties for derived and primarily-measured quantities, the error propagation law can be written for the elements of the matrix as:

$$d_{ij} = \sum_k \sum_l \frac{\partial D_i}{\partial r_k} r_{kl} \frac{\partial D_j}{\partial r_l} = D_{ik} r_{kl} D_{lj}$$

or in the matrix form with \mathbf{D}^T designating the matrix transposed to \mathbf{D} :

$$\mathbf{d} = \mathbf{D}^T \mathbf{r} \mathbf{D}$$

This relation is widely used in the practice of the data evaluation, as in case of data reduction, as well as at their model fit if we understand under D the model function and under r_i the model parameters ($i=1, \dots, n$).

Generalized and Bayesian approaches to the least-squares fit of the nuclear data

The generalized and Bayesian approaches are widely used in the model and non-model least-squares fits of the nuclear data. Under the models we understand here mathematical or physical models, providing good fit of the data through the adjustment of their parameters. Non-model approach can be called rather conditionally, because the model of reduction of the different experimental data (e.g. measured at different energies) to the same energy nodes or the energy groups used in the evaluation is based in any case on (probably rather simple) model. In non-

model approaches (if any data reduction is absent), the evaluated parameters are just evaluated values in the nodes or the groups, so that the square matrix of the sensitivity coefficients of the evaluated values to the parameters is a unit matrix.

Examples of the implementation of these approaches at the level of the programming can be the following computer codes and program complexes:

- R- matrix model codes using generalized least-squares method: EDA, RAC;
- R- matrix model codes generally using Bayesian least-squares method: SAMMY;
- Non-model codes using generalized least-square method: GMA, SOK;
- Non-model code using Bayesian least-squares method : GLUCS.

As it is known, the Bayesian approach differs from the generalized one; in this approach «a priori» evaluation is used as a starting point and experimental data sets are introduced in the evaluation sequentially, a «posteriori» evaluation at each stage is obtained from a prior evaluation and addition of the adjustment vector (matrix) to the evaluated central values (covariance matrix of uncertainties). Generalized least-squares method does not use a prior evaluation.

General relations of the least-squares method:

Generalized approach [1]

Bayesian approach [2]

$$T' = (G^+ V^{-1} G)^{-1} G^+ V^{-1} R$$

$$M' = (G^+ V^{-1} G)^{-1}$$

$$T' = T + \delta T = T + M G^+ (G M G^+ + V)^{-1} (R - T)$$

$$M' = M + \delta M = M - M G^+ (G M G^+ + V)^{-1} G M$$

where T' is a vector of (a posteriori) evaluated data,
 T is a vector of a priori evaluated data,
 M' is a covariance matrix of uncertainties of (a posteriori) evaluated data,
 M is a covariance matrix of uncertainties of (a priori) evaluated data,
 R is a vector of experimental data,
 V is a covariance matrix of uncertainty of the experimental data,
 G is a matrix of the coefficients of the data reduction or the model, upper indexes (+) and (-1) means the operators of the matrix transposing or the matrix inversion.

Results of the evaluation in the Bayesian approach does not depend from the order of the experimental data sets in their sequential input. One of the conditions of the use of this approach is the absence of the correlations between sequentially introduced experimental data sets. The scheme of the work with the data in the Bayesian approach is the following:

«a priori» evaluation (1) → experimental data (1) → «a posteriori» evaluation (1)
 «a priori» evaluation (2) (=evaluation (1)) → experimental data (2) → «a posteriori» evaluation (2)

 «a priori» evaluation (n) (=evaluation (n-1)) → experimental data (n) → final evaluation

Numerically, generalized and Bayesian approaches lead strictly to the same evaluation in the non-model fit, if as «a priori», one of the experimental data set is taken as pseudo-evaluation in the non-model fit is taken and, approximately, if the non-informative evaluation is used as a prior evaluation as a prior evaluation. Non-informative prior evaluation is evaluation which do not influence at the posterior evaluation (or numerically it is close to the posterior evaluation, but has very large assigned uncertainties). Strictly analytical, it was shown by Nancy Larson [3]. Bayesian approach is also interesting by the way how any evaluation can be improved with appearance of the new experimental data without any consideration of the old experimental data,

which were a part of the previous evaluation. Generalized approach allows also do this, treating previous evaluation as a pseudo-experimental data set.

Non-informative prior evaluation can be used in the generalized least-squares method (e.g. in the GMA complex) as pseudo-experimental data set for initial filling up of the nodes of evaluated data by non-empty values, or for interpolation of the experimental data to the same nodes used in the non-model evaluation.

Further, we will limit all our consideration by the non-model least-squares fit of the data.

Construction of covariance matrices of the uncertainties of the experimental data

Most consistent approach to the preparation of the covariance matrices of the uncertainties of the experimental data is the application of the uncertainty propagation law to the equation of the data reduction. As it is known, the primarily-measured quantities in the experiment are usually the number of the detector counts per channel depending from different conditions (measurements with and without sample, measurements with monitor sample, etc.), allowing to determine the efficiency of the detector, account the different type of the background events, to introduce all needed corrections. Using the statistical uncertainties of the primarily-measured quantities (and uncertainties of other types are absent) and relations for the reduction of the primarily-measured quantities to the data which experimentalist would like to present, the most reliable covariance matrix of the uncertainty of the reduced data can be obtained. R-matrix code SAMMY describing the cross sections in the resonance region can use this type of approach, if all sets of primarily-measured quantities are available.

Unfortunately, most compilations in the experimental database EXFOR do not contain the primarily-measured quantities and give only final data obtained by the authors with the use of the equations of the data reduction. In the best case they give also estimation of the different component of the uncertainties of the data. These components can be characterized by the different correlative properties of the components of the uncertainties. They can be separated at three groups, accordingly responsible for short-energy range correlations (SERC – statistical uncertainties), medium-energy range correlations (MERC – related with uncertainties of the introducing of many corrections, efficiency of the detector registration, etc.) and large-energy range correlations (LERC- uncertainties in the mass of the sample, quantum yields and so on). Using this classification, we can obtain the following expression for the covariance matrix of the uncertainty of the experimental data set.

If $d_i = D(r_i, q_1, q_2, q_3, \dots, q_m, p^1_1, p^1_2, p^1_3, \dots, p^i_n)$ is an equation of the reduction of the data, where d_i is a final data, and r_i is a primarily-measured quantity at the point i , and q_k and p^i_l are the parameters (k and l are indexes of the components of the uncertainty) having different correlative properties contributing in the final component of the uncertainty, then the elements of the covariance matrix V_{ij} , presenting the averaged value from product of variation between different points, can be presented (using the error propagation law in the approximation that there is no correlations between parameters q and p):

$$V_{ij} = \langle \delta d_i \delta d_j \rangle = \delta_{ij} \frac{\partial D_i}{\partial r_i} \Delta^2 r_i \frac{\partial D_i}{\partial r_i} + \sum_k \sum_l \frac{\partial D_i}{\partial q_k} \langle \delta q_k \delta q_l \rangle \frac{\partial D_j}{\partial q_l} + \sum_k \sum_l \frac{\partial D_i}{\partial p^i_k} \langle \delta p^i_k \delta p^j_l \rangle \frac{\partial D_j}{\partial p^j_l}$$

where $\Delta^2 r_i$ is a mean-square of the variation of the primarily-measured quantity, δ_{ij} – Kronecker's delta-symbol, $\langle \delta q_k \delta q_l \rangle$ and $\langle \delta p^i_k \delta p^j_l \rangle$ - covariance matrices of parameters with

different correlative properties and $\frac{\partial D_i}{\partial r_i}$ - partial derivatives. If $\langle \delta q_k \delta q_l \rangle = \delta_{kl} \Delta^2 q_k$, then, the covariance matrix of uncertainties takes the form:

$$V_{ij} = \delta_{ij} \frac{\partial D_i}{\partial r_i} \Delta^2 r_i \frac{\partial D_i}{\partial r_i} + \sum_k \frac{\partial D_i}{\partial q_k} \Delta^2 q_k \frac{\partial D_j}{\partial q_k} + \sum_l \frac{\partial D_i}{\partial p_l^i} \Delta p_l^i C_{ij}^l \Delta p_l^j \frac{\partial D_j}{\partial p_l^j}$$

where $\Delta^2 q_k$ is a mean-square variation of the parameter, and $\langle \delta p_k^i \delta p_l^j \rangle = \delta_{kl} \Delta p_l^i C_{ij}^l \Delta p_l^j$ with C_{ij}^l - correlation matrix of p_l parameter.

In case if authors give only reduced final experimental data, estimation of total uncertainty and its components, but primarily-measured quantities and total formulas for data reduction are not given, total covariance matrix of the data uncertainty can be approximated by sum of the components responsible for the short-energy range (SERC), medium-energy range (MERC) and large-energy range (LERC) components of the uncertainties:

$$V_{ij} = \delta_{ij} (\Delta_{SERC} D_i)^2 + \sum_k \Delta_{LERC} D_i^k \Delta_{LERC} D_j^k + \sum_l \Delta_{MERC} D_i^l C_{ij}^l \Delta_{MERC} D_j^l$$

or if designate the variation of the components of the uncertainty reduced final quantities through:

$$V_{ij} = \delta_{ij} \Delta_{Si}^2 + \sum_k \Delta_{Li}^k \Delta_{Lj}^k + \sum_l \Delta_{Mi}^l C_{ij}^l \Delta_{Mj}^l$$

If present first and second term of the last equation through corresponding correlation matrices, the final result can be presented as:

$$V_{ij} = \Delta_{Si}^2 C_{Sij} + \sum_k \Delta_{Li}^k C_{Lij}^k \Delta_{Lj}^k + \sum_l \Delta_{Mi}^l C_{Mij}^l \Delta_{Mj}^l$$

Square correlation matrices C_{Sij} and C_{Lij} can be presented as:

$$C_{Sij} = \begin{vmatrix} 1.0 & 0.0 & 0.0 & \dots & 0.0 \\ 0.0 & 1.0 & 0.0 & \dots & 0.0 \\ 0.0 & 0.0 & 1.0 & \dots & 0.0 \\ \dots & \dots & \dots & \dots & \dots \\ 0.0 & 0.0 & 0.0 & \dots & 1.0 \end{vmatrix} \quad \text{and} \quad C_{Lij} = \begin{vmatrix} 1.0 & 1.0 & 1.0 & \dots & 1.0 \\ 1.0 & 1.0 & 1.0 & \dots & 1.0 \\ 1.0 & 1.0 & 1.0 & \dots & 1.0 \\ \dots & \dots & \dots & \dots & \dots \\ 1.0 & 1.0 & 1.0 & \dots & 1.0 \end{vmatrix}$$

Square correlation matrix C_{Mij} is more complex and has units on the diagonal but elements, which are less on absolute value than unit out of diagonal. Some off-diagonal values can be equal one on the absolute values. Example of such correlation matrix is shown below:

$$C_{Sij} = \begin{vmatrix} 1.0 & 0.9 & 0.7 & \dots & 0.1 \\ 0.9 & 1.0 & 0.8 & \dots & 0.2 \\ 0.7 & 0.8 & 1.0 & \dots & 0.3 \\ \dots & \dots & \dots & \dots & \dots \\ 0.1 & 0.2 & 0.3 & \dots & 1.0 \end{vmatrix}$$

As a rule, pure phenomenological approach is used with the evaluation of the length of correlation for each component of the uncertainty and some model function, which describes the correlation of the uncertainties between two energy points. Such length of correlations for introducing of the uncertainty at the multi-scattering correction can be for example such minimal distance between two energy points, when introducing of the correction at one point does not influence practically at the value of the correction at another point. Usually, the linear dependencies are used for the fit of the correlation function in case of medium-energy range correlations.

Total covariance matrix of the experimental data set can be obtained by the summation of all components and should be positive definite and realistic in the sense, that it should be more close to the matrix which can be obtained when data reduction formulas are used for construction of covariance matrix of this experimental data set. In case of under evaluation of the component of the uncertainties of the data, and high contribution of the large-energy range correlation component of the uncertainty, the covariance matrices constructed from these components can lead to the appearance of the effect of the Peelle's Pertinent Puzzle (PPP) — substantial bias of the evaluated central value. PPP effect and methods of its exclusion will be discussed below.

Covariance matrices describing the covariances between energy points are quadratic and symmetric relative the major diagonal. Because of this, for their presentation it is enough to show the low triangle of the matrix (correlation matrix in this case):

1.0
0.9 1.0
0.7 0.8 1.0
.....
.....
0.1 0.2 0.3.....1.0

The same methods, detectors or samples can be used in different measurements done the same group of the experimentalists. This can lead to the appearance of the noticeable correlations between the uncertainties in these measurements. Then in the least-squares fit the blocks of the covariance matrices of the experimental data should be used which combine beside the square matrix for each experimental data set the rectangular blocks which describes the covariances (correlations) between different energy points of the different experimental data sets. Example of such matrix consisting from two data sets, which were obtained using the same samples and detectors is shown below. Data were prepared by Wolfgang Poenitz for the evaluation of the standards of neutron cross sections. 100% correlations in the uncertainty of the sample masses, 80% correlations in the uncertainty of the efficiency of the registration by the detector and 50% correlations in the uncertainty of the correction at multiple scattering and decreasing of the neutron flux in the sample have been accounted. The low triangles of the correlation matrices for each data set and rectangular block describing cross-data set correlations are shown by different color.

```

DATABLOCK***** DATASET*****
  DATA SET  853  RATIO                U8 (n, f)                U5 (n, f)
YEAR 1983 TAG  1  AUTHOR:  A.A.GOVERDOVSKII ET AL.                83KIEV,  ,159
ENERGY/MEV  VALUE  ABS. UNCERT.  PRIOR/EXP UNCERT./%  DIFF./%  VAL.*SQRT(E)
0.5500E+01  0.5020E+00  0.2385E-01  1.0496  4.8  -4.7  1.1773

```

0.5800E+01	0.5423E+00	0.1065E-01	1.0099	2.0	-1.0	1.3060
0.6200E+01	0.5807E+00	0.1112E-01	0.9977	1.9	0.2	1.4459
0.6500E+01	0.6068E+00	0.1070E-01	1.0104	1.8	-1.0	1.5470
0.7000E+01	0.6037E+00	0.1083E-01	1.0104	1.8	-1.0	1.5972
0.7500E+01	0.5743E+00	0.9780E-02	1.0119	1.7	-1.2	1.5728
0.7750E+01	0.5715E+00	0.1095E-01	0.9970	1.9	0.3	1.5910
0.8000E+01	0.5674E+00	0.1062E-01	0.9989	1.9	0.1	1.6048
0.8500E+01	0.5612E+00	0.9897E-02	1.0031	1.8	-0.3	1.6362
0.9000E+01	0.5631E+00	0.9786E-02	1.0092	1.7	-0.9	1.6893
0.1000E+02	0.5658E+00	0.9833E-02	1.0084	1.7	-0.8	1.7892

APRIORI NORM 12 1.0066 853 A.A.GOVERDOVSKII ET AL.

*****DATASET*****

DATA SET	854	RATIO	U8(n, f)	U5(n, f)
YEAR 1984 TAG	1	AUTHOR:	A.A.GOVERDOVSKII ET AL.	AE 56,164(1984)

ENERGY/MEV	VALUE	ABS. UNCERT.	PRIOR/EXP UNCERT./%	DIFF./%	VAL.*SQRT(E)	
0.1400E+02	0.5405E+00	0.1348E-01	1.0207	2.5	-2.0	2.0224
0.1450E+02	0.5568E+00	0.1610E-01	1.0204	2.9	-2.0	2.1202
0.1500E+02	0.5499E+00	0.2197E-01	1.0597	4.0	-5.6	2.1298

APRIORI NORM 12 1.0277 854 A.A.GOVERDOVSKII ET AL.

CORRELATION MATRIX OF DATA BLOCK

```

1.00
0.29 1.00
0.27 0.70 1.00
0.28 0.73 0.80 1.00
0.25 0.65 0.72 0.83 1.00
0.25 0.64 0.71 0.81 0.87 1.00
0.23 0.55 0.60 0.69 0.74 0.84 1.00
0.23 0.56 0.60 0.68 0.73 0.83 0.77 1.00
0.25 0.59 0.61 0.68 0.72 0.83 0.76 0.81 1.00
0.25 0.60 0.62 0.67 0.69 0.79 0.72 0.77 0.87 1.00
0.25 0.60 0.62 0.67 0.66 0.69 0.64 0.68 0.78 0.84 1.00
0.11 0.27 0.28 0.30 0.29 0.31 0.28 0.29 0.30 0.30 0.30 1.00
0.09 0.23 0.24 0.26 0.25 0.27 0.24 0.25 0.26 0.26 0.26 0.77 1.00
0.07 0.17 0.17 0.19 0.18 0.19 0.17 0.18 0.19 0.19 0.19 0.52 0.85 1.00

```

DATABLOCK*****

As it is known from practice of the evaluation, the account of the uncertainty correlations of this type (cross-data-sets correlations) is very important for realistic evaluation of the uncertainties of the evaluated data. Without account of such correlations, the uncertainties of the evaluated data can be substantially underestimated. Also, with account of such correlations, the uncertainty of the evaluated data based at the multiple measurements in the frameworks of the same method, cannot reach unrealistically low values. Accuracy of the data cannot be better than accuracy of the standards or fundamental constants used in the data reduction. Sure that account of the correlations between uncertainties of different data lead to the comprehension of the evaluation and to the substantial increase of the matrix dimension. Strictly speaking, the uncertainties of the measurements of any observable are correlated and the task of the evaluator to account such correlations which can affect at the results of the evaluation, including as the central values as well as their uncertainties.

Requirements to the covariance matrices of the uncertainties of the experimental and evaluated data

Requirements of the semi-positive definiteness of the covariance matrix of the uncertainties of the experimental or evaluated data are explained by the fact: only such matrix guarantees the

positive value of the uncertainty of any quantities calculated with these data. All eigenvalues of such matrix should not be negative. In the numerical calculations, order of the ratio of the maximal to the minimal eigenvalue should not be larger than the length of the word with which all computations are done at the computer. With any matrix operations, the numerical scheme should be used which does not lead to the loss of the preciseness of such calculations. Namely, when we have summation of large number of elements with variable signs and large difference in the absolute values, the scheme of summation should be used which does not lead to the loss of accuracy.

As an example, we may show the results of calculations of eigenvalues of the covariance matrices of the uncertainties of the evaluation of ${}^6\text{Li}(n,t)$ (5 data sets reduced to 51 points on energy) with the use of double precision calculations at the 64-bit word computer (length of word is 128 bits). Evaluations were done with the use of non-model GMA and GLUCS codes and PADE2 code based on mathematical model of analytical approximation. But eigenvalues were calculated with old version of the ACORNS code, widely used in the neutron reactor dosimetry for the checking of the evaluated covariance matrices at the semi-positive definiteness implemented at 32-bit PC with ordinary accuracy. Because the range of eigenvalues of the matrix obtained in PADE2 with 10-parameters fit is out of the range (about 6.5 orders of magnitude in the decimal scale) of the length of the mantissa storage, all PADE2 fit eigenvalues starting from number 11 calculated with this version of ACORNS is just computer garbage (they should be zeros precisely) and do not characterize the matrix. For non-model fit (GMA, GLUCS), the difference between largest and lowest eigenvalues fitted in the limit of 3 orders of magnitude. If this difference exceeded 6 - 7 orders of magnitude, the eigenvalues with low values have been calculated with high loss of accuracy. Taking this into account, the ACORNS code was updated by the author (E.J. Szondi, INT, Budapest) for calculations with the word length in 64 bits.

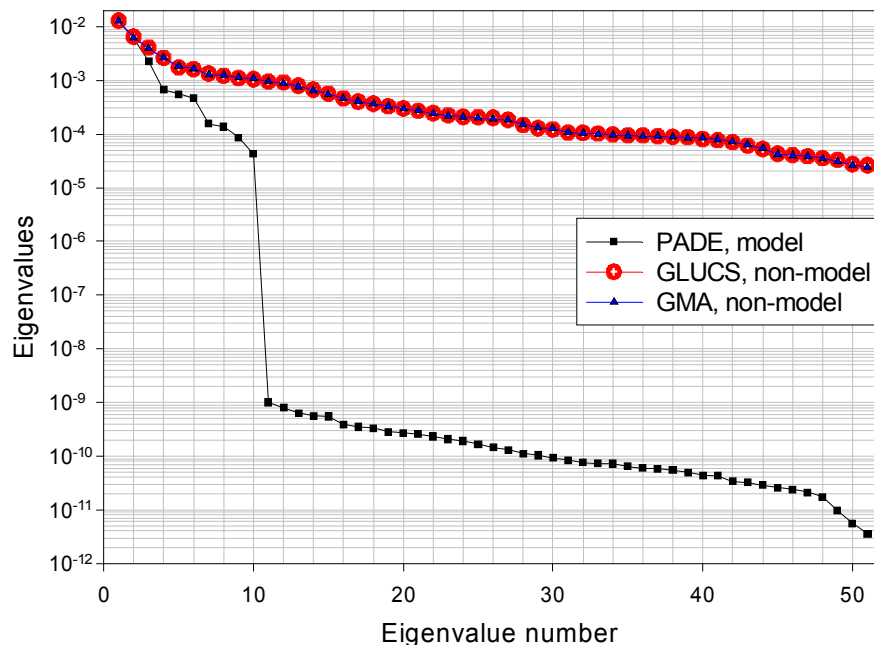


Fig. 1. Eigenvalues of the covariance matrices of the uncertainty of the ${}^6\text{Li}(n,t)$ cross section evaluated in the model (PADE, 10 parameters) and non-model (GMA, GLUCS) least-squares fits.

Results of the calculations of the eigenvalues for covariance matrices of the evaluated uncertainties ordered in the direction of their decreasing for one model and two non-model fits are shown in Fig. 1. The difference between calculations in two non-model codes GMA and

GLUCS is in the limits of machine accuracy. All 51 eigenvalues obtained in the non-model fits are positive definite. In PADE fit the mathematical model of analytical expansion with 10 parameters is used. In this case the covariance matrix of uncertainties of the cross sections obtained from parameters in 51 energy nodes has 10 non-zero (positive) values and should have 41 zero value. In the 32-bit machine presentation these zero values are presented by the numbers, which at 6-7 orders lower than the largest eigenvalue. If λ_l and λ_n are maximal and minimal eigenvalues of the covariance matrix, then important ratio λ_l/λ_n set the requirements to the accuracy with which calculations should be done to avoid the loss of accuracy and conversion of the initially positive definite covariance matrix in the non-positive definite.

For matrices with large difference between maximal and minimal eigenvalues their storage in the files of the evaluated data is very important problem. Existing formats of the evaluated data allow the storage of the mantissa of the numbers with not more than 7 digits in decimal presentation and this led to the cut of the mantissa of the numbers of the covariances obtained with high precision in the calculations. As result the initially determined as positive or semi-positive matrix, it may be converted in the negative definite matrix. The size of the covariance matrices obtained in the combined fit of many reactions can be very large (e.g. 1200*1200). For storage of the covariance matrices of the large size the formats have been proposed, where for economy of the space, the corresponding elements of correlation matrices are presented by two decimal digits. This also may lead to the loss of the semi-positive definiteness of such cutted matrices.

The natural requirement to the covariance matrix of the uncertainties is the set of the following inequality between the elements of covariance matrices $V_{ij} \leq \sqrt{V_{ii}V_{jj}}$. This inequality provides, that all non-diagonal elements of the corresponding correlation matrix should be less or equal 1 (diagonal elements), or correlation of uncertainties between two points should not exceed 1.

More strict requirements to the constructed covariance matrices of the experimental data are requirements of such properties, that could not lead to the appearance of the PPP effect at evaluation of these data. PPP effect is not appeared at the fit of the data which have only statistical uncertainties and can be rather large if the contribution of the components of the uncertainty presenting long-range correlations is substantially overestimated. More detailed discussion of the PPP effect and those requirements to the experimental data, which allow to reduce and even to avoid it, will be given below.

Use of Bayesian code GLUCS for combined fit of the cross sections and preparation of the evaluated data files and covariances for neutron-induced reactions above the resonance region

GLUCS program complex developed at the Oak Ridge National Laboratory (USA) [4] and updated by Siegfried Tagesen [5] to the combined evaluation of the all cross sections for one nucleus at the Institute for Radium Study and Nuclear Physics (IRK, Austria) is based at the use of the Bayes approach in the evaluation of the cross sections. Complex consists from 3 codes INPUT, GLUCS и OUTPUT, which work independently and sequentially, using as input data the output data sets prepared by the previous modules. INPUT module reads a prior evaluation cross sections and covariance matrices in the ENDF-6 format and prepares the files of input data for GLUCS module. Experimental data, also needed for GLUCS (least-squares fitting code) run, are prepared by some auxiliary programs and include the uncorrelated sets of experimental data consisting from the experimental cross sections reduced to the same energy groups, total per-cent uncertainty and low triangle of the correlation matrix of the uncertainty. After CLUCS run with least-squares fit, the files with posterior evaluation are prepared which in its turn after OUTPUT module run are converted in posterior evaluation in the ENDF-6 format of the evaluated data

files. The procedure is repeated up to the input of the last set of experimental data. Constraints and physical relations between the data (different cross sections) are accounted in the process of the evaluation and influence rather substantially at the final results (cross section and covariances). As result the size of the total evaluated covariance matrix is increasing with inclusion of blocks of elements of uncertainties of all partial cross sections considered in the evaluation and can be very large.

As example $^{52}\text{Cr}+n$ evaluation-flow chart with Bayesian inclusion of new data is shown at Fig. 2. The neutron energy interval for all reactions included is between 0.64 and 20 MeV. Some old evaluation (mostly from EFF-2) was taken as a prior for all reaction channels with a rather large (non-informative) prior uncertainties. At the first step the partial channels for which the experimental data are available have been evaluated, at the second step, all other reactions and constraints/relations between partial and total cross sections have been added in the fit. These constraints are: total inelastic scattering is a sum of inelastic scattering with excitation of the discrete and continuum levels, sum of all reaction cross sections is equal to non-elastic cross section, sum of non-elastic and elastic cross-sections is equal to total cross section.

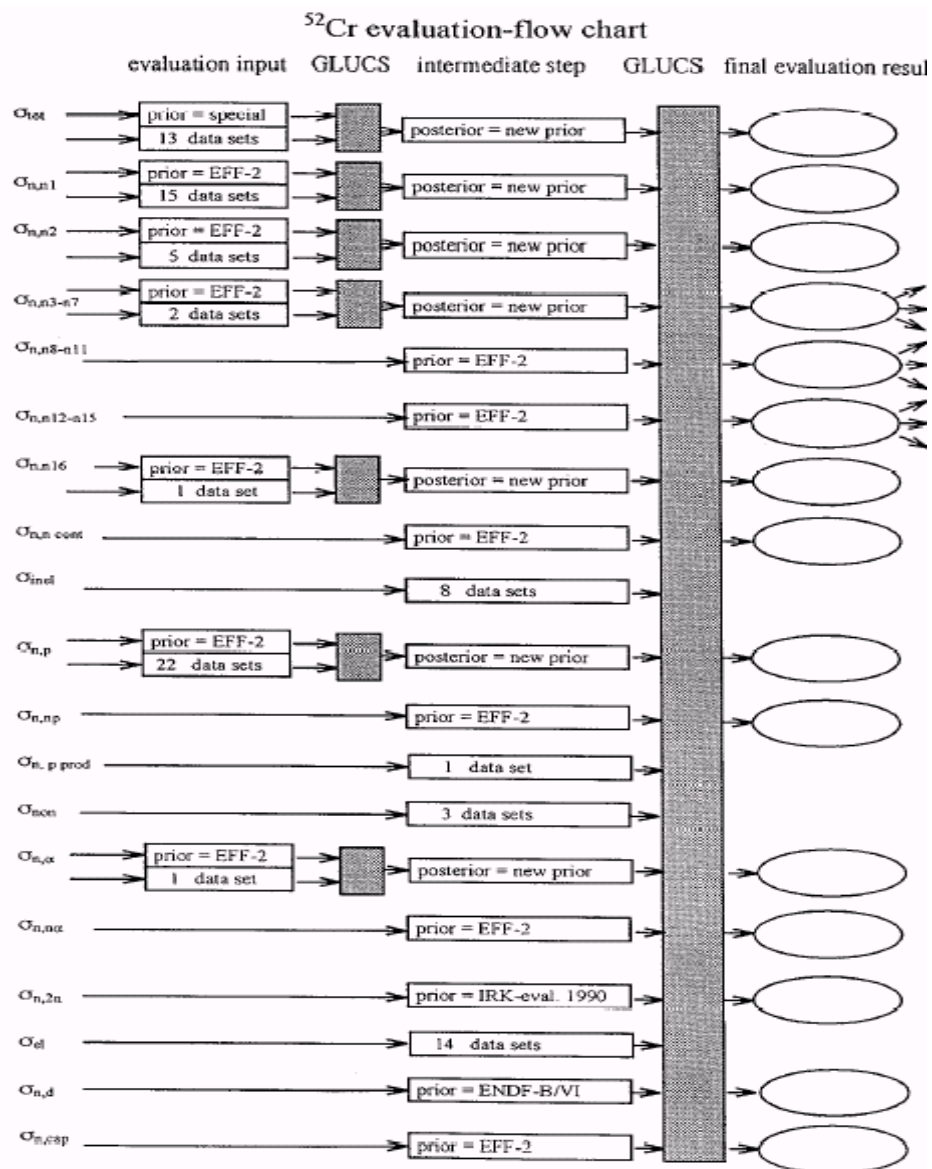


Fig.2 $^{52}\text{Cr}+n$ evaluation flow-chart in Bayesian approach.

Final evaluation result includes evaluation of all considered partial and total cross sections, and full covariance matrix including all cross-energy and cross-reaction covariances. Because of used constraints, even prior cross sections, which had no experimental data, were improved in posterior evaluation.

Group averaged experimental total cross sections prepared for evaluation is shown in Fig. 3 in comparison with old EFF-2 evaluation and Cierjacks68 data which were selected as «prior», and the results of the final fit with the account of 92 experimental data sets is shown on Fig. 4. The evaluated uncertainty achieved for total cross section is between 0.5 and 1.5 %, what probably seems to low taking into account of 5-8 % spread of experimental data of the total cross sections, but other cross section contributing in the evaluation and general chi-square of the order 1 per degree of freedom may justify this value.

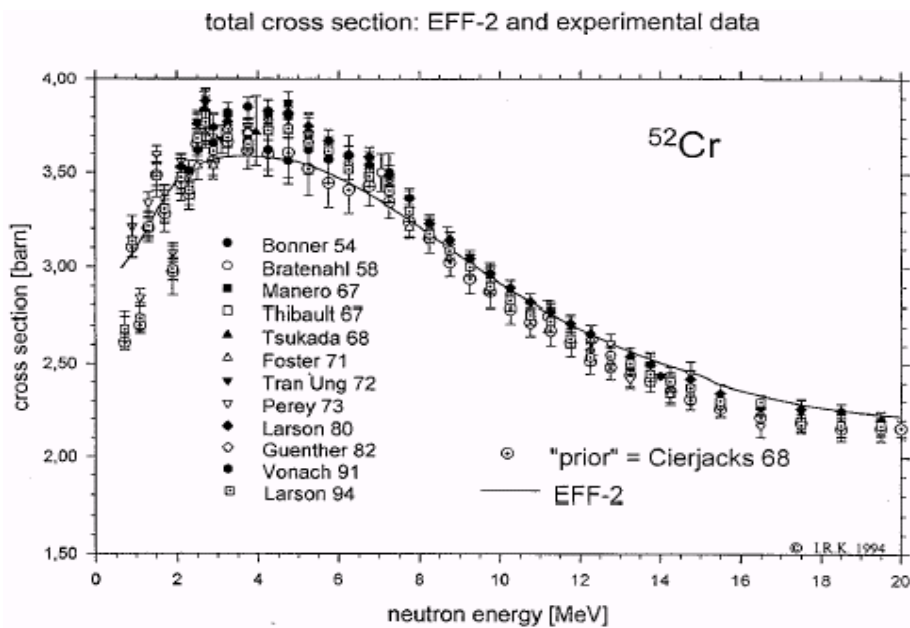


Fig. 3. Comparison of the experimental data for total cross section with the EFF-2 old evaluation and a prior evaluation.

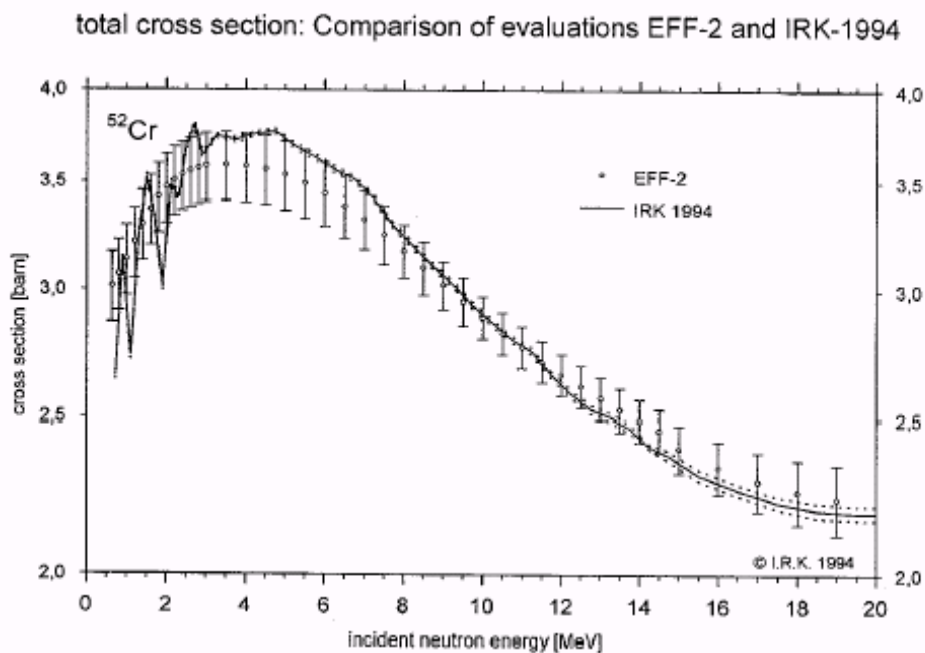


Fig. 4. Comparison of the old and new evaluation for the total cross section.

Large number of experimental data on elastic scattering cross section is shown at Fig. 5 in comparison with the EFF-2 evaluation taken as a prior and the results of the obtained fit which has rather large uncertainties comparing with the total cross section is shown at Fig. 6.

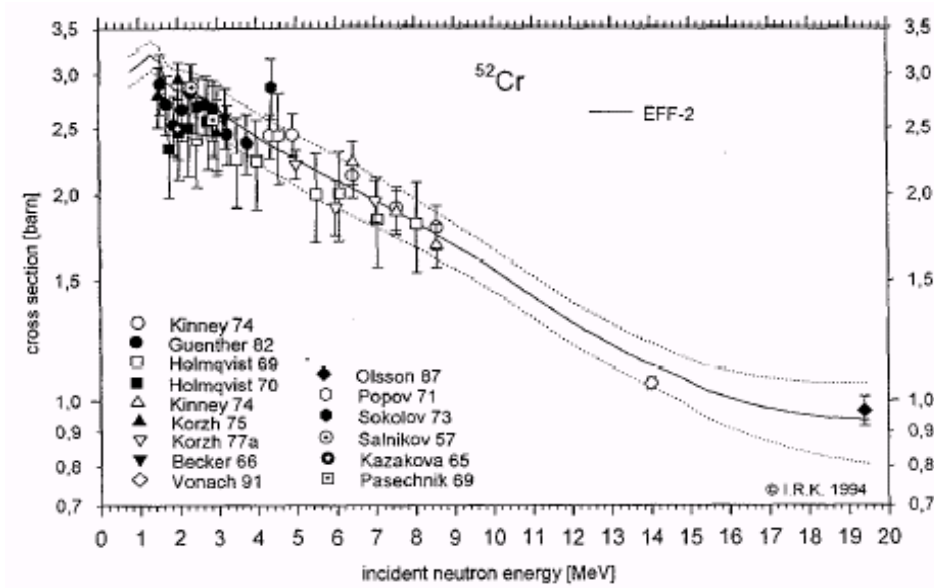


Fig. 5. Comparison of the experimental data for elastic cross section with the EFF-2 old evaluation and a «prior» evaluation.

Figure 7

elastic cross section: Comparison of evaluations EFF-2 and IRK-1994

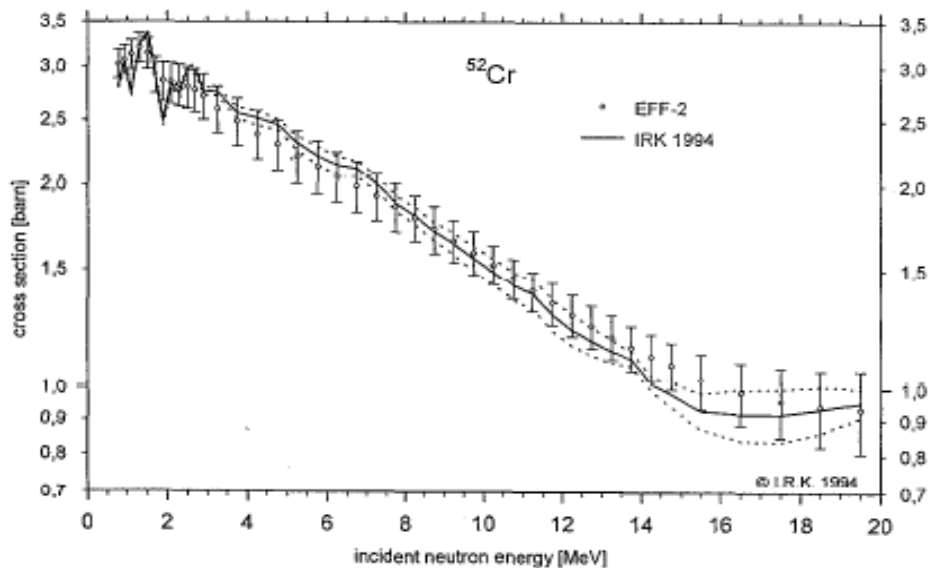


Fig. 6. Comparison of the old and new evaluation for the elastic scattering cross section.

Evaluation of total inelastic scattering cross section is shown in Fig. 7 and inelastic scattering cross section with excitation of the first level in Fig. 8. The correlation matrices of the evaluated data for total cross section and inelastic scattering cross section with the excitation of the first level are shown in Fig. 9. Correlation matrix for total cross sections shows strong correlations between 2 and 10 MeV. Matrices for both reactions have very specific behavior at 14 MeV point, where large number of high accuracy data contributes in the evaluation.

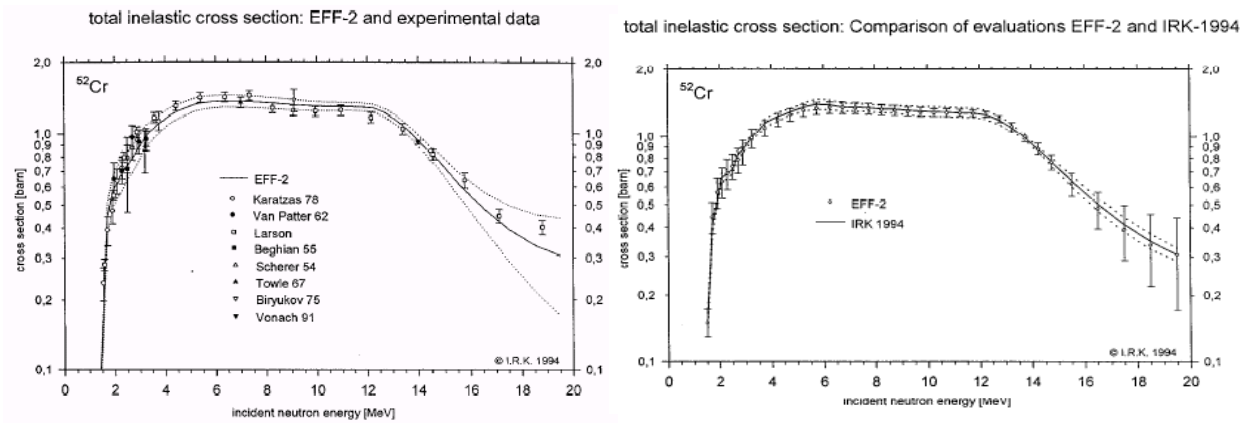


Fig. 7. Comparison of the experimental data for total inelastic cross section with the EFF-2 old «prior» evaluation (left plane) and old and new evaluation (right plane).

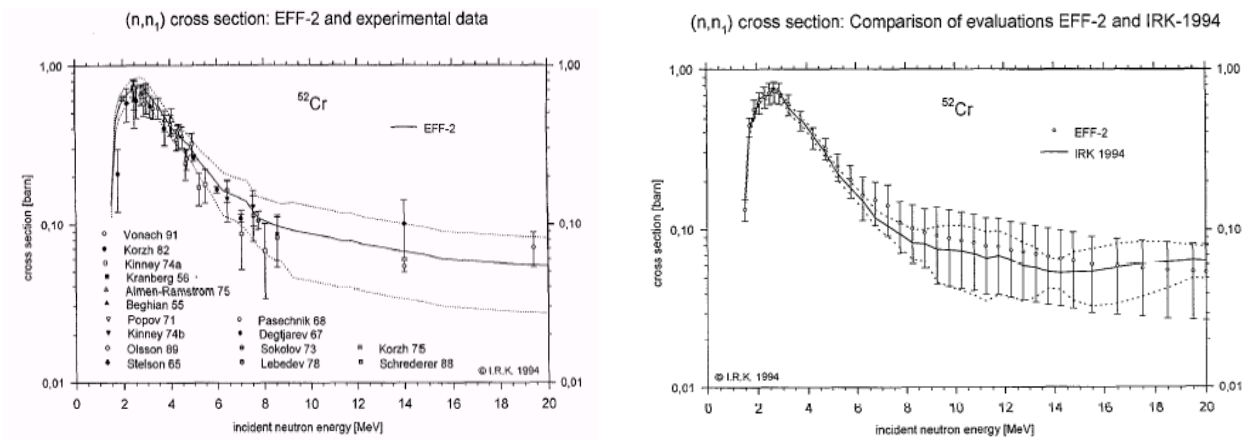


Fig. 8. Comparison of the experimental data for inelastic scattering cross section with excitation of the first level with the EFF-2 old «prior» evaluation (left plane) and old and new evaluation (right plane).

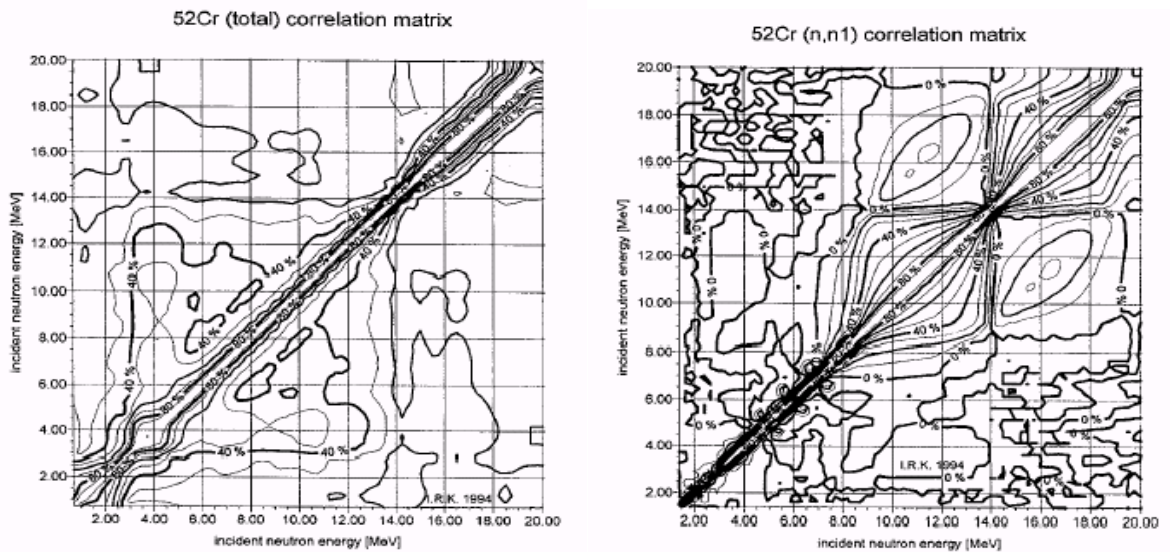


Fig. 9. Correlation matrices of the evaluated uncertainties describing cross-energy correlations for total cross section (left panel) and for inelastic scattering with the excitation of the first level (right panel).

Evaluation was done more than 15 years ago. The uncertainties of the evaluation are rather low. To show how the evaluated data are consistent with some results of modern measurements [6], the comparison of the yield if the 1434.07 keV gamma-line formed as result of all gamma-transition passing through de-excitation of the first level in ^{52}Cr is given in Fig. 10. In average, 92 to 100% of all inelastic scattering reactions ended up with this gamma-transition in neutron energy range below 20 MeV. IRK evaluation for total neutron inelastic scattering, which were taken was taken in Joint European File was re-calculated in the 1434.07 keV gamma-line production yield and compared with the results of measurements. Generally the consistency is good (in the limits of 5 - 10%). The existing discrepancies can be related more to the experimental data. Level of the experimental cross section at the energy of 5 - 7 MeV (1.6 barn) is too high, because it is fixed well by total, elastic and non-elastic cross sections. There is no physical justification why the experimental gamma-yield begins the growth to the 8 MeV (near threshold of the (n,2n) reaction). Also cross section in 14 - 15 MeV range is well established and known at least with 2 - 3 % uncertainty. Natural chromium as one of the constituent of the stainless still widely used in the construction of experimental setups may create some background problem for 1434.07 keV gamma-line.

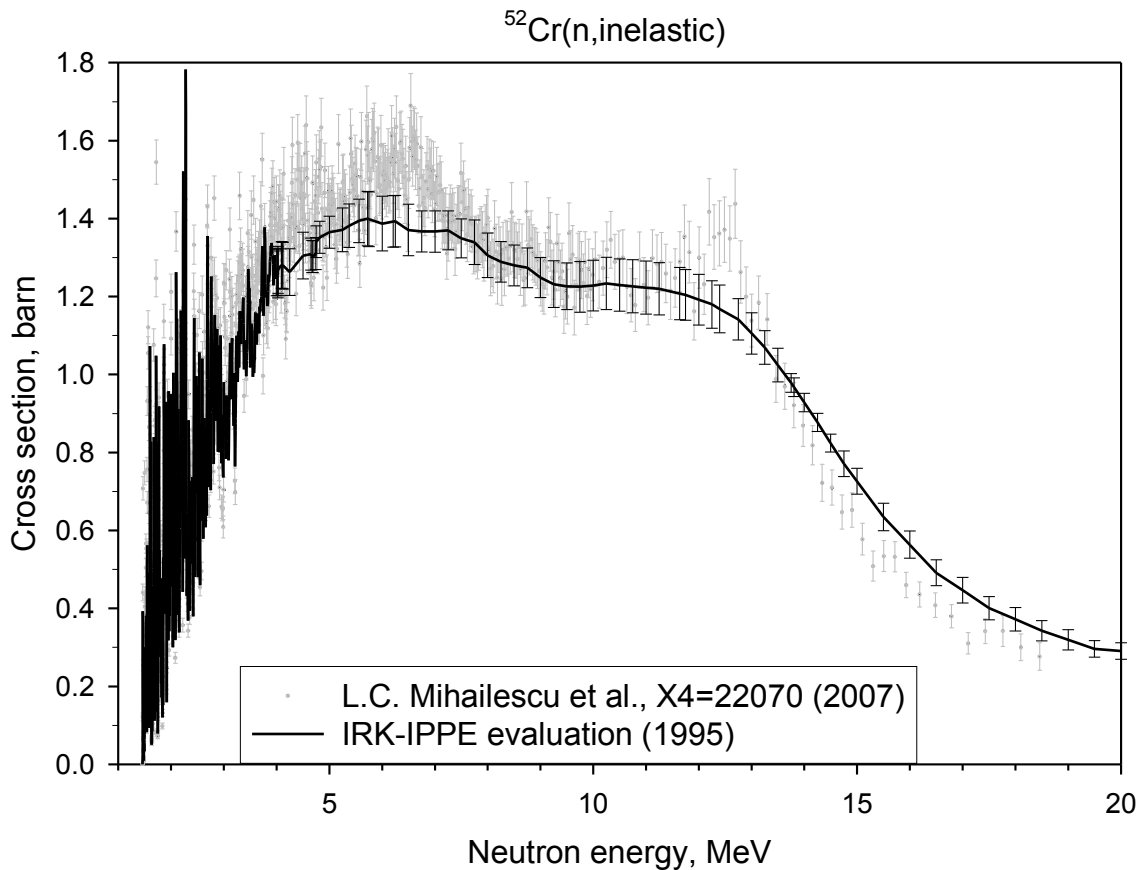


Fig. 10. Comparison of the evaluated (GLUCS, 1995) 1434.07 keV gamma-production cross section with the results of latest measurements (L.C. Mihailescu et al., EXFOR Entry 22870 (2007)).

Bayes approach to the description of the complex multi-step, multi-particle break-up processes in the case of $^9\text{Be}+n$ reactions

In difference from the reactions with incident neutrons up to energy in 20 MeV at ^{52}Cr , where major part of the processes with the emission of the nucleons and more heavy particles go mostly through the simple single-step reactions, reactions induced by neutrons at ^9Be nucleus have

larger diversity and some of them present the combination of the sequential two-particle reactions with three-particle decay [7]. Specificity of these reactions is that the final reaction products (for exclusion of small yield of protons, deuterons and ^3He) are 2 neutrons and 2 α -particles practically at all incident energies. This reaction can be used as an effective neutron multiplier in the blankets of the thermonuclear installations for transmutation of the fertile materials in the fissile materials for nuclear power plants.

Main mechanisms of the reactions of interaction of neutrons with energy above 2 MeV with ^9Be leading to break-up of the ^{10}Be compound system at 2 neutrons and 2 alpha-particles are shown in Fig. 11. Reactions beginning with the inelastic scattering with of different levels at the first step of the reaction contribute largest in these processes. ^8Be residual nuclei decays for nuclear time at two alpha-particles.

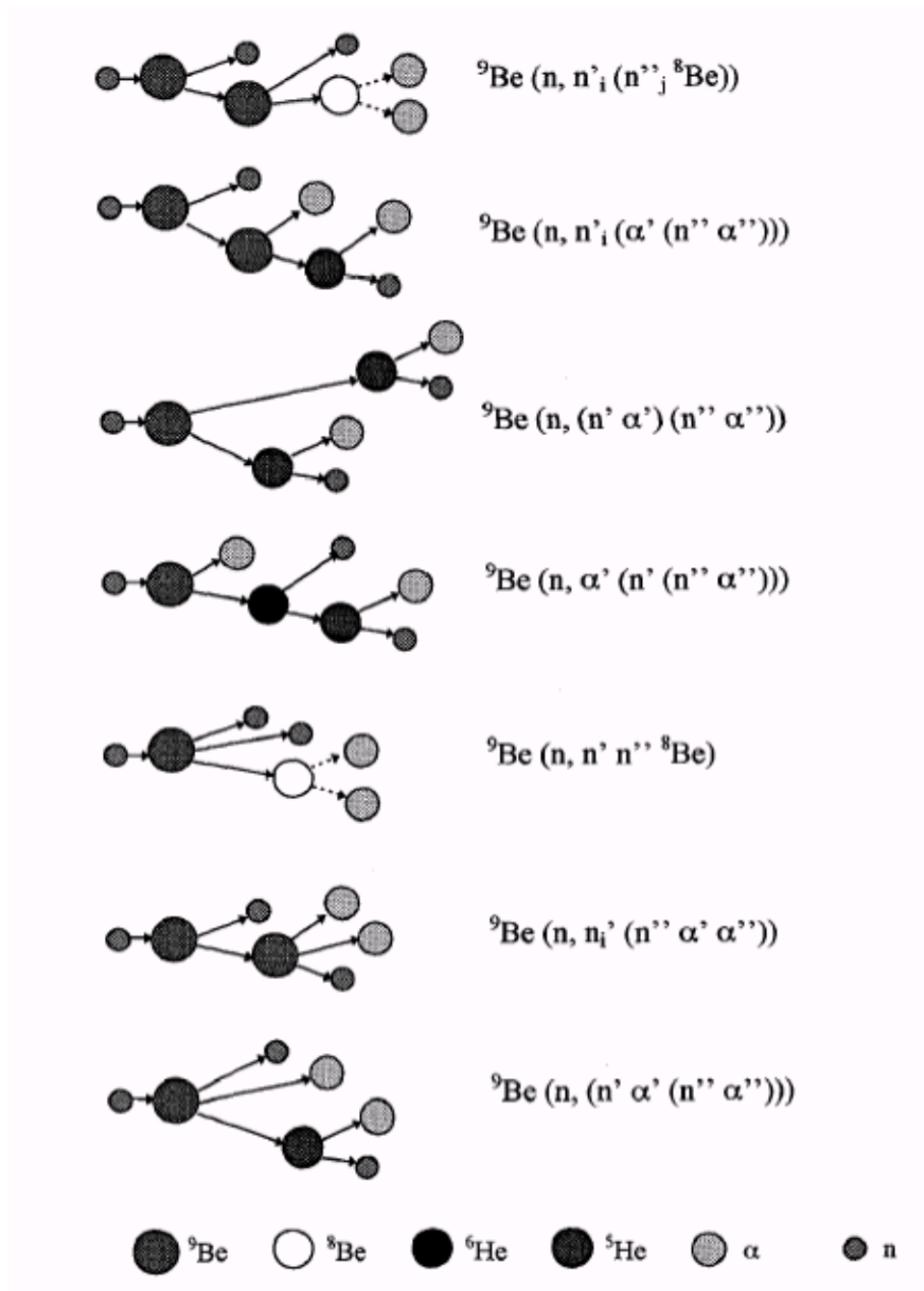


Fig. 11. Processes in $^9\text{Be}+n$ reaction leading to the decay at 2 neutrons and 2 alpha-particles.

Main channels of the reaction, including their intermediate states, widths and branching coefficients are shown in the Table 1. Because the direct experimental data on many reaction channel cross sections are absent, but some cross sections can be obtained from the model estimations and there are experimental data on the total energy-angular distributions of emitted neutrons for neutrons with incident energy 5.9, 10.1, 14.1 and 18 MeV and alpha-particles for neutrons with 14 MeV neutron energy, the Bayesian approach was used for evaluation of the contribution of different channels in the total reaction cross section.

Table 1. Characteristics of the reactions with excitation of ${}^9\text{Be}$ levels in the inelastic scattering of neutrons.

N	Elev. MeV	J _p	Γ _{tot} , MeV	Branching Ratio for decay to final state				
				${}^8\text{Be}$ g.s. BR1	${}^8\text{Be}$ 1-st BR2	${}^5\text{He}$ g.s. BR3	${}^5\text{He}$ 1-st BR4	(nαα)-3-body BR5
0	0.0 (g.s.)	3/2-	0.0(stable)	0.0	0.0	0.0	0.0	0.0
1	1.684	1/2+	0.217	1.00	0.0	0.0	0.0	0.0
2	2.4294	5/2-	0.00077	0.07	0.0	0.0	0.0	0.93
3	2.78	1/2-	1.08	1.00	0.0	0.0	0.0	0.0
4	3.049	5/2+	0.282	0.87	0.13	0.0	0.0	0.0
5	4.704	3/2+	0.743	0.13	0.87	0.0	0.0	0.0
6	5.59	3/2-	1.33	0.5	0.5	0.0	0.0	0.0
7	6.38	7/2-	1.21	0.02	0.55	0.43	0.0	0.0
8	6.76	9/2+	1.33	0.0	1.0	0.0	0.0	0.0
9	7.940	1/2-	1.00	0.5	0.5	0.0	0.0	0.0
10	11.283	9/2-	1.10	0.02	0.14	0.84	0.0	0.0
11	11.81	5/2+	0.400	0.20	0.80	0.0	0.0	0.0
12	13.79	5/2-	0.590	0.0	1.0	0.0	0.0	0.0
13	14.392	3/2-	0.000381	0.049	0.386	0.565	0.0	0.0
14	14.4	1/2-	0.8	0.5	0.5	0.0	0.0	0.0
15	15.1	7/2-	0.35	0.0	1.0	0.0	0.0	0.0
16	15.9	5/2-	0.31	0.0	1.0	0.0	0.0	0.0
17	16.672	5/2+	0.041	0.0	0.0	1.0	0.0	0.0
18	16.975	1/2-	0.00049	0.07	0.0	0.0	0.0	0.93
19	17.298	5/2-	0.20	0.0	1.0	0.0	0.0	0.0
20	17.493	7/2+	0.047	0.0	0.0	1.0	0.0	0.0

Figure 1: ${}^9\text{Be}$ evaluation-flow chart (integral cross sections)

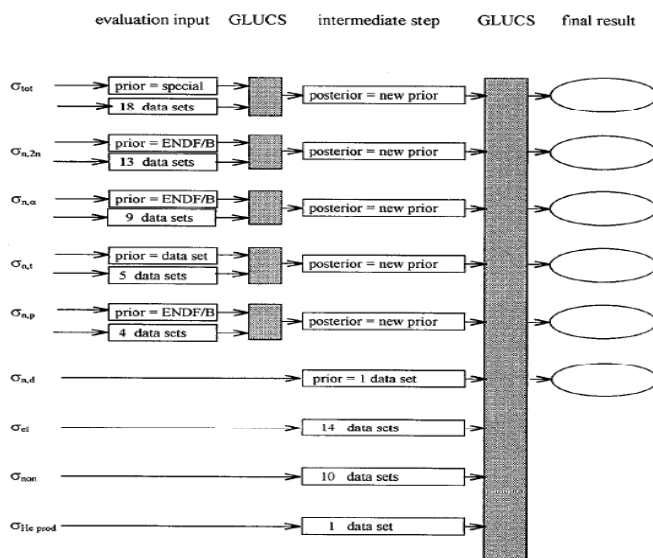


Рис. 12. Evaluation-flow chart in the evaluation of the integral cross sections with available experimental data for ${}^9\text{Be}+n$ reaction cross section.

At the first stage the evaluation of integral cross sections for all channels was prepared basing at a prior and experimental data shown at the evaluation flow-chart (Fig. 12). For those channels, for which the experimental data were absent (as for inelastic scattering with excitation of high-lying unstable levels) the calculations of inelastic scattering cross sections was done with account of direct and statistical mechanisms contribution using ECIS and TNG codes. For channels with no experimental data at all and absence of any possibilities for model estimation of their cross sections, a prior expert estimation was done with large assigned uncertainties (usually about 100 %). Results of the evaluation for the integral cross sections obtained at this stage are shown in Table 2 and for cross sections with largest number of available experimental data are shown in Fig. 13.

Table 2. A prior evaluation of contribution of different channels in the ${}^9\text{Be}+n$ cross section obtained with ECIS and TNG codes and expert's evaluation of cross sections for complex reaction channels (energies are given in MeV, cross sections in mb).

En	2.0	3.0	4.0	5.0	5.9	7.0	8.0	9.0	10.1	11.0	12.0	13.0	14.1	15.0	17.0	20.0
σ_{tot}	2102	2005	1885	1842	1798	1754	1733	1722	1676	1640	1584	1528	1473	1436	1375	1315
σ_{el}	2010	1700	1389	1295	1218	1170	1135	1117	1094	1065	1037	1006	971	949	912	870
σ_{non}	92	305	496	547	580	584	598	605	582	575	547	522	502	487	463	445
$n,n1$	31.3	46.9	38.0	36.0	31.5	24.1	19.8	15.5	11.6	9.90	8.17	6.98	5.43	4.63	3.45	2.06
$n,n2$		122	212	252	271	272	249	236	215	198	180	158	140	129	112	102
$n,n3$			23.6	22.6	21.5	19.2	18.8	15.8	12.0	10.3	8.53	7.23	5.43	4.60	3.73	2.60
$n,n4$			49.2	46.9	42.5	39.6	35.6	31.2	25.0	22.8	19.3	16.6	12.9	11.0	9.21	6.73
$n,n5$					16.4	16.9	17.4	16.7	14.4	12.9	11.6	9.19	7.94	6.47	4.69	
$n,n6$						11.9	13.5	13.4	12.4	12.8	12.0	11.3	9.03	7.83	6.58	5.08
$n,n7$							50.1	65.2	72.1	79.7	82.1	79.0	77.6	75.1	70.5	64.7
$n,n8$							7.20	9.33	9.15	9.93	10.0	9.65	8.61	8.03	7.97	7.13
$n,n9$								1.49	3.68	3.67	3.59	3.59	3.31	3.14	2.88	2.46
$n,n10$												3.15	6.98	8.34	10.9	12.4
$n,n11$													4.50	4.69	4.55	5.05
$n,n12$															3.42	3.48
$n,n13$															1.89	2.31
$n,n14$															0.91	1.16
$n,n15$															0.80	3.62
$n,n16$																2.65
$n,n17$																2.27
$n,n18$																0.70
$n,n19$																1.59
$n,n20$																1.34
$n,\alpha0$	45	105	85	65	50	35	28	22	19	17	15	13	11	10	8	5
$n,\alpha1$		1.50	55.4	70.0	62.6	53.4	40.4	33.5	32.2	27.4	23.9	21.3	18.6	17.1	13.6	9.24
$n,\alpha2$				4.2	25.1	36.4	32.1	31.1	34.0	30.8	28.3	26.6	24.5	23.3	19.5	14.4*
$n,{}^3\text{He}^5\text{He}$			5.0	22.0	31.0	37.0	36.0	33.0	28.0	24.0	19.0	14.0	10.0	8.0	5.0	5.0*
$n,nn^8\text{Be}$		16.0	22.0	25.0	27.0	29.0	31.0	33.0	34.0	36.0	37.0	38.0	39.0	40.0	41.0	42.0*
$n,n\alpha^7\text{He}$				3.0	11.0	20.0	48.0	60.0	78.0	88.0	102	115	124	131	136*	

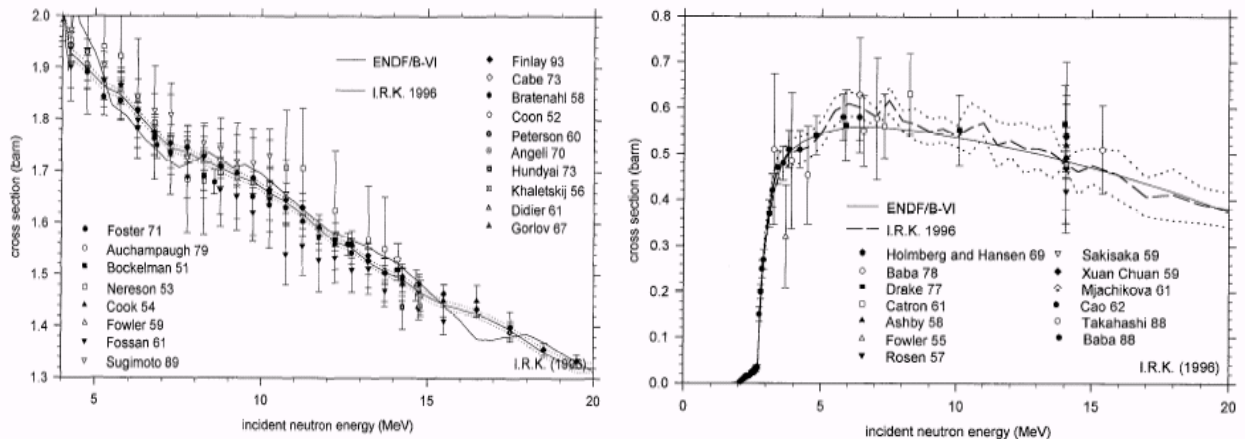


Fig. 13. Description of the total cross section (left panel) and (n,2n) cross section (right panel).

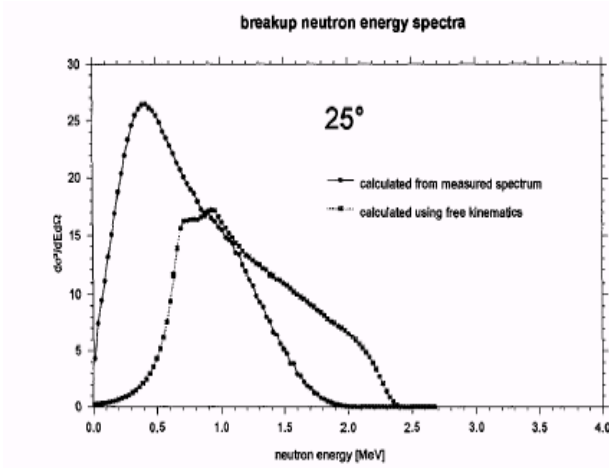


Fig. 14. Comparison of the second neutron energy distribution under the angle of 25 degree in the laboratory system for the reaction ${}^9\text{Be}(n,n'(n''\alpha'\alpha''))$ in case of free-kinematics break up and with account of the interaction between particles. Free kinematics 3-body break up predicts more haard spectrum for the neutron.

At the next step of the evaluation we have used least-squares fit of the experimental data on neutron emission spectra at 4 initial energies (5.9, 10.1, 14.1 and 18.1 MeV) for a large number of the angles. Bayesian method allows introduce sequentially in the fit of the new experimental data, which improve the evaluation. In this case, the cross section for each channel at these 4 energies was considered as the parameter for which a prior evaluation is known. Fit of emission spectra was done for different angles with sequential adjustment of the integral cross section for each channel. Shape of the spectrum for each partial channel was determined from kinematics transformation of spectra in the laboratory system of the coordinate from center of mass system. Two-body or three-body decays in the center of mass system were taken as obtained in the model calculations or from experiment where they were measured or isotropic in all other cases. For example the emission spectra for second neutron at 25 degrees in laboratory system from ${}^9\text{Be}(n,n'(n''\alpha'\alpha''))$ reaction are compared for two cases: free 3-body decay versus using of experimental data on energy distribution of neutrons in 3-body ($n''\alpha'\alpha''$) decay. As it is seen the neutron spectrum is substantially softer because alpha-particles have higher energy mostly due to Coulomb expulsion not accounted in the free 3-body decay. For transformation of the energy-angular distributions in sequential multi-step multi-body break up processes from the center of mass in the laboratory system the direct methods of multiple numerical integration on angles and energies were used in the cases where analytical expressions and codes developed by T. Beynon [8] were not available.

In the results of the least-squares fit of the neutron emission spectra for 4 incident neutron energies at 5.9, 10.1, 14.1 and 18.1 MeV the contribution of some channels, in particular those, the prior values for which were obtained by an expert evaluation, were changed substantially, and uncertainties of their contributions at these energies were reduced. The comparison of the prior and posterior evaluation obtained in such fit for spectra with incident neutron energy 5.9 MeV is shown in Table 3. Total correlation matrix of the uncertainties of the contribution of the channels contains the elements describing the correlation between different channels. Some correlation coefficients have negative sign, showing that the contribution of the channels, which are close on the form and contribute at the same energy range of the emission spectra are at strong competition. The correlation matrices for four incident energies are shown in Table 4.

Table 3. Variation of cross sections and uncertainties for different channels in the least-squares fit of the 5.9 MeV neutron emission spectrum under different angles.

Channel	Prior c.s.	Posterior c.s.
(n,n'1)		
(n, α 2)	25.1 (100.)	50.7 (49.)
(n,n'2)	271 (5.)	258 (4.6)
(n,n'(3+4))	58.8 (100.)	0
(n,n'5)	16.4 (100.)	18.4 (78.)
(n, α 1)	62.6 (50.)	45 (40.)
(n, ⁵ He ⁵ He)	31 (100.)	44.6 (60.)
(n,n'n'' ⁸ Be)	27 (100.)	31.2 (80.)
(n,n' α ⁵ He)	30 (100.)	57.8 (48.)

Table 4. Correlation coefficients (multiplied at 100) between uncertainties of contribution of different channels after least-squares fit of energy-angular distributions for 4 incident neutron energies.

$E_n=5.9$ MeV

	1	2	3	4	5	6	7	8	9	10
1 (n,n1')	100									
2 (n,n2')	-12	100								
3 (n,n3')	0	5	100							
4 (n,n4')	-16	1	-51	100						
5 (n,n5')	3	-4	0	1	100					
6 (n,a1)	2	-24	0	0	-28	100				
7 (n,a2)	-12	0	0	-4	-7	-18	100			
8 (n, ⁵ He ⁵ He)	-4	1	0	-1	-12	-30	-20	100		
9 (n,n'n'' ⁸ Be)	-25	-12	0	-9	-2	10	-14	-10	100	
10 (n,n' α ⁵ He)	-11	0	0	-3	-12	-14	-22	-26	-24	100

$E_n=10$ MeV

	1	2	3	4	5	6	7	8	9	10	11	12	13	14
1 (n,n1')	100													
2 (n,n2')	-6	100												
3 (n,n3')	3	3	100											
4 (n,n4')	0	0	0	100										
5 (n,n5')	-2	-5	7	6	100									
6 (n,n6')	1	1	0	0	0	100								
7 (n,n7')	-8	6	15	12	-2	12	100							
8 (n,n8')	-5	9	18	16	-1	16	-45	100						
9 (n,n9')	1	12	-13	-13	0	-1	16	2	100					
10 (n,a1)	0	-11	-2	-2	0	-3	0	5	-1	100				
11 (n,a2)	7	-18	-27	-24	2	-9	-19	-1	-20	-9	100			
12 (n, ⁵ He ⁵ He)	-2	-14	-7	-7	0	3	-11	-15	-4	-3	-25	100		
13 (n,n'n'' ⁸ Be)	0	0	0	0	0	-36	-26	-12	0	6	26	15	100	
14 (n,n' α ⁵ He)	-13	-24	-19	-24	-4	-18	-15	-15	-10	-5	-23	-18	-37	100

$E_n=14$ MeV

	1	2	3	4	5	6	7	8	9	10	11	12	13	14	15	16
1 (n,n1')	100															
2 (n,n2')	-6	100														
3 (n,n3')	0	0	100													
4 (n,n4')	0	-1	0	100												
5 (n,n5')	1	1	0	0	100											
6 (n,n6')	0	0	0	0	0	100										
7 (n,n7')	-10	-11	0	-1	1	1	100									
8 (n,n8')	3	8	0	0	-36	-36	-33	100								
9 (n,n9')	0	7	0	0	20	20	21	-18	100							
10(n,n10')	-2	-2	0	0	0	0	-4	1	0	100						
11(n,n11')	0	0	0	0	0	0	0	0	0	0	100					
12(n,a1)	-3	-10	0	0	0	0	-6	4	1	-1	0	100				
13(n,a2)	0	-10	0	0	2	2	3	0	-14	0	0	-3	100			
14(n,5He5He)	-10	-7	0	-1	10	9	-9	0	-3	-3	0	1	-67	100		
14(n,n'n'8Be)	-11	-25	0	-1	-10	-10	-34	5	-32	-4	0	13	43	-20	100	
16(n,n'a5He)	4	9	0	0	-13	-13	-6	0	19	1	0	-18	-46	7	-46	100

$E_n=18$ MeV

	1	2	3	4	5	6	7	8	9	10	11	12	13	14	15	16
1 (n,n1')	100															
2 (n,n2')	-7	100														
3 (n,n3')	-1	2	100													
4 (n,n4')	-3	-11	0	100												
5 (n,n5')	-1	-6	0	-1	100											
6 (n,n6')	0	3	0	0	0	100										
7 (n,n7')	-3	-25	0	-5	-3	-32	100									
8 (n,n8')	2	7	-3	1	0	-32	-31	100								
9(n,n9')	0	-3	-5	0	0	-7	12	0	100							
10(n,n10')	0	-6	-5	-1	0	-7	10	0	0	100						
11(n,n11')	0	-2	-5	0	0	-7	13	0	0	-30	100					
12(n,a1)	-1	-1	-35	0	0	0	0	0	0	-2	0	100				
13(n,a2)	0	-4	8	0	0	-22	12	0	0	-33	0	15	100			
14(n,5He5He)	0	0	9	0	0	-5	0	0	0	-9	0	15	-34	100		
15(n,n'n''8Be)	0	-1	15	0	0	-6	2	0	0	-45	0	53	64	18	100	
16(n,n'a5He)	-3	-25	-11	-5	-3	12	-15	3	-2	34	-1	-53	-68	-13	-89	100

A final evaluation of the contribution of different channels in the full energy range 2 - 20 MeV (see Table 5 and Fig. 15) was obtained by simple interpolation using the model dependence, where they are known. Based on Bayesian procedure, the evaluation includes all knowledge available to us about these reactions: experimental data on partial and total cross sections, spectroscopic information about the states, their widths, decay modes and branching coefficients, results obtained from model calculations. It gives prediction of the cross sections in the channels, which were not directly observable, like channels with 3-body break-ups.

Table 5. Final evaluation of the contribution of different channels in the neutron emission cross section. Neutron energies where adjustment to the emission spectra was done are marked.

E_n , MeV	n,n ₁	n,n ₂	n,n ₃	n,n ₄	n,n ₅	n,n ₆	n,n ₇	n,n ₈	n,n ₉	n,n ₁₀	n,n ₁₁	n,a ₁	n,a ₂	n, ⁵ He ⁵ He	n,n'n'' ⁸ Be	n,na ⁵ He	n,2n
2	0	0	0	0	0	0	0	0	0	0	0	0	0	0	2.27	0	2.27
2.2	0	0	0	0	0	0	0	0	0	0	0	0	0	0	8.46	0	8.46
2.4	0	0	0	0	0	0	0	0	0	0	0	0	0	0	17.62	0	17.62
2.6	0	0	0	0	0	0	0	0	0	0	0	0	0	0	27.54	0	27.54
2.7	5.06	0	0	0	0	0	0	0	0	0	0	0	0	0	31.5	0	36.56
2.8	48	114.06	0	0	0	0	0	0	0	0	0	0	0	0	34	0	196.06
3	82.6	219.31	0	0	0	0	0	0	0	0	0	3.5	0	0	35.2	1	341.61
3.2	72	292.82	5	0	0	0	0	0	0	0	0	17	0	0	34	3.3	424.12

3.4	62	304.63	10.5	0	0	0	0	0	0	0	0	0	51	0	0	33	8.8	469.93
3.6	54	270.16	14.5	32	0	0	0	0	0	0	0	0	66	0	0	32.5	17	486.16
3.8	49.5	272.09	18	40	0	0	0	0	0	0	0	0	66	0	2	32	25	504.59
4	46.7	260.74	20.3	42.3	0	0	0	0	0	0	0	0	61.5	0	8.6	32	33.2	505.34
4.5	43	256.13	18.5	38	0	0	0	0	0	0	0	0	56	0	27	32.25	44	514.88
5	40.3	286.78	14.6	30.2	0	0	0	0	0	0	0	0	52.1	4.7	35.9	32.5	48.2	545.28
5.5	35.9	304.57	12	24	6.5	0	0	0	0	0	0	0	51.6	31	40.5	32.8	56	594.87
6	31.5	300.01	9.4	19	7.61	0	0	0	0	0	0	0	51.1	54.5	42.7	33	61.2	610.02
6.5	27.8	283.42	8.1	16.2	7.73	2	0	0	0	0	0	0	46.8	71	41.5	32.7	63	600.25
7	24.1	268.85	6.78	13.3	7.84	7.83	0	0	0	0	0	0	42.4	71.7	40.5	32.3	65.7	581.3
7.5	20.1	309.26	6.71	12.7	7.96	8.33	2	0	0	0	0	0	40.4	67	39	32.8	70.2	616.46
8	16	250.1	6.64	11.9	8.07	8.83	16.2	6.7	0	0	0	0	38.4	63.7	38	33.3	74.7	572.6
8.5	14.5	236.94	6.11	11.2	7.91	8.83	28	8	0	0	0	0	35.7	61	37.3	32.7	76.4	564.59
9	13	214.96	5.58	10.5	7.75	8.82	38.3	8.68	1.44	0	0	0	32.9	60	36.7	32	78	548.63
9.5	12.3	216.14	4.91	9.5	7.29	8.49	45	8.26	2.8	0	0	0	32.1	59	34.8	33.3	81.1	554.99
10	11.6	197.72	4.24	8.4	6.82	8.16	49.5	8.51	3.55	0	0	0	31.2	58.2	33	34.6	84.1	539.6
10.5	10.8	214.46	3.94	8.03	6.75	8.29	52.1	8.87	3.55	0	0	0	28.6	57	32	36	88.1	558.49
11	9.9	224.79	3.64	7.66	6.68	8.42	54.7	9.23	3.55	0	0	0	26	54.1	31	37.4	92	569.07
11.5	9.04	181.58	3.33	7.07	6.34	8.16	55.5	9.27	3.51	0	0	0	24.3	50	30.5	37.2	95	520.8
12	8.17	197.22	3.01	6.48	5.99	7.9	56.3	9.3	3.47	0	0	0	22.5	45	30	37	98	530.34
12.5	7.76	181.73	2.85	6.18	5.83	7.87	56.7	9.38	3.57	0	0	0	20.8	41	30	37.7	101.5	512.87
13	7.35	178.89	2.69	5.88	5.67	7.84	57.1	9.45	3.66	3.29	0	0	19	38	30	38.4	105	512.22
13.5	6.53	163.46	2.36	5.22	5.08	7.04	56.5	8.94	3.51	6	2	0	17.7	33	30.5	39.3	113.4	500.54
14	5.71	147.21	2.02	4.55	4.48	6.24	55.9	8.42	3.36	7.26	2.34	0	16.3	30.9	31.5	40.1	121.8	488.09
14.5	4.87	130.17	1.63	3.88	3.83	5.35	50.55	7.48	3.01	7.53	2.2	0	14.2	25.7	29	37.6	115.4	442.4
15	4.88	136.1	1.54	3.88	3.88	5.42	54.2	7.87	3.19	8.7	2.45	0	14.7	27.1	31.6	41.7	129.6	476.81
16	4.14	123.21	1.5	3.48	2.74	4.77	51.8	7.6	3	10	2.36	0	11.9	21.7	31	39.3	135.5	454
17	3.27	106.21	1.25	2.93	2.25	4.11	45.9	7.04	2.64	10.2	2.14	0	9.48	17.1	27.5	34.6	132.8	409.42
18	2.83	103.8	1.15	2.65	2.06	3.79	45.4	6.79	2.56	11.01	2.14	0	8.64	15.4	24	34.9	146.2	413.32
19	2.3	96.49	0.97	2.29	1.76	3.33	42.3	6.25	2.31	10.9	2.14	0	7.35	13.8	18.4	33.2	147	390.79
20	1.85	92.4	0.82	2.03	1.55	2.94	39.8	5.94	2.31	11	2.24	0	6.27	13.4	13.4	32.7	151.5	380.15

$^9\text{Be} + n$, final adjusted channel cross sections

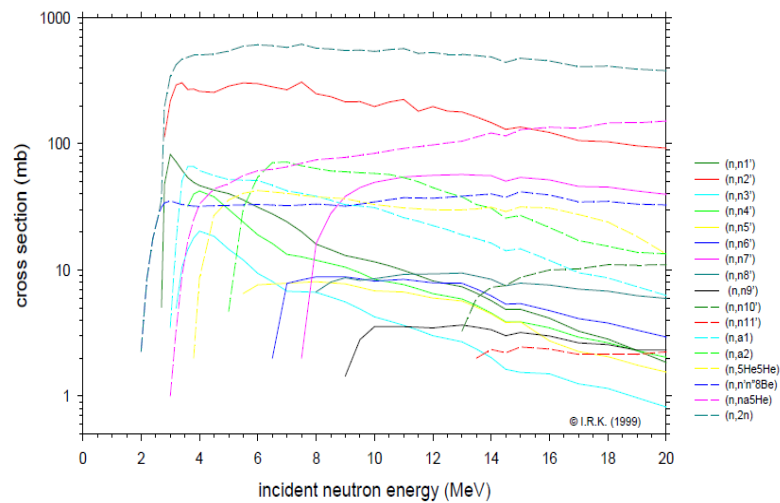


Fig. 15 Results of the evaluation of the cross sections for $^9\text{Be}+n$ reactions in Bayesian approach.

Results of evaluation of the energy-angular distributions for some reaction channels are shown in figures 16 to 18 and total secondary neutron energy-angular distribution in the figure 19.

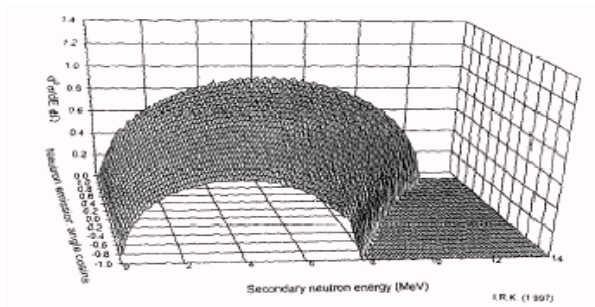


Fig. 16. Energy-angular distributions for the reaction channel ${}^9\text{Be}(n,n'{}^8\text{Be})$ for 14 MeV neutron incident energy.

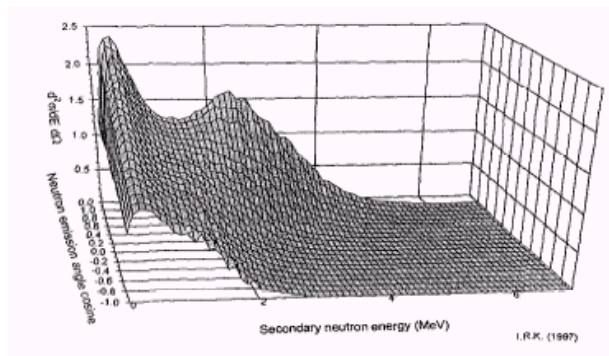


Fig. 17. Energy-angular distributions for the reaction channel ${}^9\text{Be}(n,(n'\alpha')(n''\alpha''))$ for 14 MeV neutron incident energy.

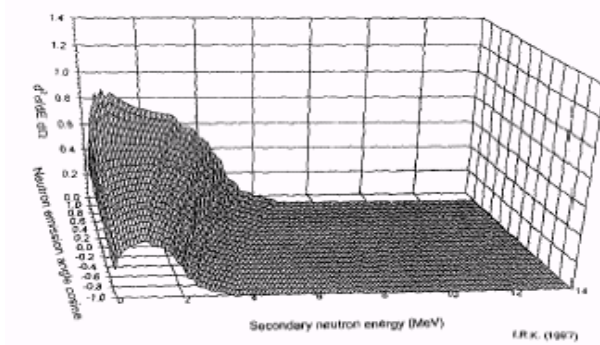


Fig. 18. Energy-angular distributions for the reaction channel ${}^9\text{Be}(n,n_1'(\alpha_0'(n''\alpha''))$ for 14 MeV neutron incident energy.

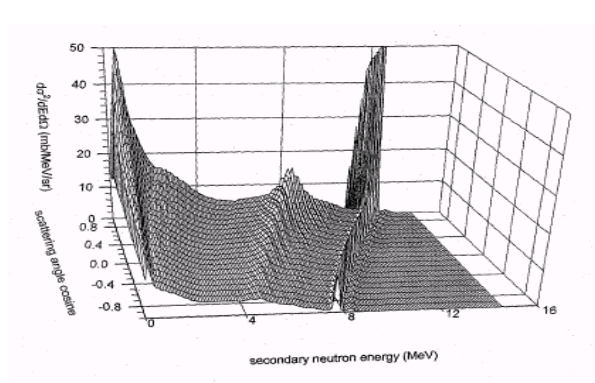


Fig. 19. Evaluated energy-angular distributions for secondary neutrons emitted in ${}^9\text{Be}+n$ reaction.

Comparison of the experimental and evaluated spectra of the neutrons emission under different angles for 14 MeV incident neutrons at ${}^9\text{Be}$ are shown in Fig. 20.

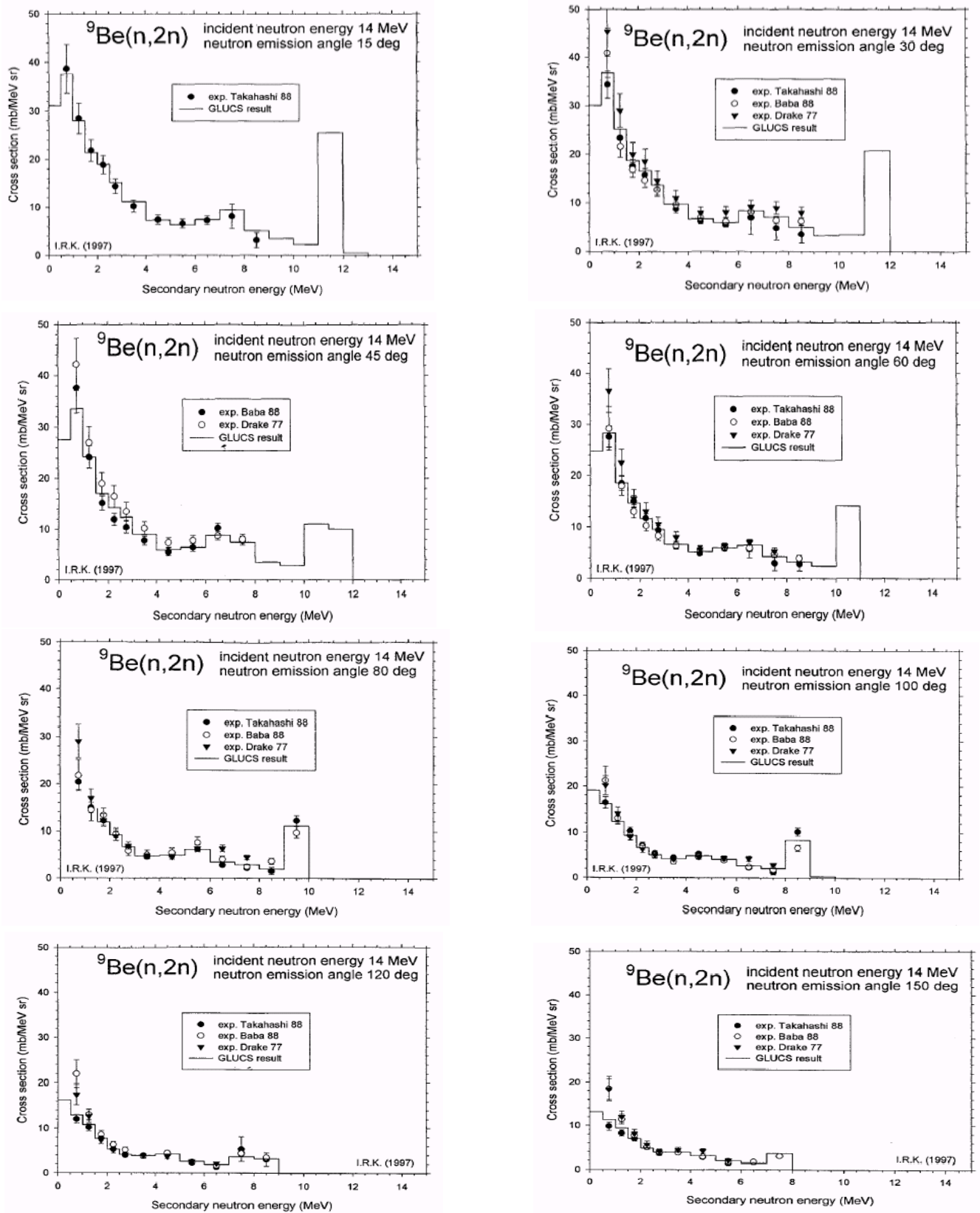


Fig. 20. Comparison of the experimental and evaluated spectra of the neutrons emission under 8 angles in the laboratory system for 14 MeV incident neutrons at ${}^9\text{Be}$.

Experimental data on the emission of the alpha-particles were not used in the evaluation because of their small number and low accuracy. But they can be used for checking and justification of the evaluation and used methods. The comparison of the experimental data on the emission of the alpha-particles with the results of the evaluation is shown in Fig. 21. The contributions of most important channels are shown separately. Generally, a good consistency is observed for exclusion of the part of the spectra below 3 MeV, where Coulomb interaction in the break-up at two charged products in the center of mass system may play some role, which is not properly accounted in free kinematics break-ups.

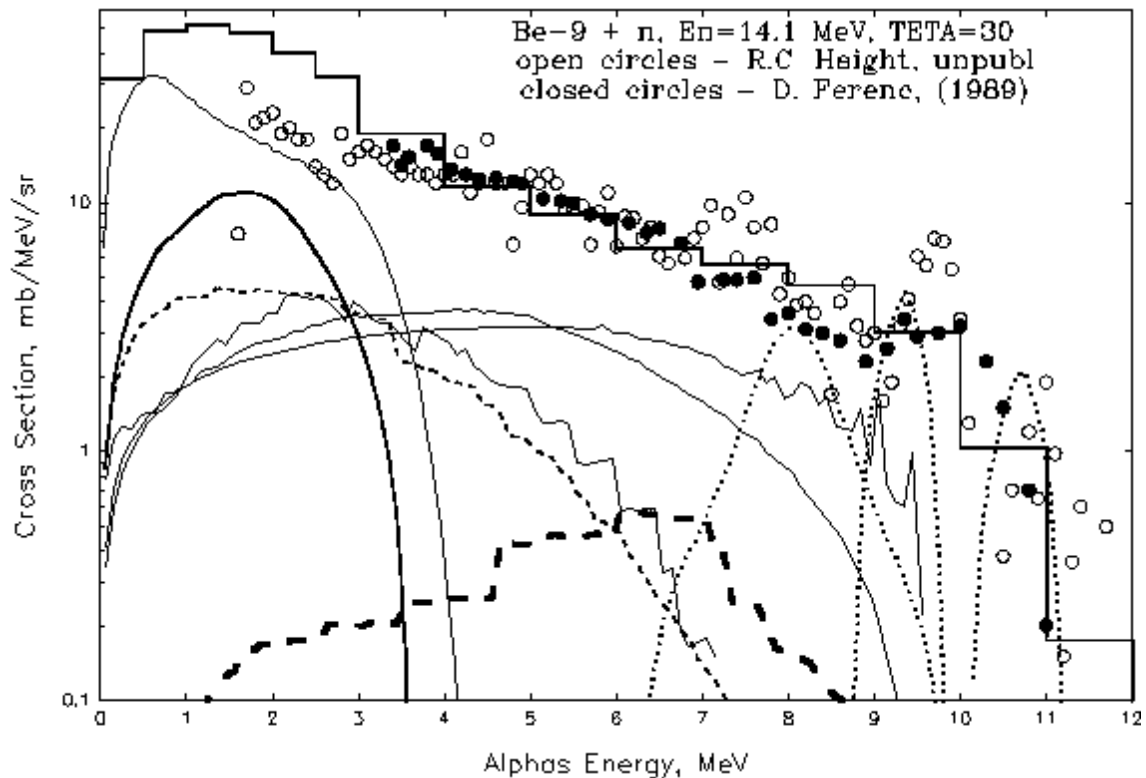


Fig. 21. Comparison of the experimental data on emission of alpha-particles under 30 degrees in the laboratory system for reaction ${}^9\text{Be}(n,x)\alpha$ induced by 14-MeV neutrons. Experimental data by Ferenc for 14.6 MeV incident neutrons (closed circles, D. Ferenc et al., Nucl. Sci. Eng. **101**, 1 (1989)) and by Haight for 15 MeV neutrons (open circles, R.C. Haight, unpublished (1993)). Legend: dotted lines – (n,α_0) , (n,α_1) , (n,α_2) ; two thin lines covering practically all spectrum – $(n,n\alpha^5\text{He})$ and $(n,n'a'(n''\alpha''))$; thin dashed line (below 7.3 MeV) – $(n,n'7(\alpha_0'(n'a'')))$; thin line (below 4.2 MeV) – $(n,n'2(n''\alpha'\alpha''))$; thin broken line – $(n,n'n''(\alpha'\alpha''))$; thick dashed line – $(n,n'7(n'_1(\alpha'\alpha'')))$; thick line – $(n,n'10(a_0'(n'a'')))$; histogram – full spectrum of the alpha-particles emission.

GMA code and simultaneous (combined) evaluation of neutron cross section standards, actinides cross sections and prompt fission neutron spectra

GMA as a system of the codes for data preparation and the generalized least-squares fit was written by Wolfgang Poenitz in 80-th and widely used by the international community for the combined evaluation of the standards of neutron cross sections. The complex consists from 2 major codes DAT and GMA. DAT code prepares the input of the experimental data for the following their general least-squares fit with GMA code. Preparation of the experimental data includes the data reduction (values and their uncertainties) to the chosen nodes on the neutron energy, which will be used for all data included in the evaluation. A prior evaluation of the data is used for the extrapolation (reduction) of the data to the nodes. This prior evaluation can be replaced by the posterior evaluation after obtaining it in the least-squares fit, and experimental

data can be reduced to the nodes using this new evaluation and procedure of least-squares fit can be repeated once more. It is normal iteration procedure which often because we do not know true values or we are not satisfied by some approximation to them before the evaluation. All components of the uncertainties in the nodes and their correlative properties are assigned separately.

The code allows account the following types of the data at their simultaneous (combined) fit:

absolute cross section measurements (measurements of total cross sections by transmission method, measurements with the associated particles method, measurements relative «absolute standard» - $^1\text{H}(n,p)$ cross section)

sum of absolute cross sections and combinations which include ratio of absolute cross section to the sum of other absolute cross sections

measurements of the shape of the cross sections (non-normalized cross sections)

ratio of absolute cross sections (absolute ratios)

ratios of the shapes of the cross sections (non-normalized ratios, shape of the ratios)

integrals on given spectrum (spectrum averaged cross sections, in particular — prompt fission neutron spectrum of $^{252}\text{Cf}(sf)$, which is standard).

The latest description of the code and standard database prepared by Poenitz is published in [9].

Code allows introducing the components of the uncertainties of different types: SERC – statistical, LERC – correlated in the whole energy range of data, such as uncertainty of the mass of the samples, MERC – medium-energy range correlated with different correlation lengths, such as uncertainties in the determination of the efficiency of the detector, uncertainties of some corrections. Beside the correlations between uncertainties of data in different energy points of the same data set, there is an opportunity to introduce correlations between uncertainties of the different data sets, e.g., if the same samples, detectors, etc., were used in different measurements, - very common case for measurements done by the same group of experimenters.

As example of the input of the correlated data sets for the preparatory code DAT, the table is shown at the next page. Three correlated data sets (№ 358, 359 и 360) are combined in the data block: absolute measurements of the $^{197}\text{Au}(n,\gamma)$ cross section at the 30 keV point, absolute measurements of the capture cross section of $^{197}\text{Au}(n,\gamma)$ in 30 keV and 60 keV points and measurements of the cross section shape in the energy range from 24.7 to 347 keV. The following correlations exist between the uncertainties of the data in the data sets 359 и 358: 100% in the correction at neutron self-shielding and scattering in the samples, 100 % in the correction at neutron attenuation and scattering at the target. Between uncertainties of the data in the data set 360 and data sets 358 and 359, there are 100 % correlations in the uncertainty of the correction at neutron self-shielding and scattering in the samples. Structure of the input data for the module DAT is given in [9].

Last simultaneous (combined) evaluation of the neutron cross section standards have included more than 400 data sets for reaction cross sections $^6\text{Li}(n,t)$, $^{10}\text{B}(n,\alpha_0)$, $^{10}\text{B}(n,\alpha_1)$, $^{10}\text{B}(n,\alpha)$, $^{197}\text{Au}(n,\gamma)$, $^{238}\text{U}(n,g)$, $^{235}\text{U}(n,f)$, $^{238}\text{U}(n,f)$ и $^{239}\text{Pu}(n,f)$ [10, 11]. 26 pre-evaluated thermal constants (thermal scattering, fission and capture cross sections, Westcott g-factors and average total fission neutron yields for ^{233}U , ^{235}U , ^{239}Pu и ^{241}Pu , as well as average total fission neutron yield in spontaneous fission of ^{252}Cf).

Evaluation of neutron cross section standards at light nuclei was done in the frameworks of R-matrix approach and has been included in the combined simultaneous evaluation of all standards as pseudo-experimental data sets. Energy range was different for different reactions in accordance with the recommendations where they can be used as the standards, but usually they cover wider energy range than range where they are used as standards. In general, the interval with account of all standards, covers the energy range from thermal point (0.0253 eV) to 200 MeV.

Main work on data preparation for the evaluation was concluded in the reduction of the data to the form of presenting primarily-measured quantities. For example, if fission cross section of ^{239}Pu was measured relative ^{235}U , but finally given by the authors in the form of absolute fission cross section of ^{239}Pu , then in the standards evaluation, data have been introduced as absolute ratio of ^{239}Pu to ^{235}U if it was possible to determine which ^{235}U standards was used by the authors in the normalization.

Analysis of the components of the uncertainties assigned by the authors, evaluation of the uncertainties due to possible non-accounted corrections, estimation of the correlation properties of different components of the uncertainties, as well as possible correlations between uncertainties in different measurements, is an important part of the evaluation process. At the last step of the evaluation, the search of discrepant data (outliers), which do not allow to reach consistent fit of data with χ^2 per degree of freedom of the order 1 is extremely important. These data require the further improvement in their presentation, namely the search of the reasons of their discrepancies and often the adding of additional component of the uncertainties (usually MERC type) which makes these data consistent with true value (or the other data at the first step of iteration process of the evaluation).

The size of the vector of the evaluated data in the evaluation of the standards was equal to 949, with the covariance matrix of the uncertainty with the dimension 949*949 for 33 different cross sections and thermal constants. Because the blocks describing correlations between uncertainties of different cross section and constants contain in some cases extremely low correlation coefficients, then they can be excluded from the total covariance matrix; this reduces substantially the volume of the information, which is needed to store in the files of the evaluated data.

Results of the combined evaluation of the standards are shown in the figures 22 to 37 in comparison with the experimental data and the results of previous evaluations. The data set numbers for experimental data given in the legends for the figures can be converted in the references using table from publication [9]. Data by shape type are marked in the legends to the figures. Because the data are reduced to the primarily-measured form, they are (in many cases) inconsistent with data which can be retrieved from EXFOR library. A prior data shown in the figures are the results of the previous evaluation of the standards (e.g. standards in ENDF/B-VI library). The graphical view of the covariance matrices of the uncertainties for evaluated standards are shown in figures 38 to 41 two-dimensional color presentation used in NJOY code and in one of the three-dimensional color presentation developed by Victor Zerkin for ZVView code.

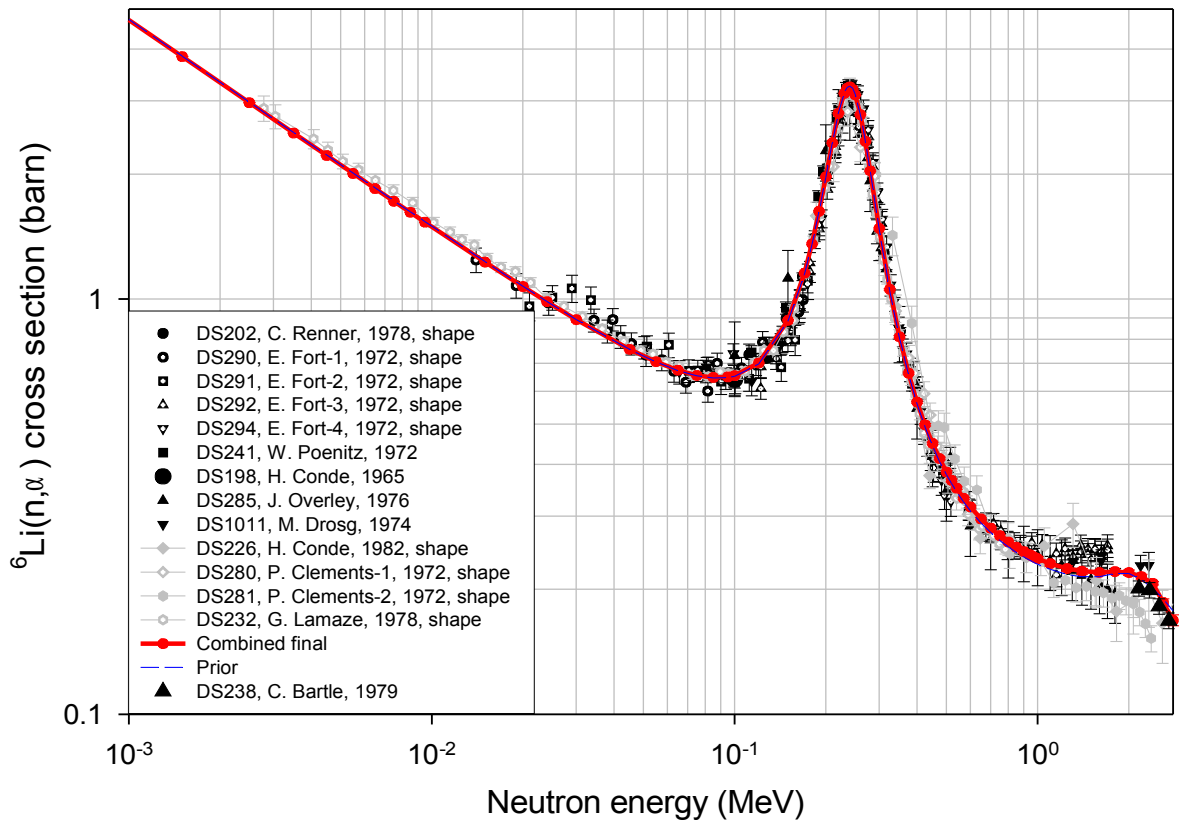


Fig. 22. Cross section of the ${}^6\text{Li}(n,t)\alpha$ reaction.

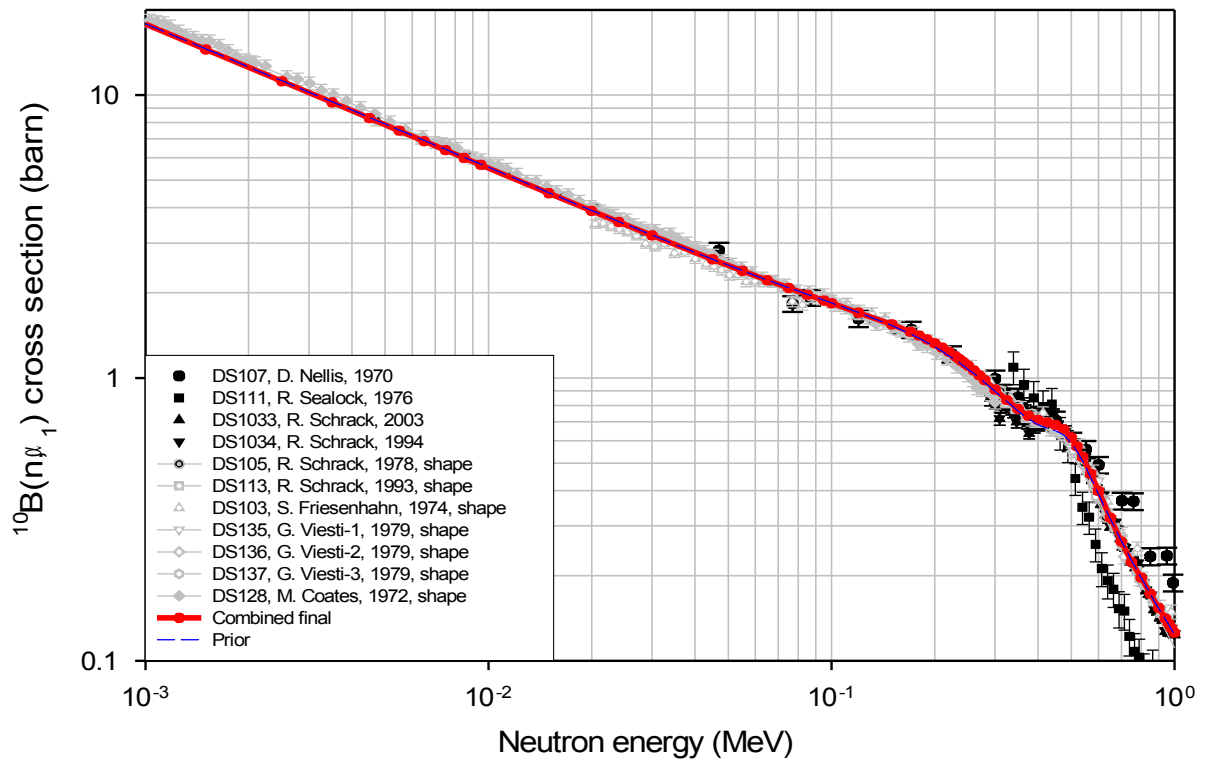


Fig. 23. Cross section of ${}^{10}\text{B}(n,\alpha_1)$ reaction.

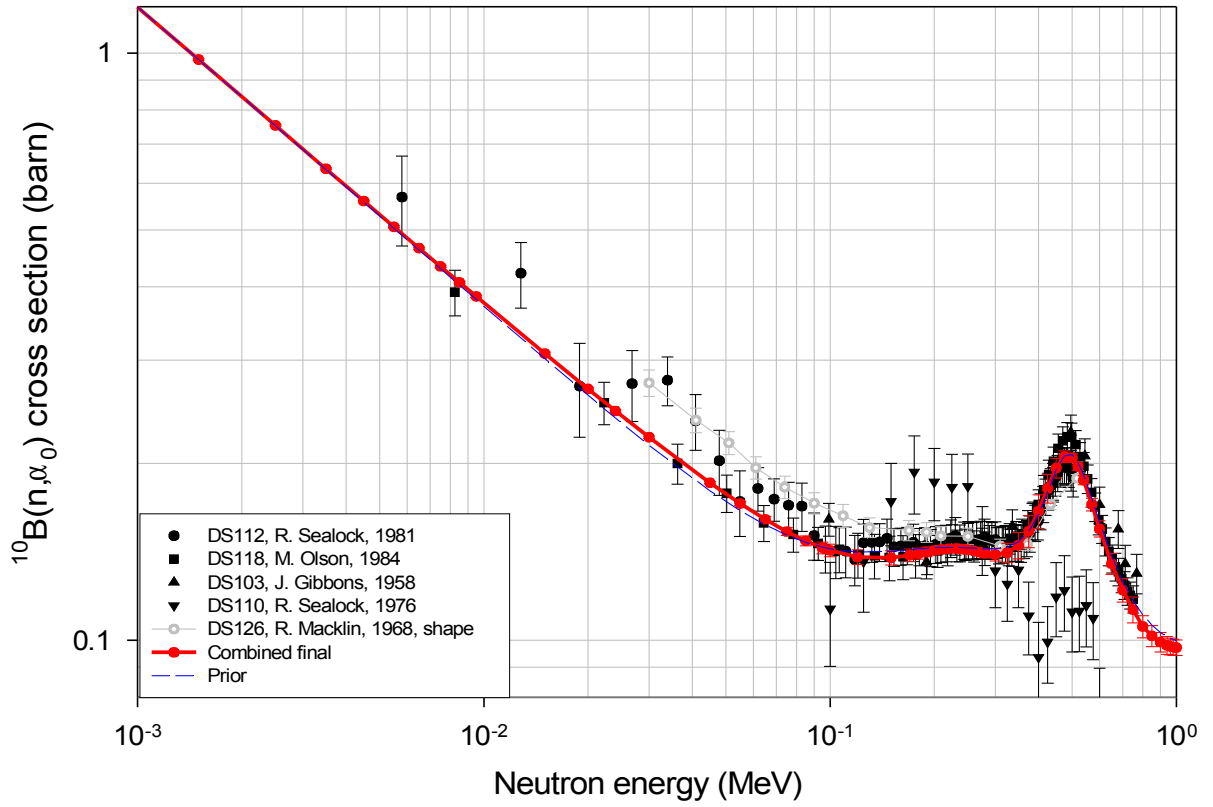


Fig. 24. Cross section of $^{10}\text{B}(n,\alpha_0)$ reaction.

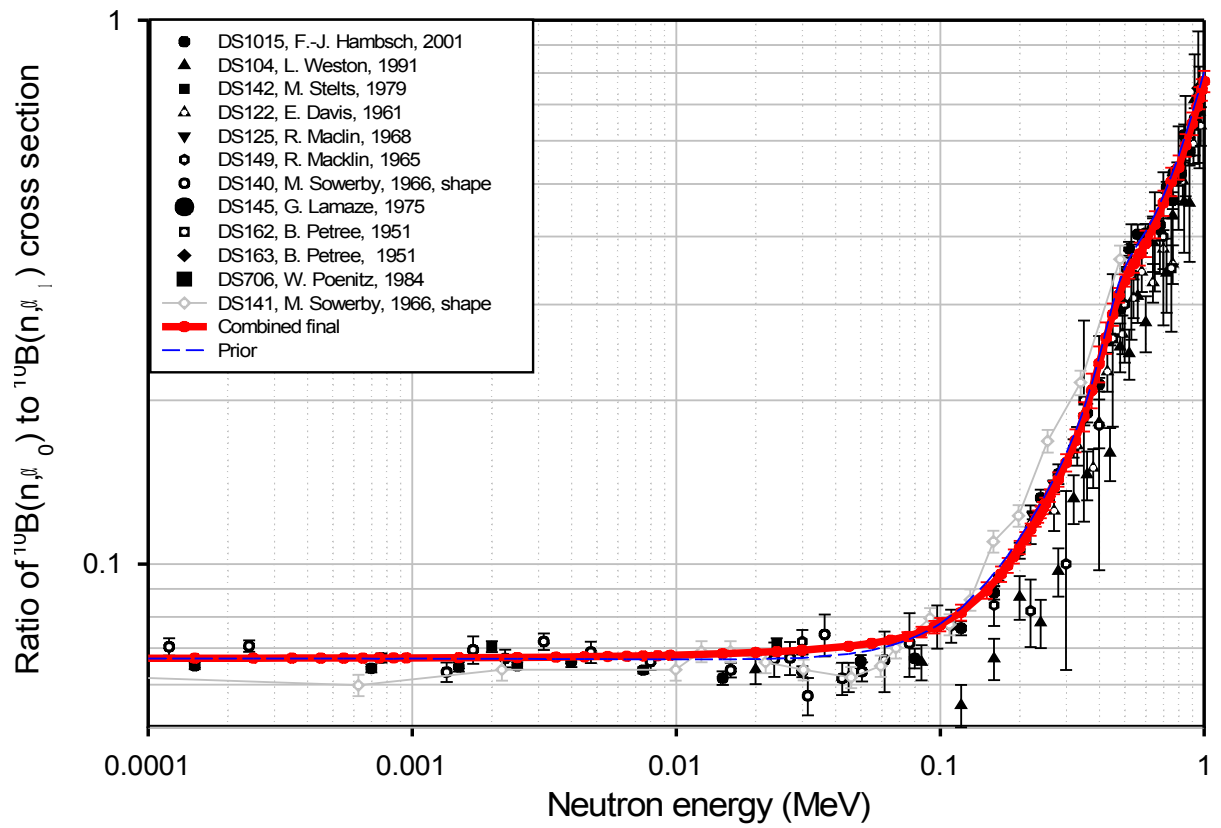


Fig. 25. Ratio of the cross sections of $^{10}\text{B}(n,\alpha_0)$ to $^{10}\text{B}(n,\alpha_1)$ reaction.

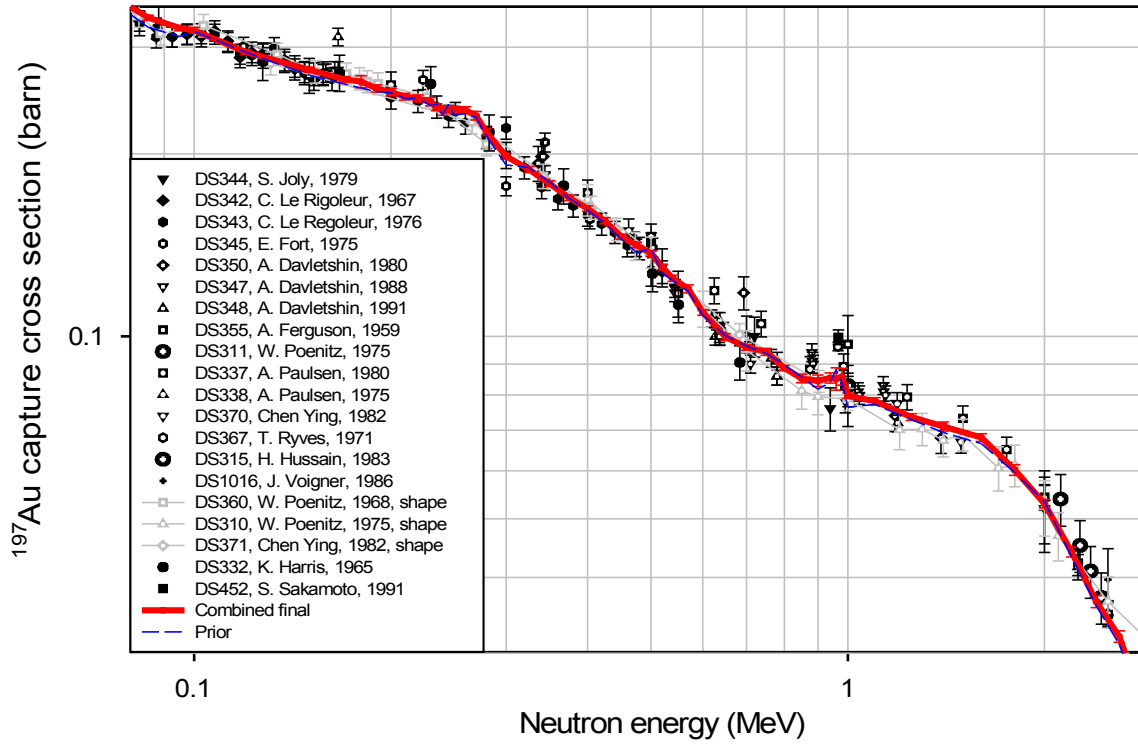


Fig. 26. Cross section of the $^{197}\text{Au}(n,\gamma)$ reaction.

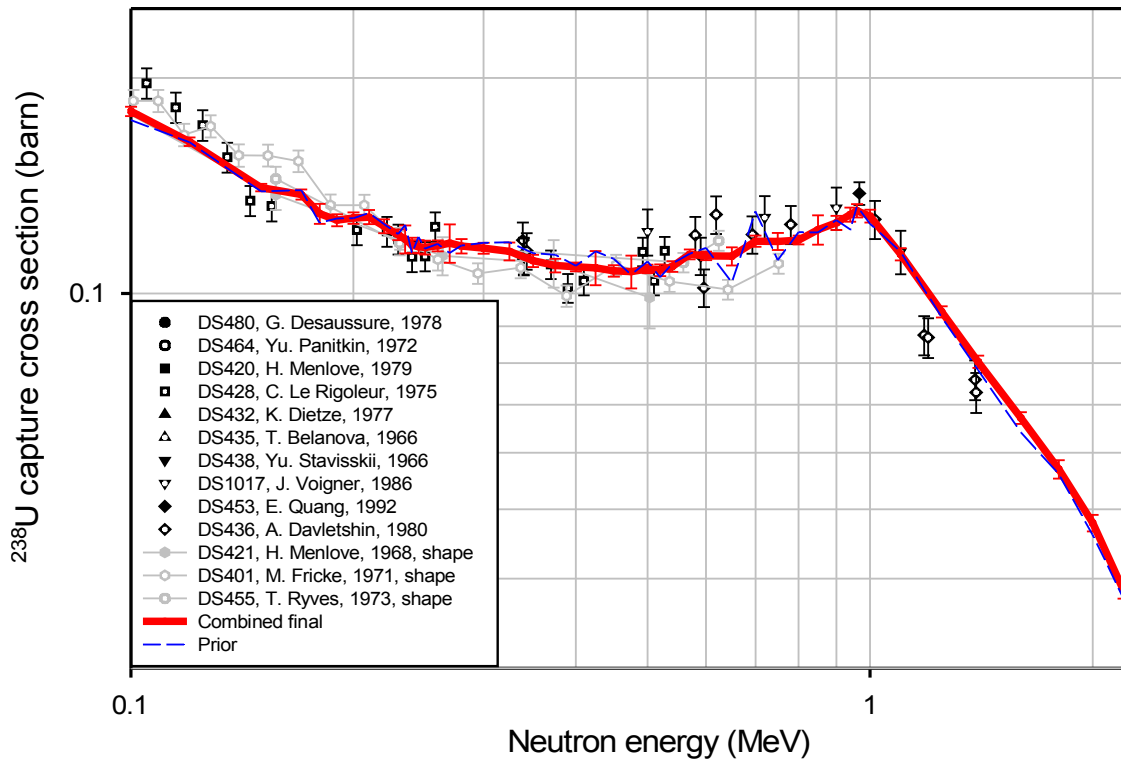


Fig. 27. Cross section of $^{238}\text{U}(n,\gamma)$ reaction.

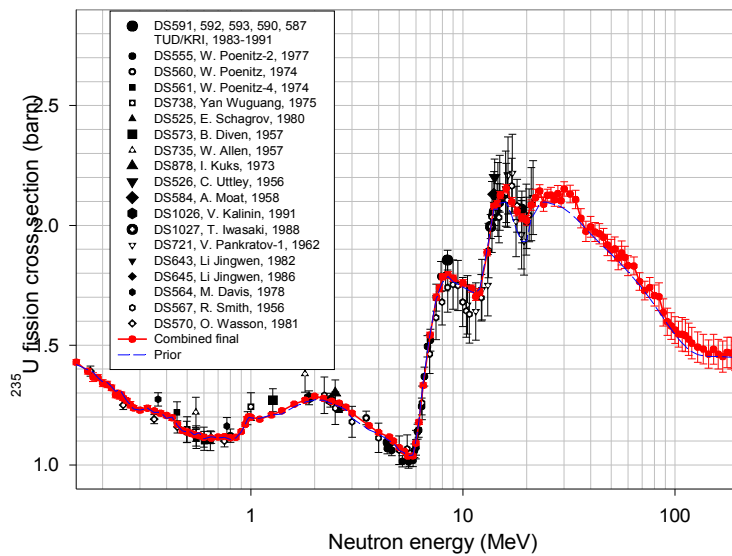
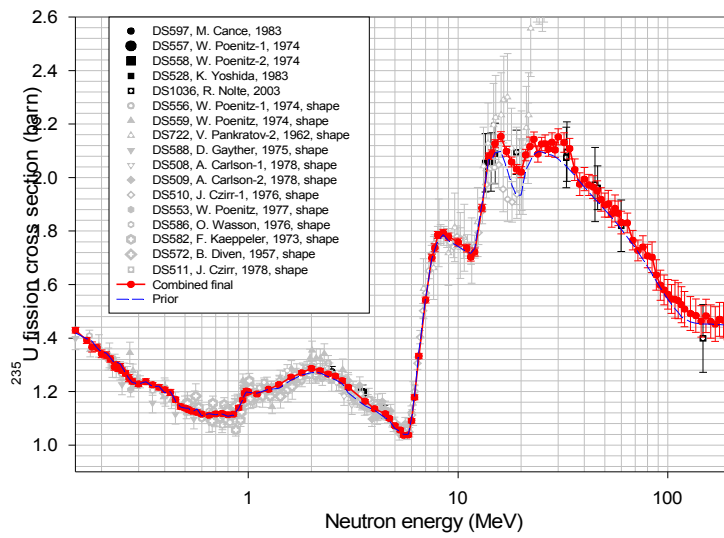
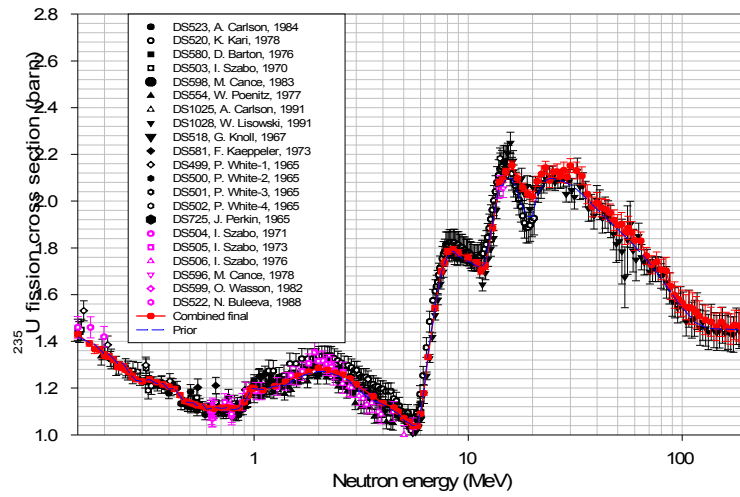


Fig. 28. Cross section of the $^{235}\text{U}(n,f)$ reaction with a largest number of experimental data available.

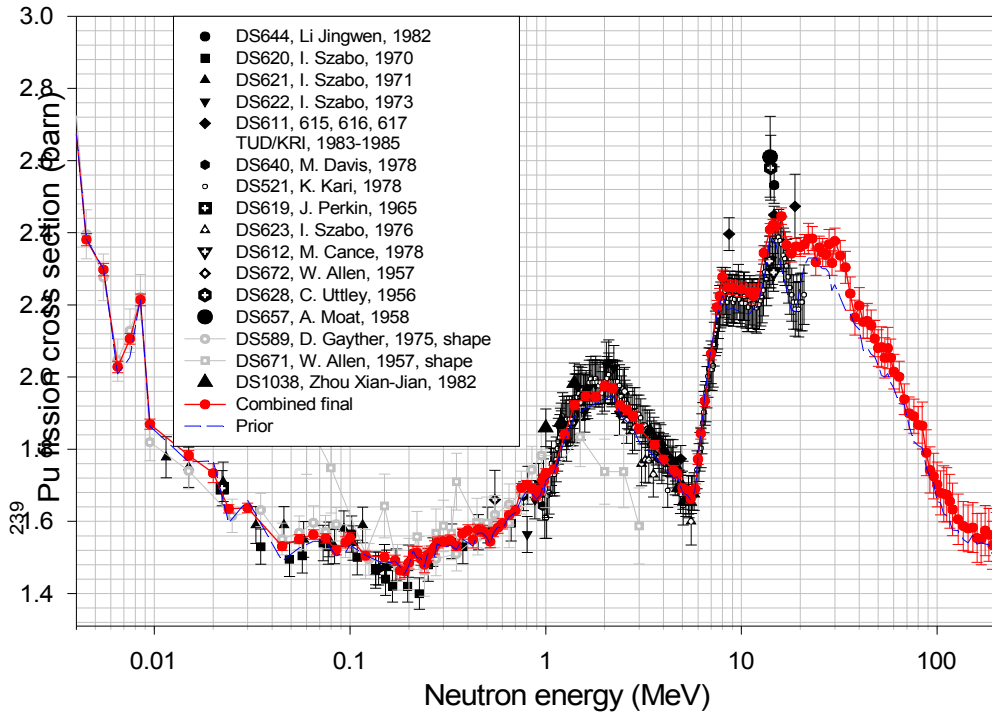


Fig. 29. Cross section of $^{239}\text{Pu}(n,f)$ reaction.

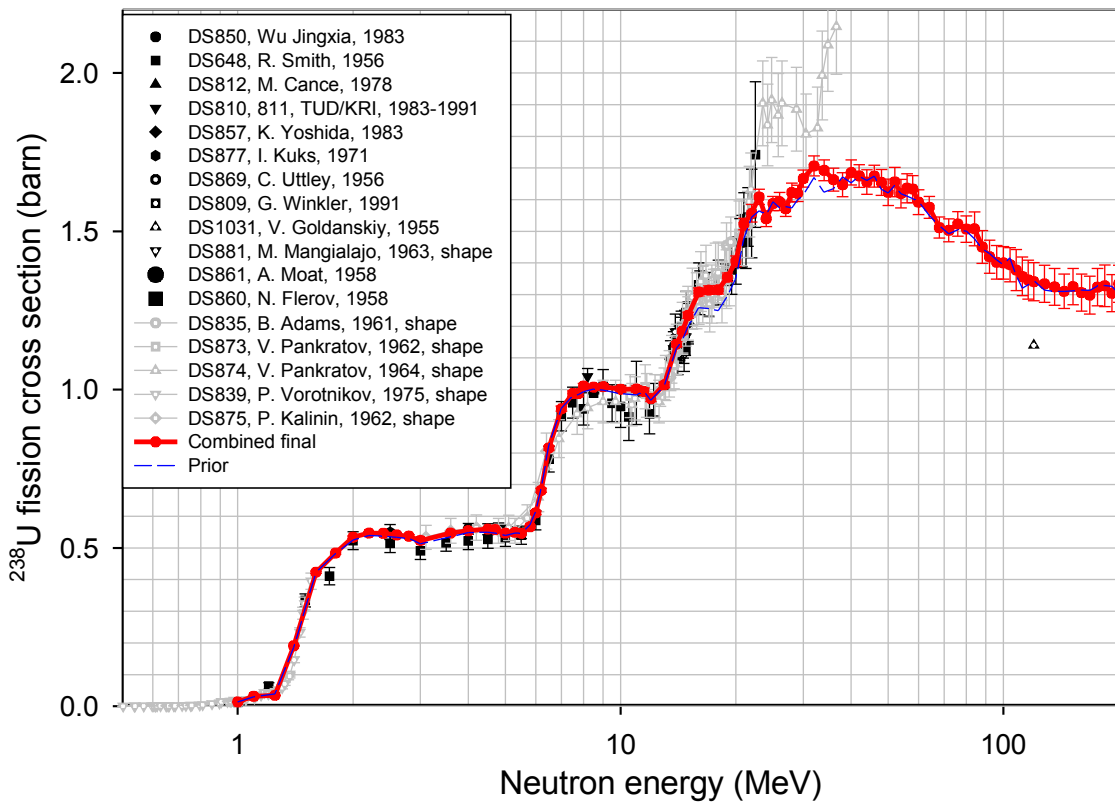


Fig. 30. Cross section of the $^{238}\text{U}(n,f)$ reaction.

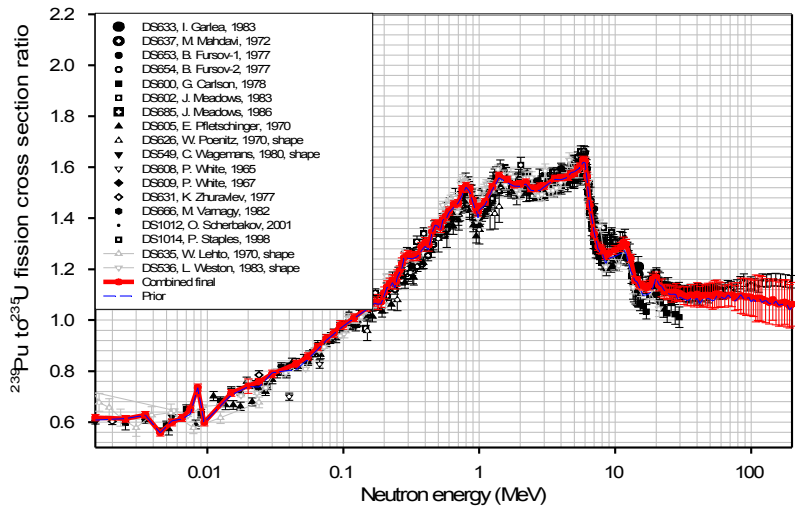


Fig. 31. Ratio of the cross sections of $^{239}\text{Pu}(n,f)$ to $^{235}\text{U}(n,f)$ reaction.

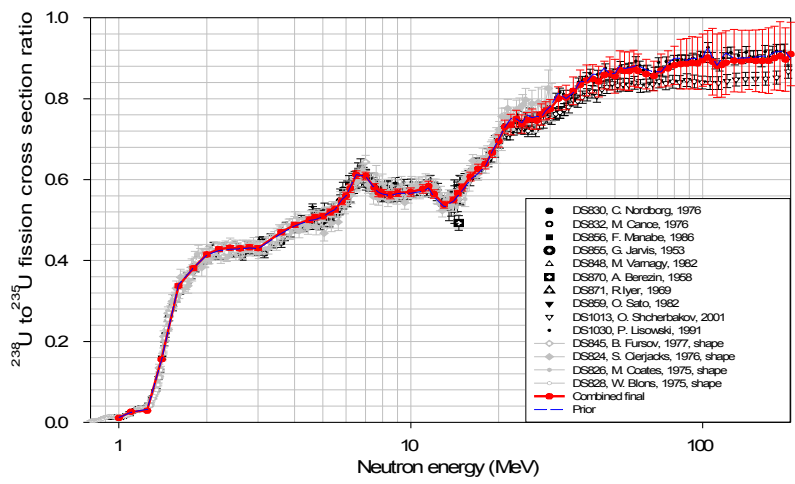


Fig. 32. Ratio of the cross sections of $^{238}\text{U}(n,f)$ to $^{235}\text{U}(n,f)$ reaction.

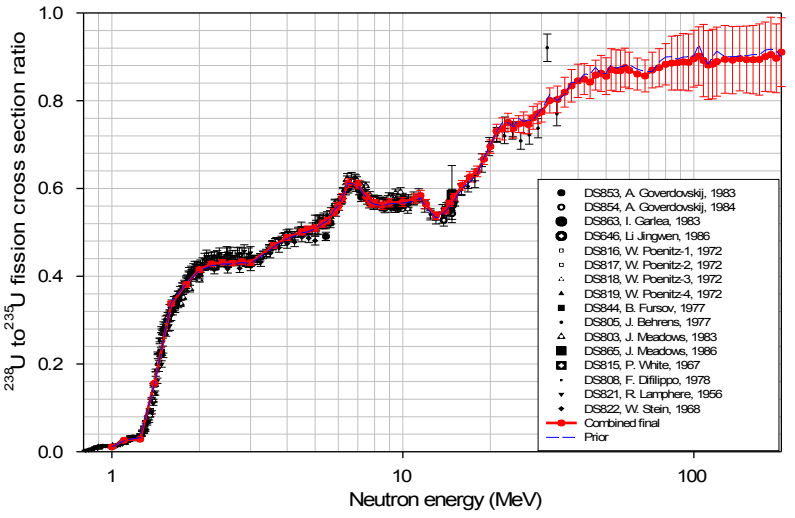


Fig. 33. Ratio of the cross sections of $^{238}\text{U}(n,f)$ to $^{235}\text{U}(n,f)$ reaction.

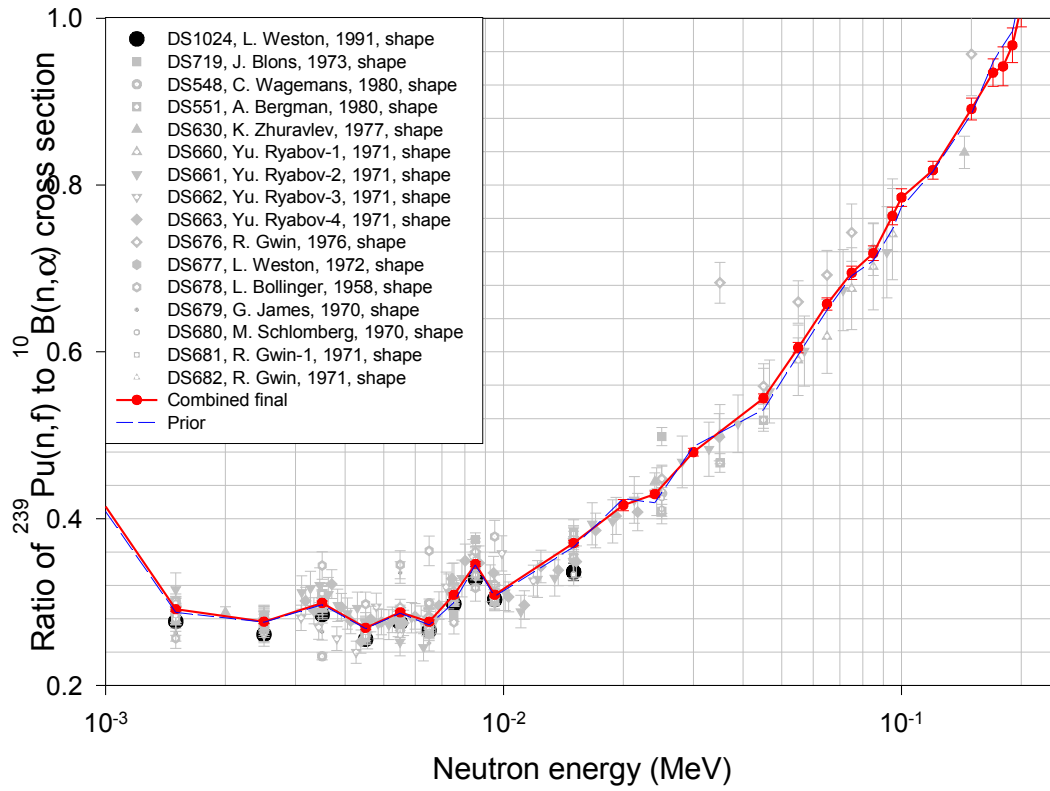


Fig. 34. Ratio of the cross sections of $^{239}\text{Pu}(n,f)$ to $^{10}\text{B}(n,\alpha)$ reactions.

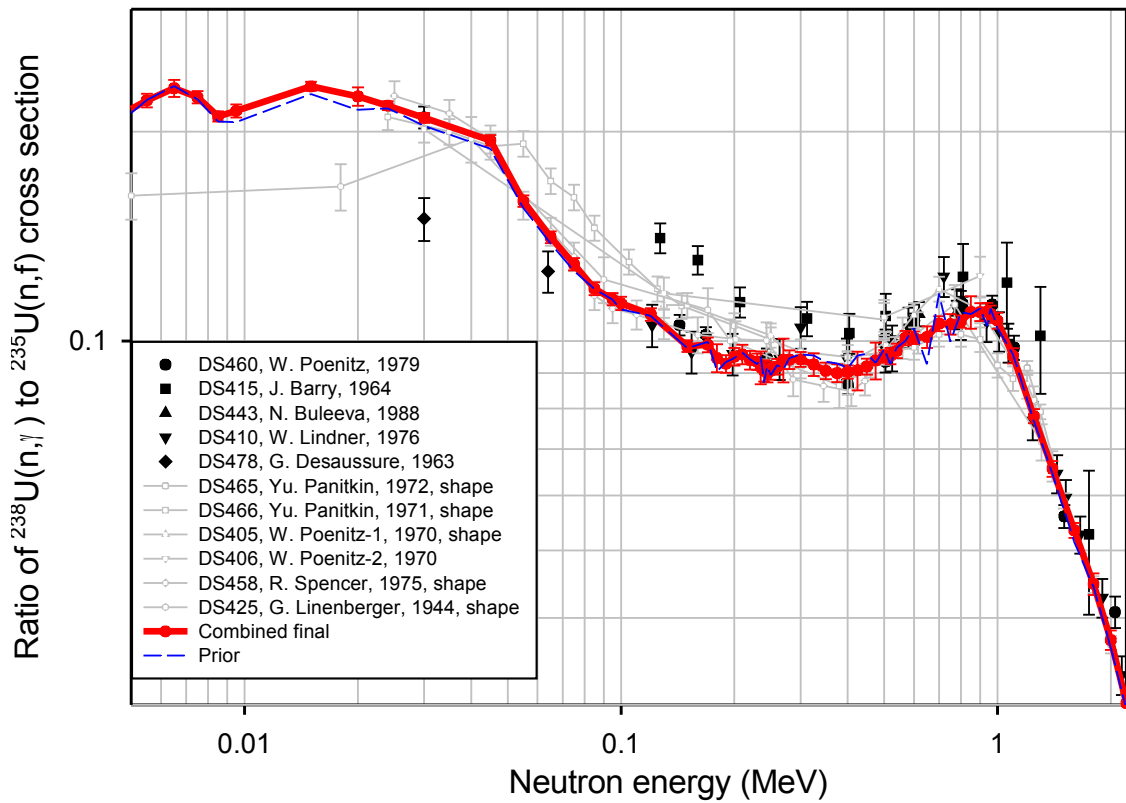


Fig. 35. Ratio of the cross sections of $^{238}\text{U}(n,\gamma)$ to $^{235}\text{U}(n,f)$ reaction.

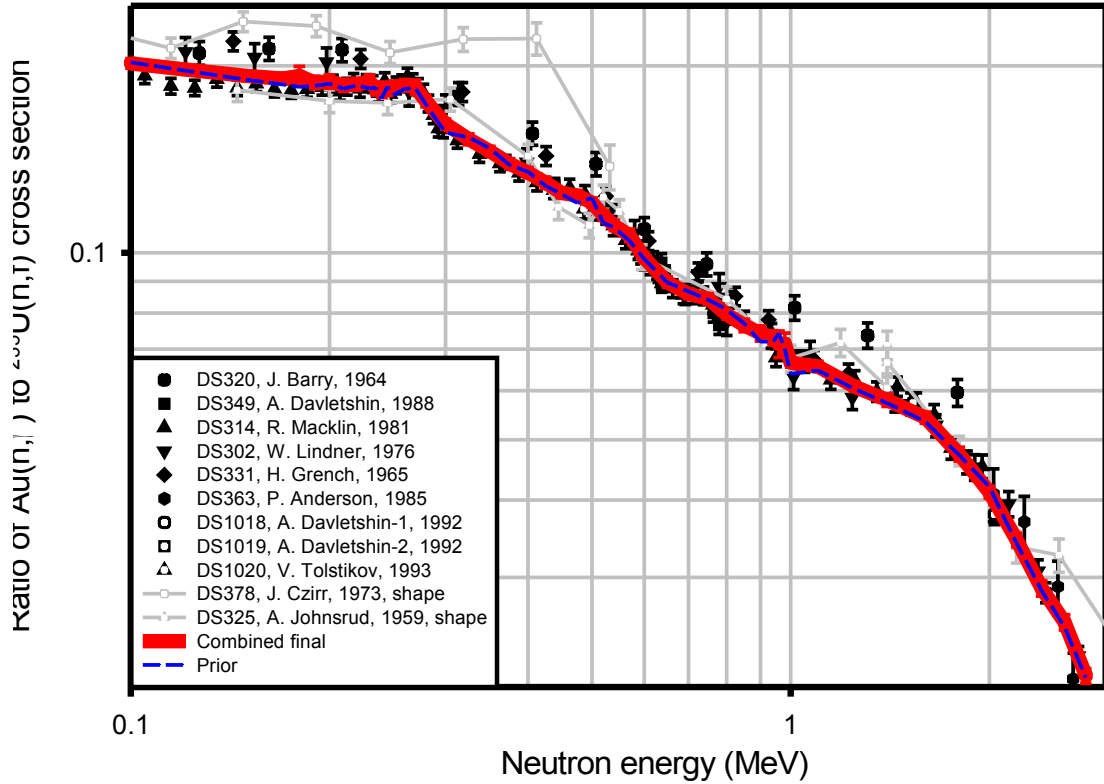


Fig. 36. Ratio of the cross sections of $^{197}Au(n,\gamma)$ to $^{235}U(n,f)$ reaction.

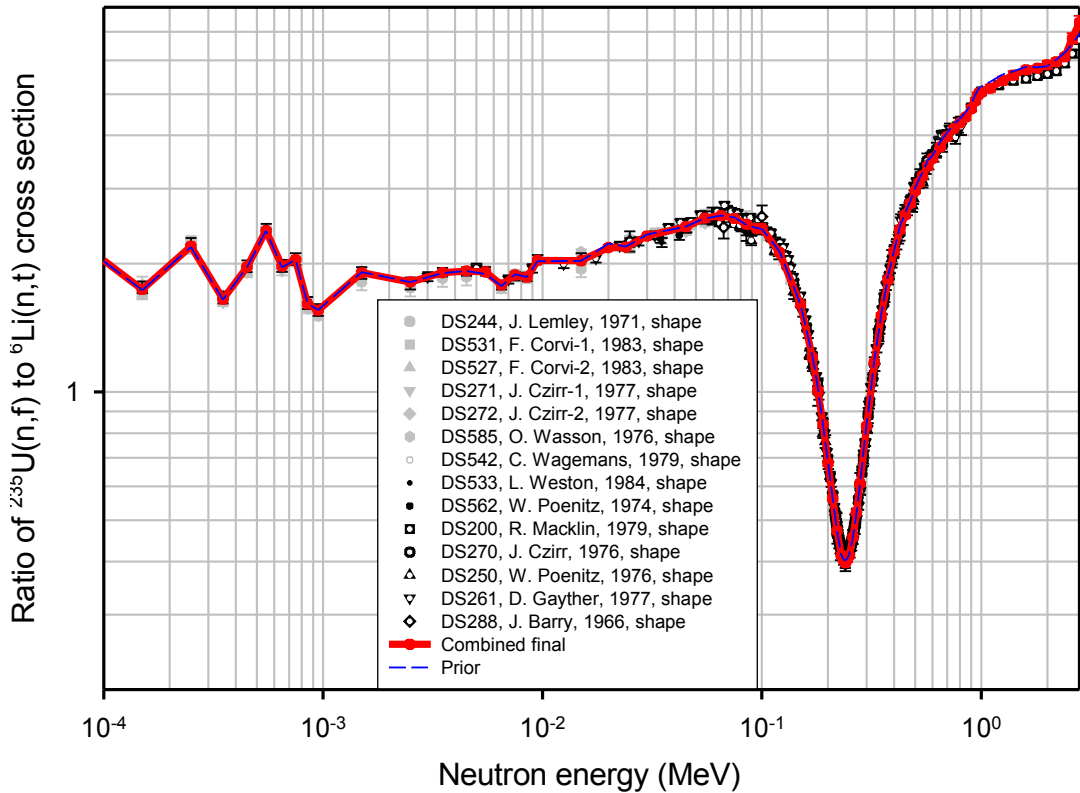


Fig. 37. Ratio of the cross sections of $^{235}U(n,f)$ to $^6Li(n,t)$ reaction.

Graphical view of the correlation matrices of the uncertainties is shown below

Fig. 38 «NJOY- style»: correlation matrix of the $^{235}\text{U}(n,f)$ standard in the two-dimensional color presentation.

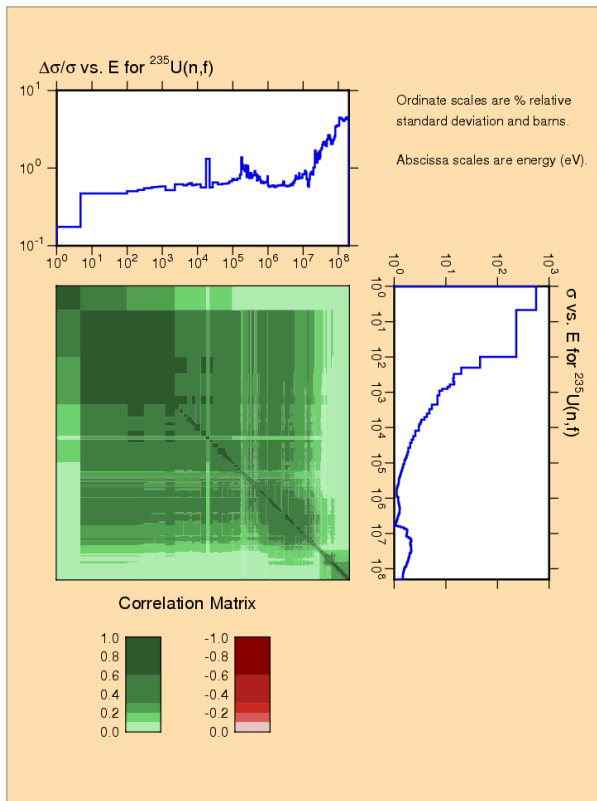
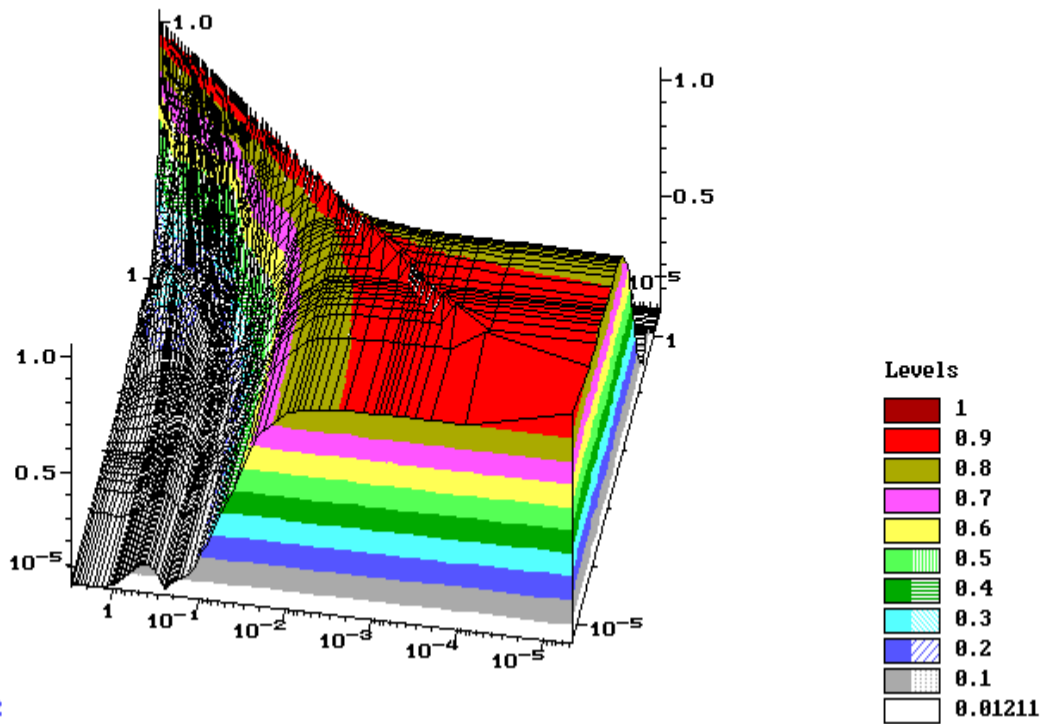


Fig. 39. One of the presentations proposed by Victor Zerkov (IAEA) as 3-dimensional rotating view for $^6\text{Li}(n,t)$.

ENDF Request 105, 2009-Jul-06,17:27:55
IAEA-STD: LI-6(N,T)HE-4



ZUView2

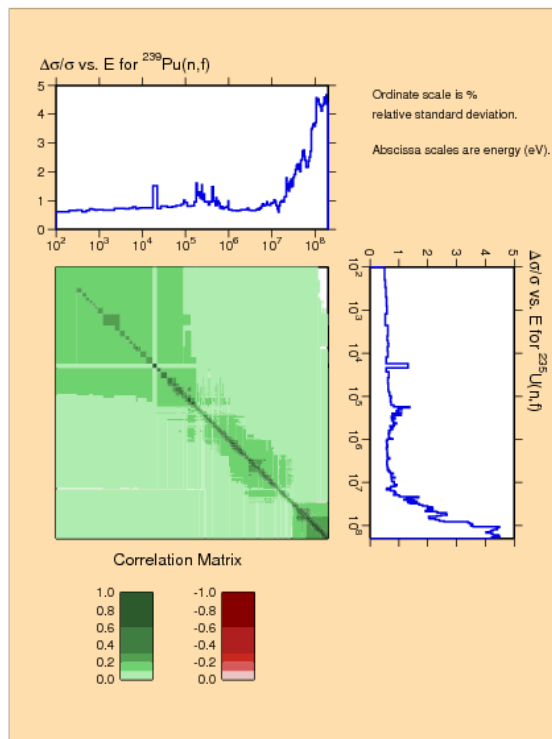
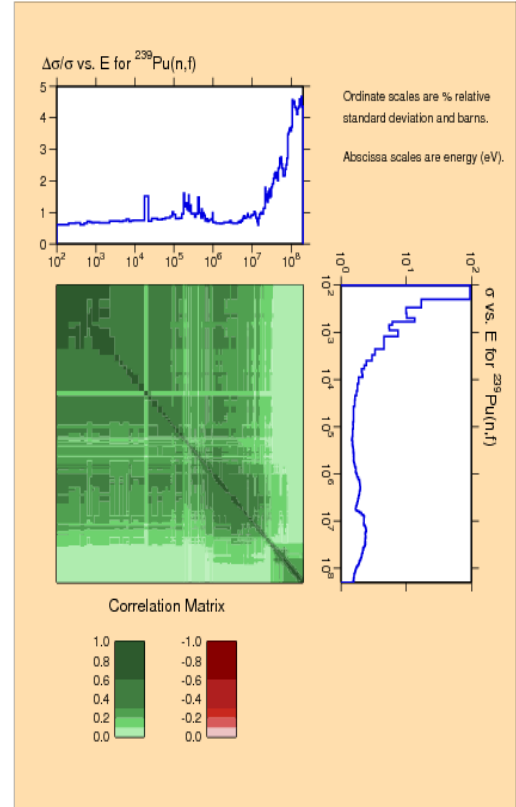
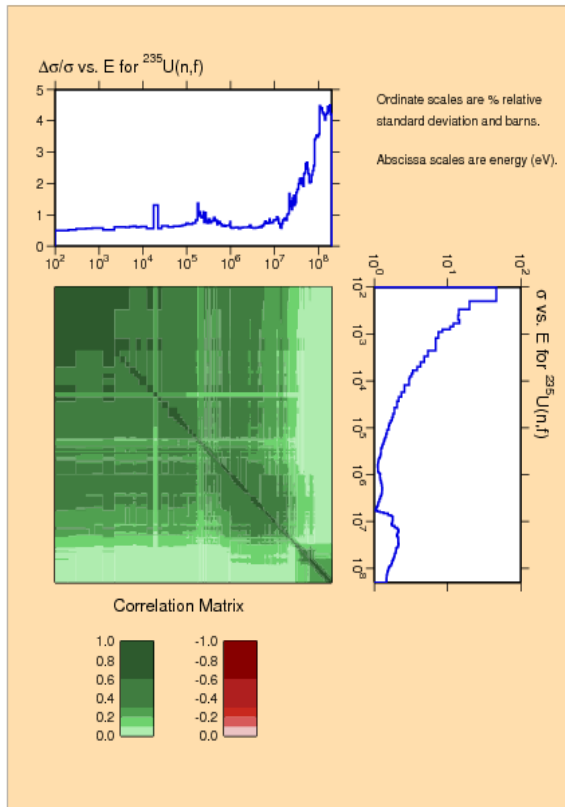


Fig. 40. Three blocks of full covariance matrix of the uncertainties of the $^{235}\text{U}(n,f)$ and $^{239}\text{Pu}(n,f)$ cross sections. Low panel shows the correlation matrix of the uncertainties between two cross sections, where only correlations between the same energies are important.

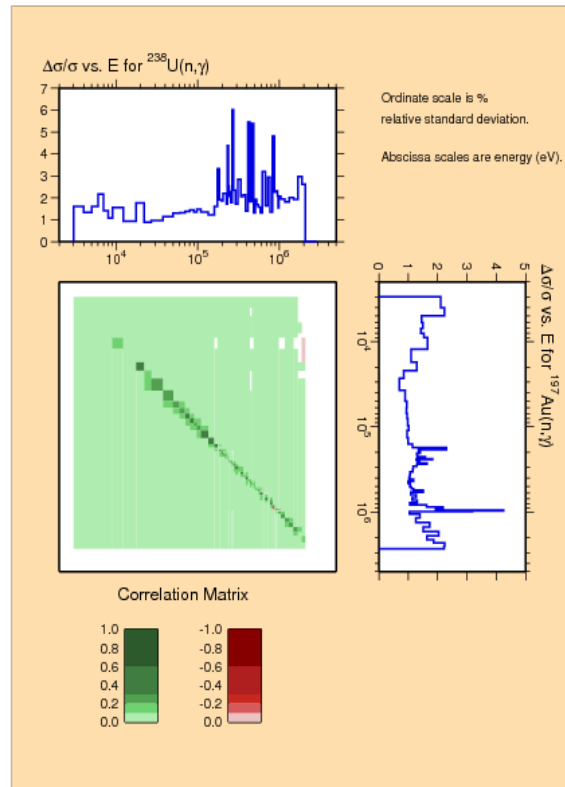
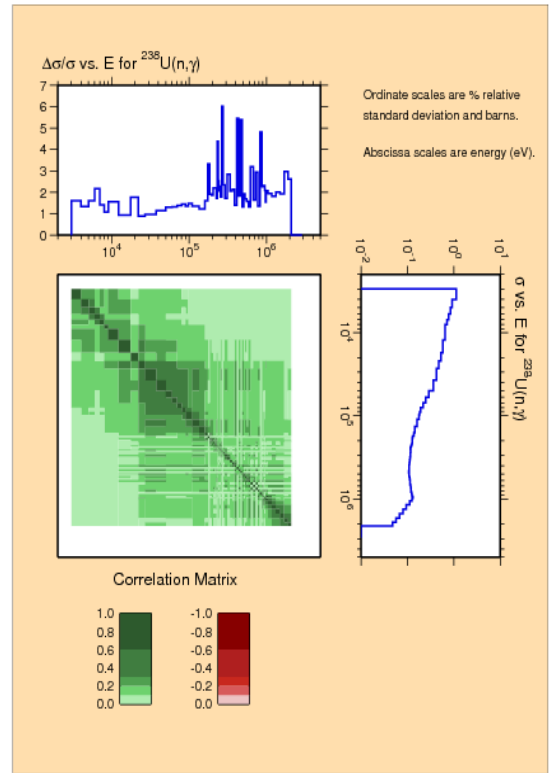
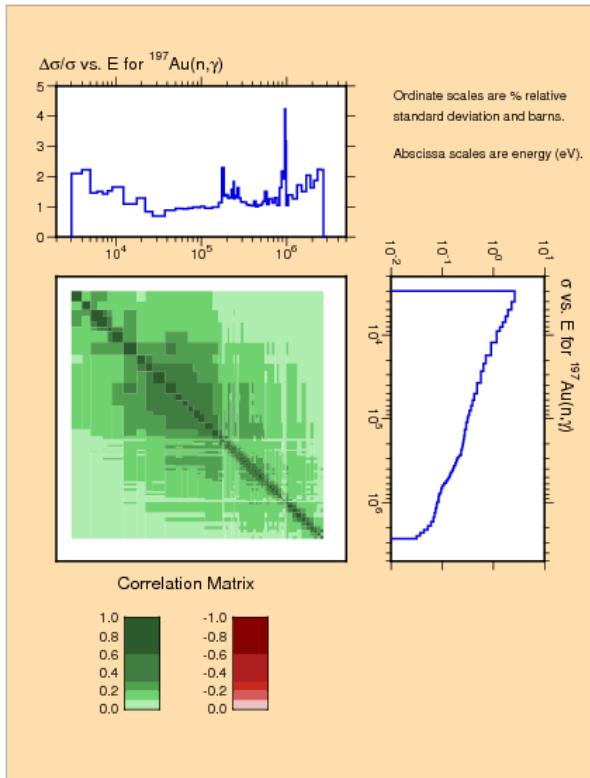


Fig. 41. Three blocks of full covariance matrix of the uncertainties of the $^{197}\text{Au}(n,\gamma)$ and $^{238}\text{U}(n,\gamma)$ cross sections. Bottom panel shows the correlation matrix of the uncertainties between two cross sections, where only correlations between the same energies are important.

Evaluation of the fission and capture cross sections of minor actinides important for the fuel cycle closing tasks can be done with the evaluated standards and their full covariance matrix of the uncertainties, either with addition of the minor actinides experimental data to the standards experimental data base and the following combined evaluation, or in the Bayesian approach, when minor actinides data are fitted together with the evaluated standards introduced in the GMA as large pseudo-experimental data set. Clearly that this also leads to the revision of the standards, although due to small number (comparing with the standards) of new data and their, as a rule, larger uncertainty, that influence at the standards is small. As the examples, the results of such evaluation done for $^{237}\text{Np}(n,\gamma)$ and $^{237}\text{Np}(n,f)$ reactions are shown in figures 42 to 44.

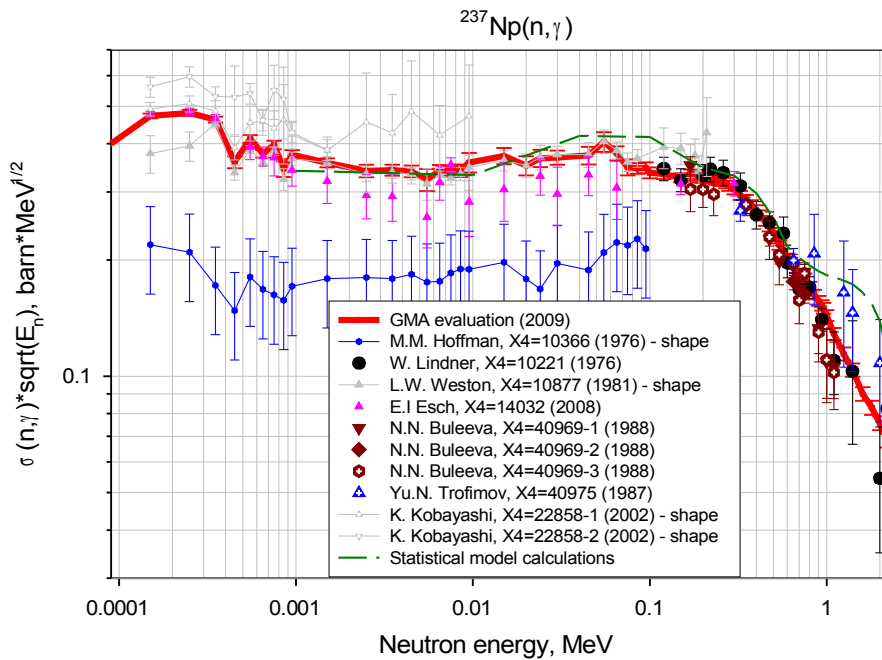


Fig. 42. ^{237}Np capture cross section, obtained in the combined evaluation with the standards.

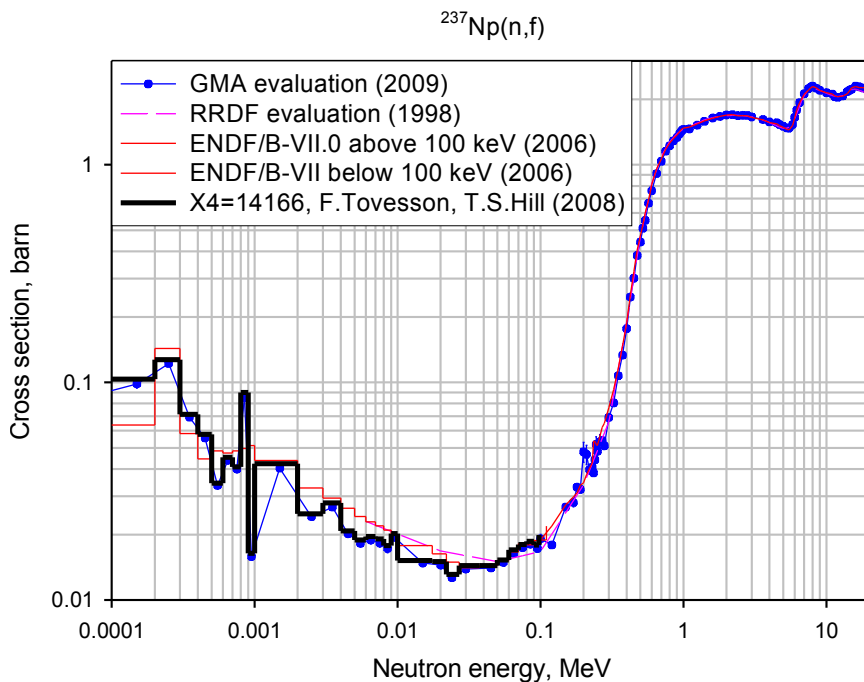


Fig. 43. ^{237}Np fission cross section, obtained in the combined evaluation with the standards.

The evaluation of the fission cross section in the sub-threshold range is under strong influence of the results of last measurements done by F. Tovesson and T.S. Hill [12]. Although these

measurements in the thermal range have rather large systematical uncertainty (about 70%), they agree in the limits of 35% with the evaluated value in the thermal point (20.4 mb). They are consistent with the results of other measurements above the fission threshold, this generally their high reliability.

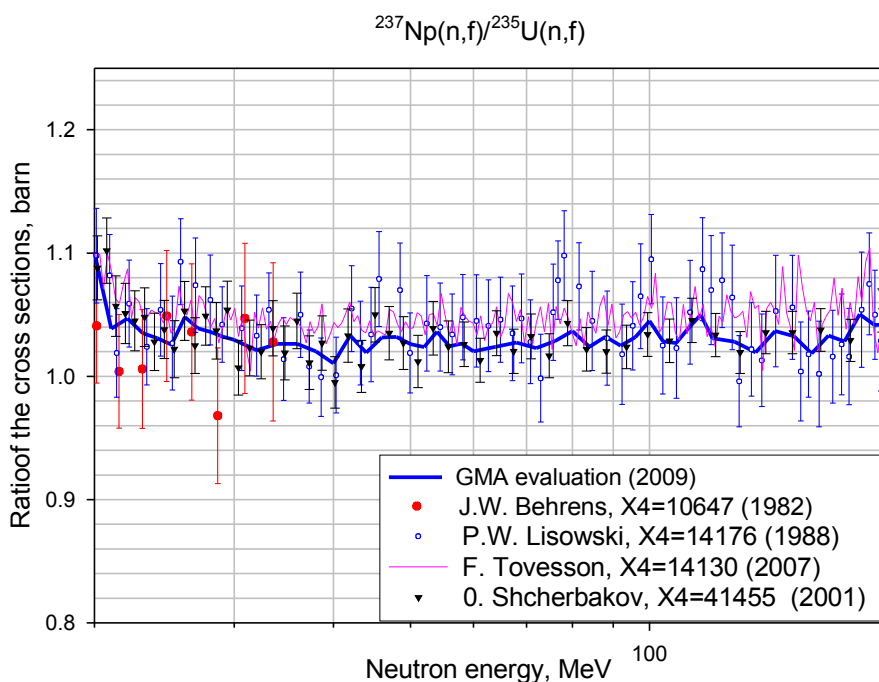


Fig. 44. ^{237}Np fission cross section in the energy range from 20 to 200 MeV, obtained in the combined evaluation with the standards data.

In the energy range above 20 MeV the measurements of the ratio of $^{237}\text{Np}(n,f)$ to $^{235}\text{U}(n,f)$ cross section have been made with good accuracy and the results of 4 independent measurements agree in the limits of 2 – 3 % in the all energy interval from 20 to 200 MeV. Cross section evaluated simultaneously with other standards has uncertainty from 1.6% at 20 MeV to 4.5% at 200 MeV. These uncertainties are comparable with the uncertainty of the $^{235}\text{U}(n,f)$ standards in this energy range, and because of this, $^{237}\text{Np}(n,f)$ cross section at least in the energy range above of the threshold of the fission also can be used as a secondary standards in other measurements.

GMA method allows also to make simultaneous evaluation of the prompt fission neutron spectra (PFNS) for thermal neutron induced fission of ^{235}U , ^{239}Pu and ^{233}U combined with PFNS from spontaneous fission of ^{252}Cf . For this, following the ideology used by Poenitz, all data in the evaluation were reduced to the form most close to the primarily-measured quantities. It concerns mainly to the time of flight measurements where ^{252}Cf standard was used for determination of the efficiency of the neutron detector.

Combined simultaneous evaluation of prompt fission neutron spectra was done in the fission neutron energy range from 0.02 to 12.8 MeV, in the region where exist the experimental data. For evaluation, all spectra (experimental and evaluated) were presented as the ratios to the Maxwellian spectrum with $kT=1.32$ MeV, which on definition is normalized at 1 in the all energy range of the secondary neutrons. This reduced substantially (from 3 to 4 orders to 1.5 — 2 times) the interval of the function variation and influence of the PPP effect. The non-model non-smoothed point-wise evaluation of the PFNS for spontaneous fission of ^{252}Cf done by W. Mannhart in 1987 was used as standard evaluation. This included the evaluation of central values and covariance matrix of uncertainties. Final recommended ^{252}Cf standard is differed from non-model point-wise evaluation by smoothing with the use of spline fit, Non-smoothed ^{252}Cf evaluation has been introduced in the GMA as pseudo-experimental set of data.

Important constraint at the PFNS evaluated in this form is the requirement of the strict spectrum normalization at 1 in the whole range of the neutron energies. Because in present case the evaluation was done in the limited interval of energy from 0.02 to 12.8 MeV, the requirements of the normalization of all spectra in this energy interval at the value 0.9985 ± 0.0003 was introduced in the least-squares fit. Uncertainty in the normalization is explained by the difference in the shape of the spectra taking part in the combined evaluation.

Strict requirement introduced by the normalization and large difference in the uncertainties at different points led to the strong changes of the spectra at the points with high uncertainties, and to the appearance of unphysical structures in the spectra. To avoid such unphysical fluctuations in the spectra, the specific function of the shape smoothing have been introduced in the fit. Usually, it has been presented by the Watt spectrum with the parameters adjusted to fit the global shape of the non-smoothed spectrum added by artificial covariance matrix with noticeable correlations only between neighboring points. This smoothing shape function allows smooth the spectrum in the neighboring points without changes of its global shape obtained in the non-model evaluation. The comparison of the PFNS evaluations obtained in the combined simultaneous evaluation of the spectra reduced to their primarily-measured form with the present ENDF/B-VII.0 evaluation is shown in the figures 45 - 50.

Major difference of new evaluation from previous one is higher yield of the prompt neutrons in the soft part of the spectra ($E_n < 1$ MeV). The impact of other spectra at the standard PFNS of ^{252}Cf is limited by the changes at 1 — 2 %, for exclusion of the range below 1 MeV, where yield of neutrons in new evaluation is higher at 3 — 4 %.

Measurements of the absolute ratios to the PFNS of spontaneous fission of ^{252}Cf can be reduced to the absolute spectra using new evaluation of the PFNS of ^{252}Cf obtained in the combined simultaneous fit of all spectra. Comparison of these spectra with the results of non-model evaluations and with model evaluation done by V. Maslov in Kornilov's model of two fragments with emission of prompt neutrons at the different moments of the Coulomb acceleration of the separated fragments is shown in the figures 51 to 53. NIAR data are given in the nodes on the energies, where the evaluation was done. As we see there is good consistency between the data in the range of the maximum of the spectra. Strong fluctuations in the data by A. Lajtai et al. are explained by the $^6\text{Li}(n,t)$ standard used in these measurements. Standard cross section has strong resonance at 235 keV, which was not reduced to the experimental resolution, when the estimation of the lithium glass neutron detector efficiency was done.

The preliminary results of testing of the files with these evaluated spectra in the critical experiments had shown that they may remove the long existing controversy between the microscopic evaluations of the PFNS and requirements to them, which follow the need to reach the criticality in the integral experiments. The major conclusion is that parameters of the criticality are very sensitive not only to the mean energy of the PFNS (and because of different neutron leakage in small and large assemblies this influence can be different), but also to the shape of the PFNS.

Comparison of new (combined evaluation) with old (based at only Cf spectra evaluations of PFNS) for spontaneous fission of ^{252}Cf is shown in Fig. 54. Combined evaluation with data for PFNS for ^{235}U , ^{239}Pu and ^{233}U leads to the increase of the yield of neutrons in the soft part of the spectrum and small decrease of the yield in the hard part of the spectrum. This trends is observed for PFNS at all considered fissile nuclei.

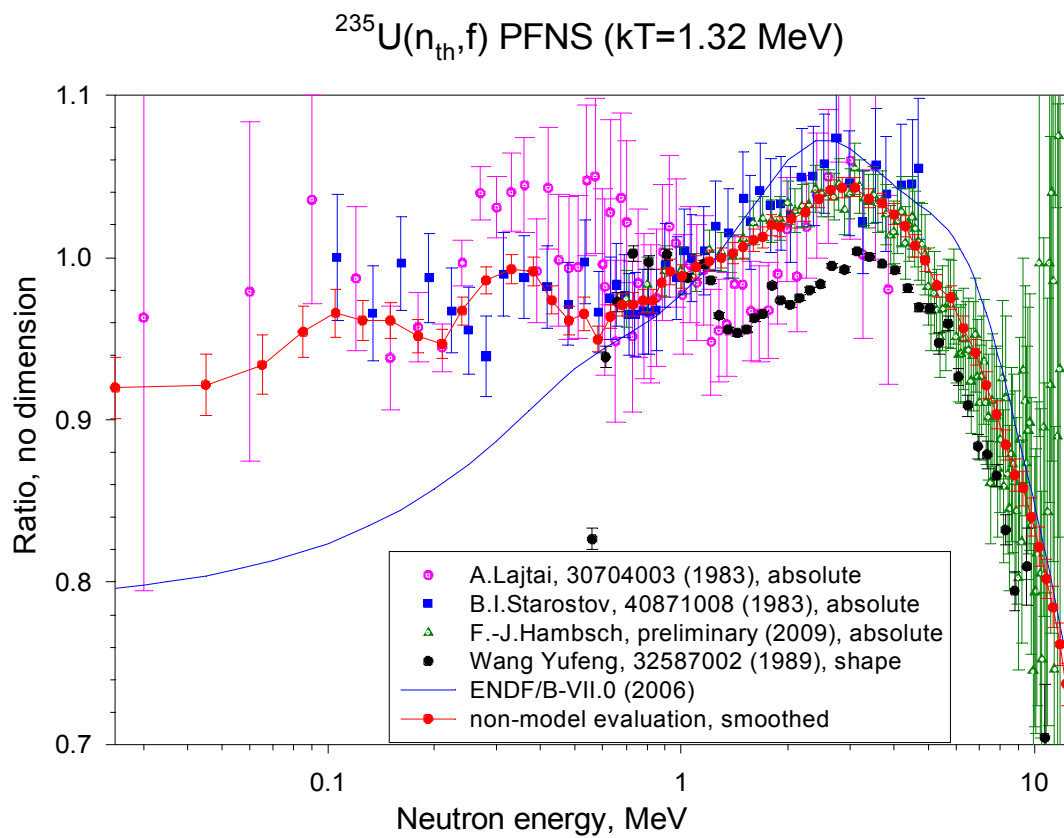
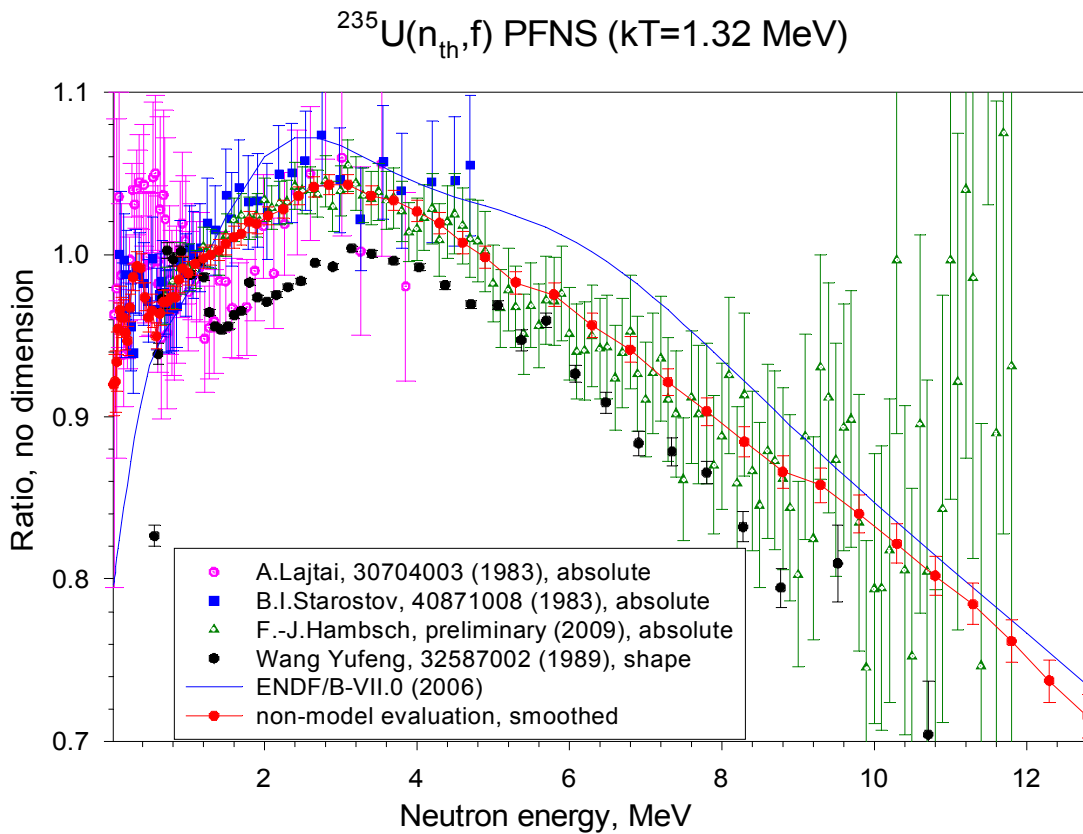


Fig. 45. Comparison of the evaluated and experimental data on PFNS for $^{235}\text{U}(n_{\text{th}},f)$ in the linear and logarithmic scale the neutron energy. The results of absolute measurements and the measurements of the shape are shown.

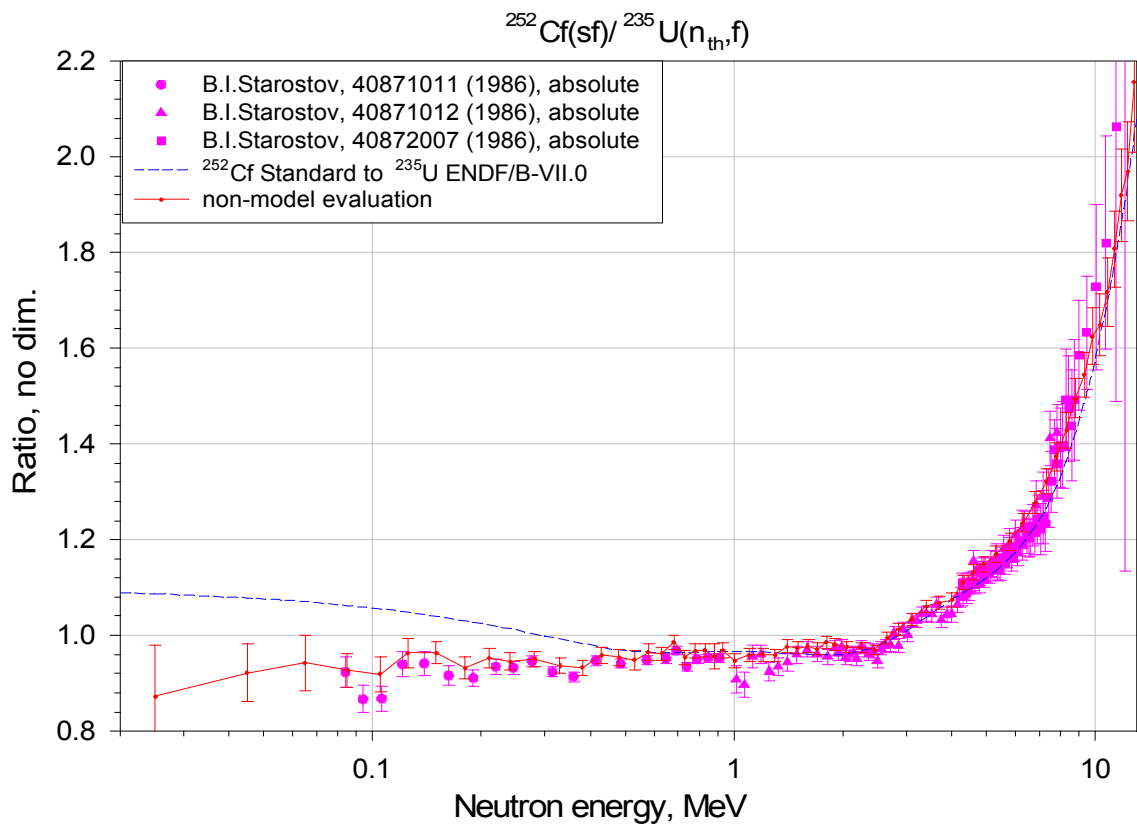
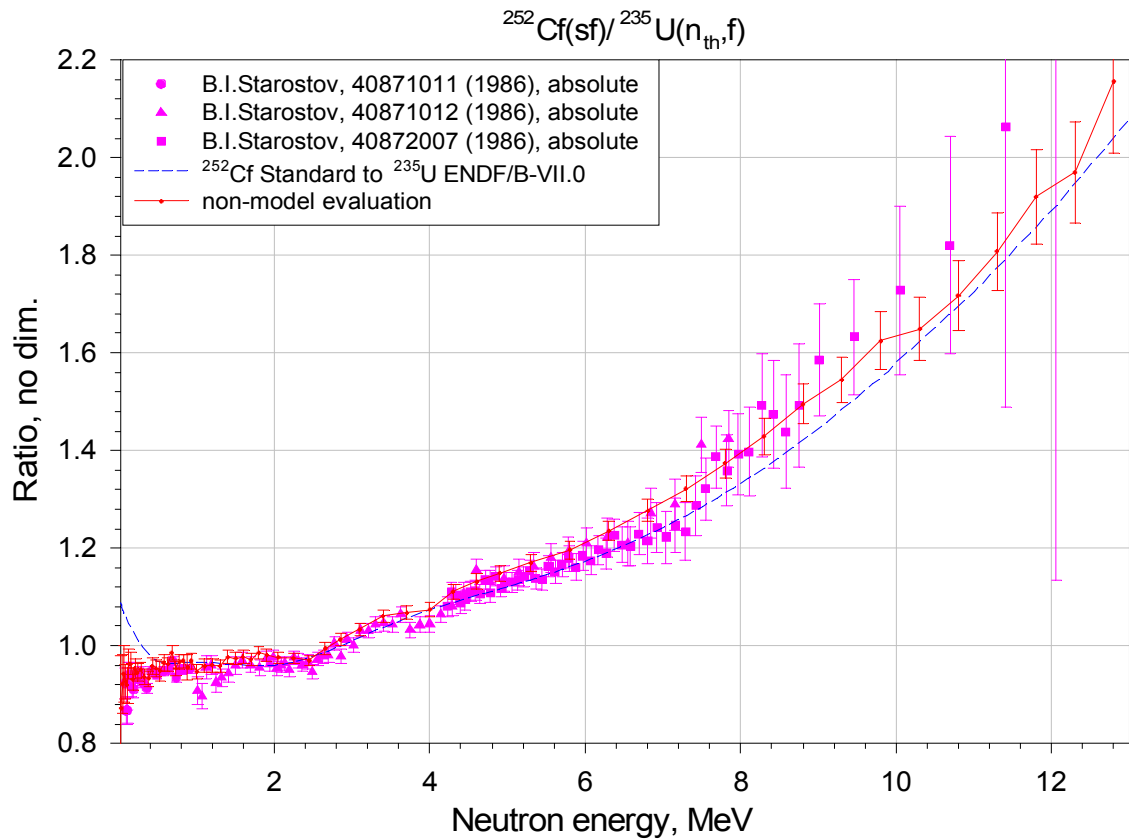


Fig 46. Comparison of the results of measurements of absolute ratio of the PFNS spectra $^{252}\text{Cf}(\text{sf})/^{235}\text{U}(n_{\text{th}},\text{f})$ in linear and logarithmic scales on neutron energy.

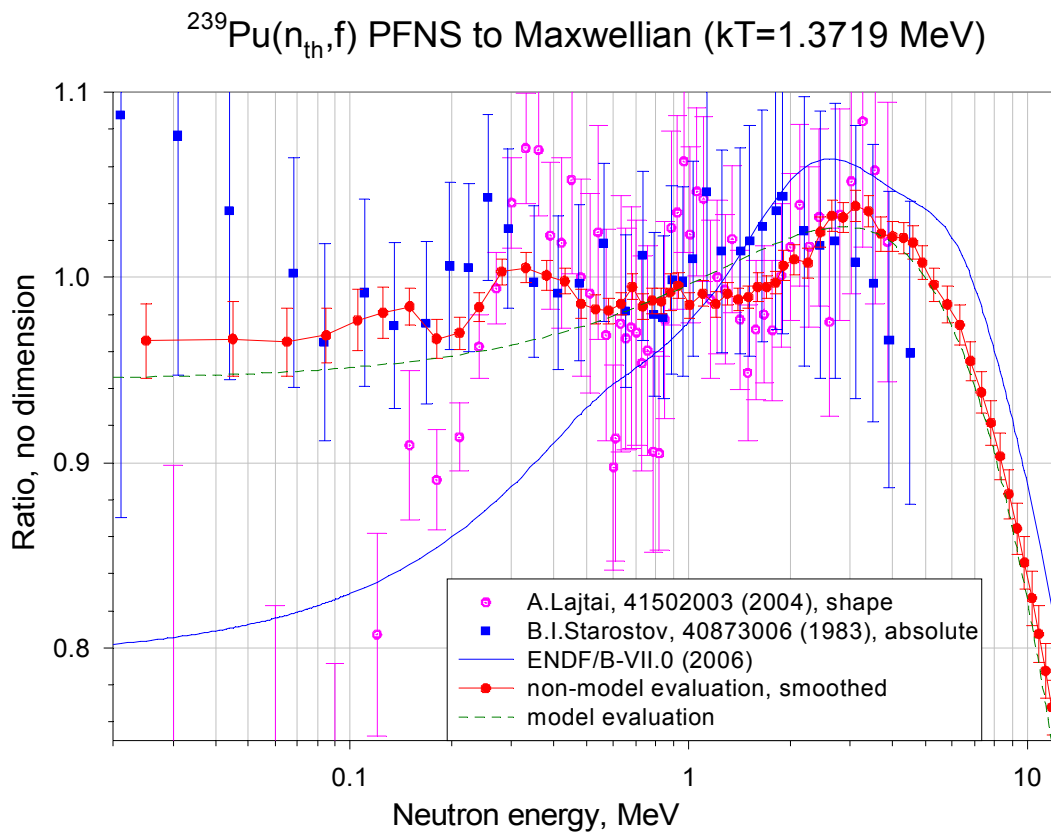
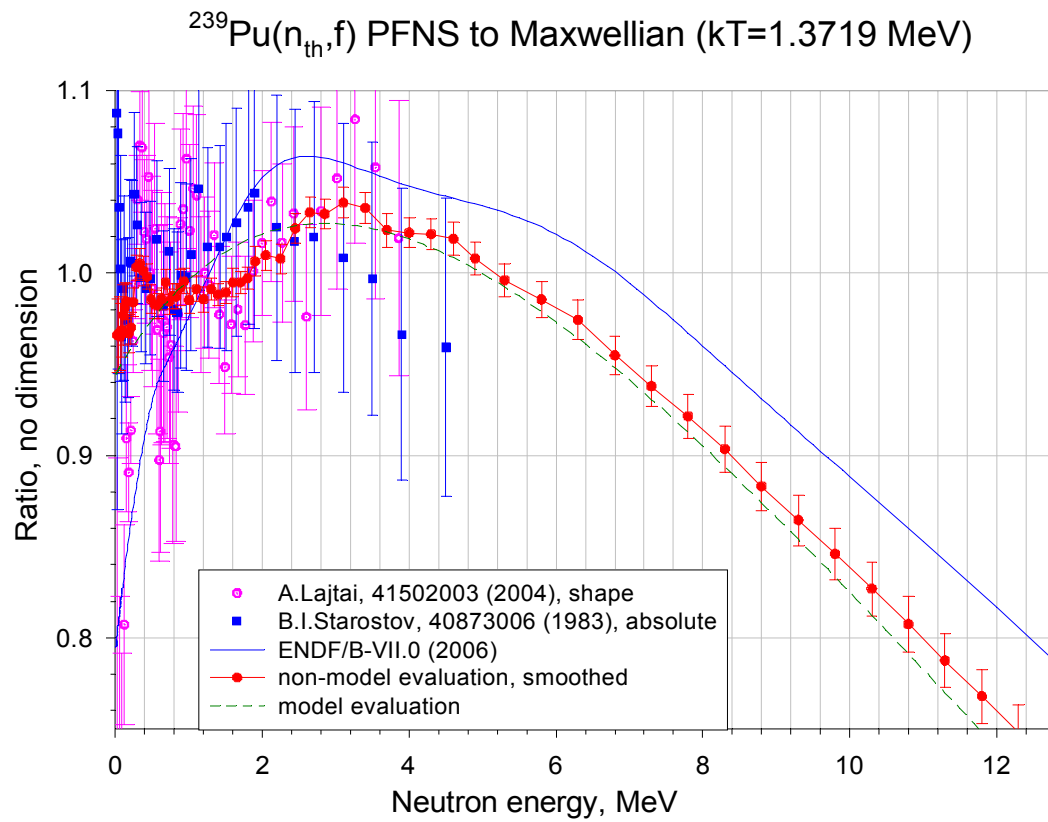


Fig. 47. Comparison of the spectra of PFNS for $^{239}\text{Pu}(n_{\text{th}},f)$ in linear or logarithmic scale on the neutron energy. The results of absolute and shape spectra measurements are shown.

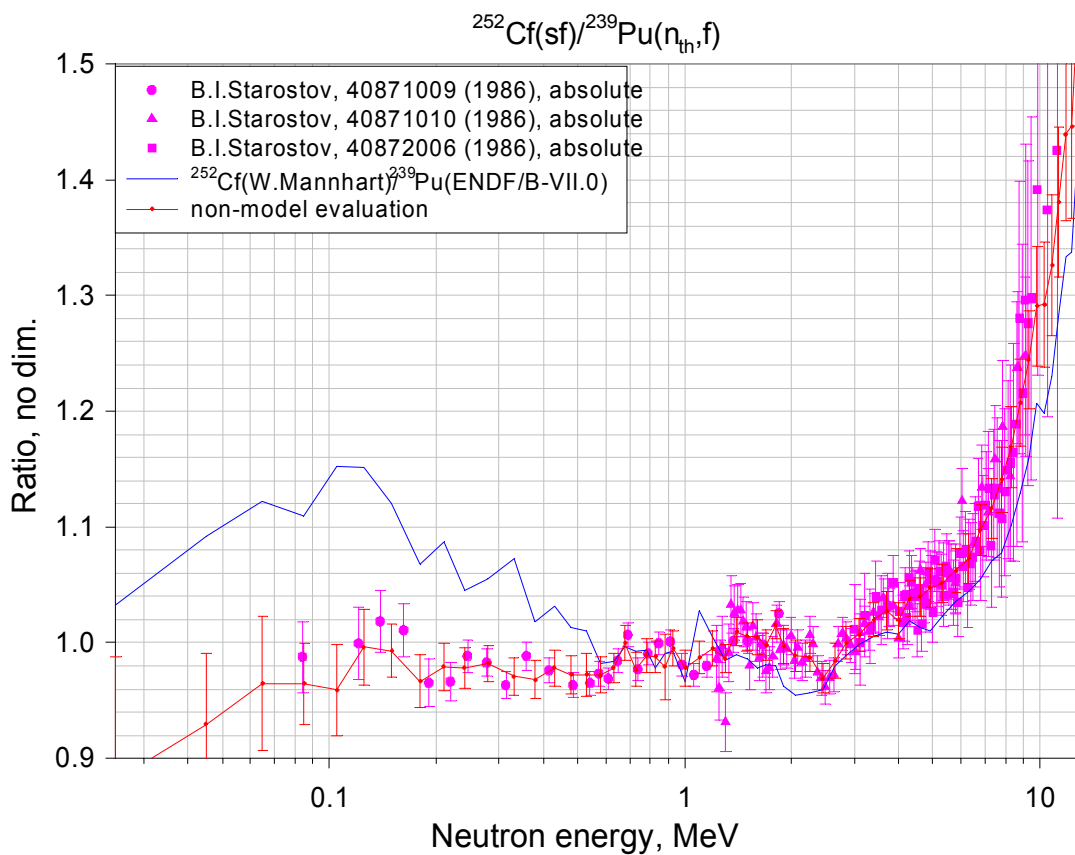
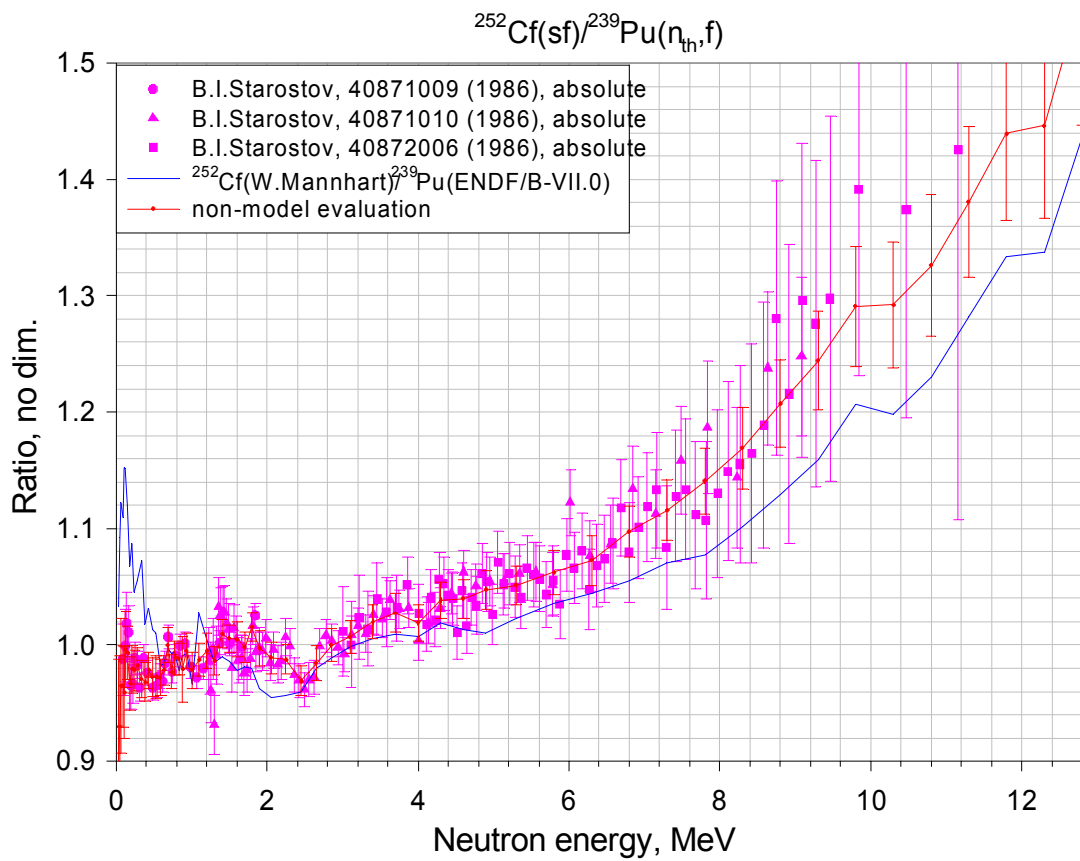


Fig. 48. Comparison of the results of measurements of absolute ratio of the PFNS spectra $^{252}\text{Cf(sf)}/^{239}\text{Pu}(n_{\text{th}},f)$ in linear and logarithmic scales on neutron energy.

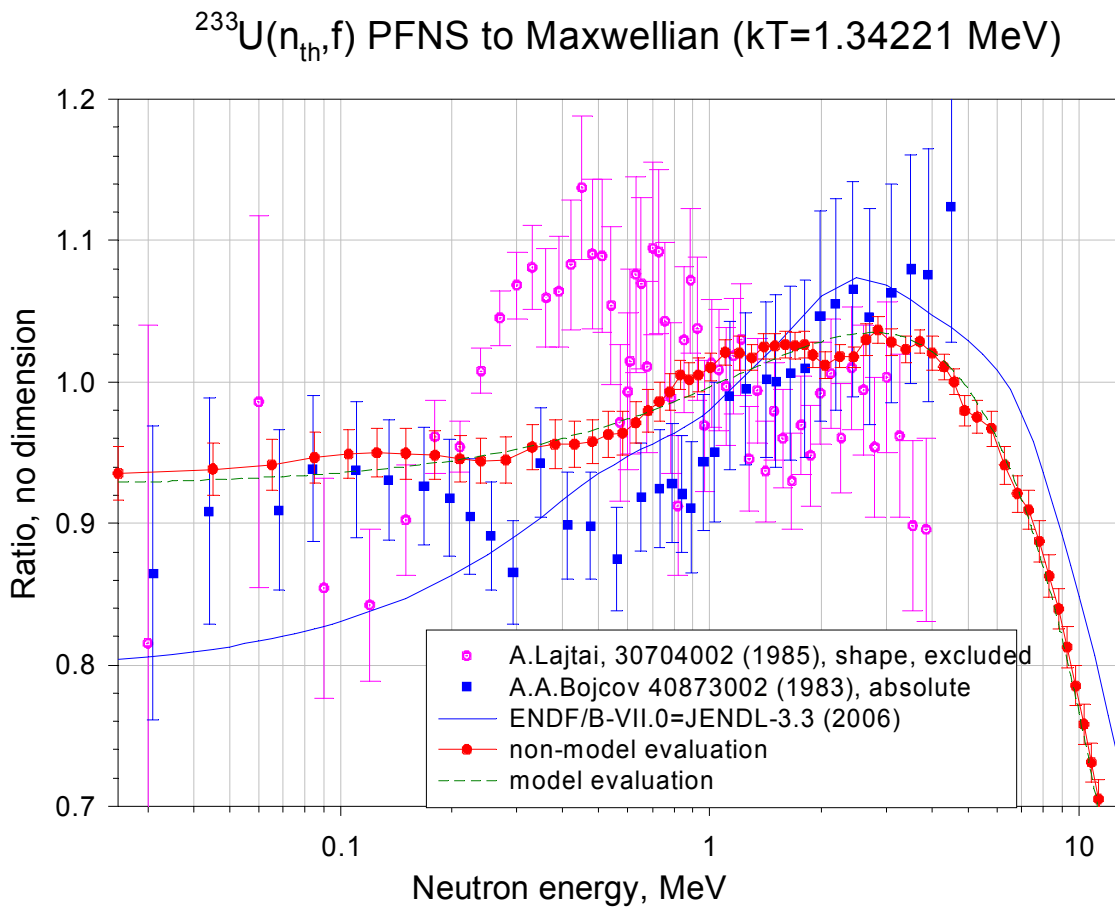
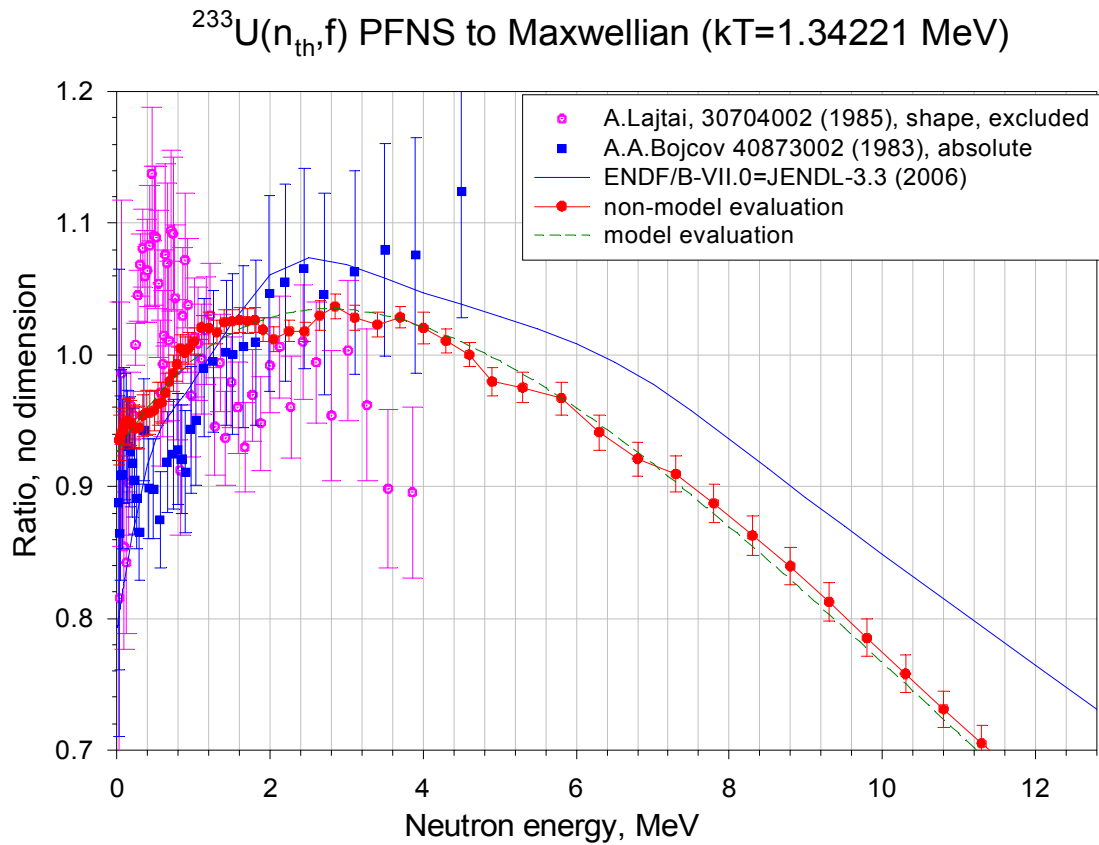


Fig. 49. Comparison of the evaluated and experimental data on PFNS for $^{233}\text{U}(n_{\text{th}},f)$ in the linear and logarithmic scale the neutron energy. The results of absolute measurements and the measurements of the shape are shown.

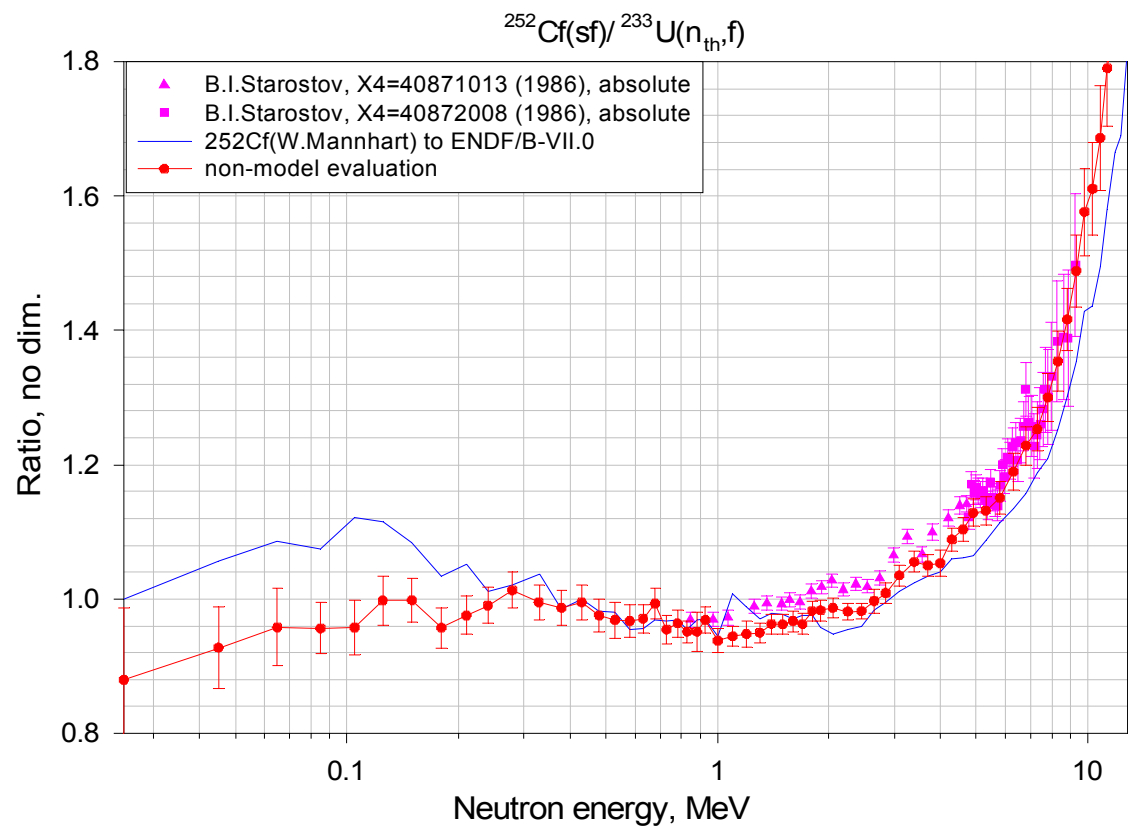
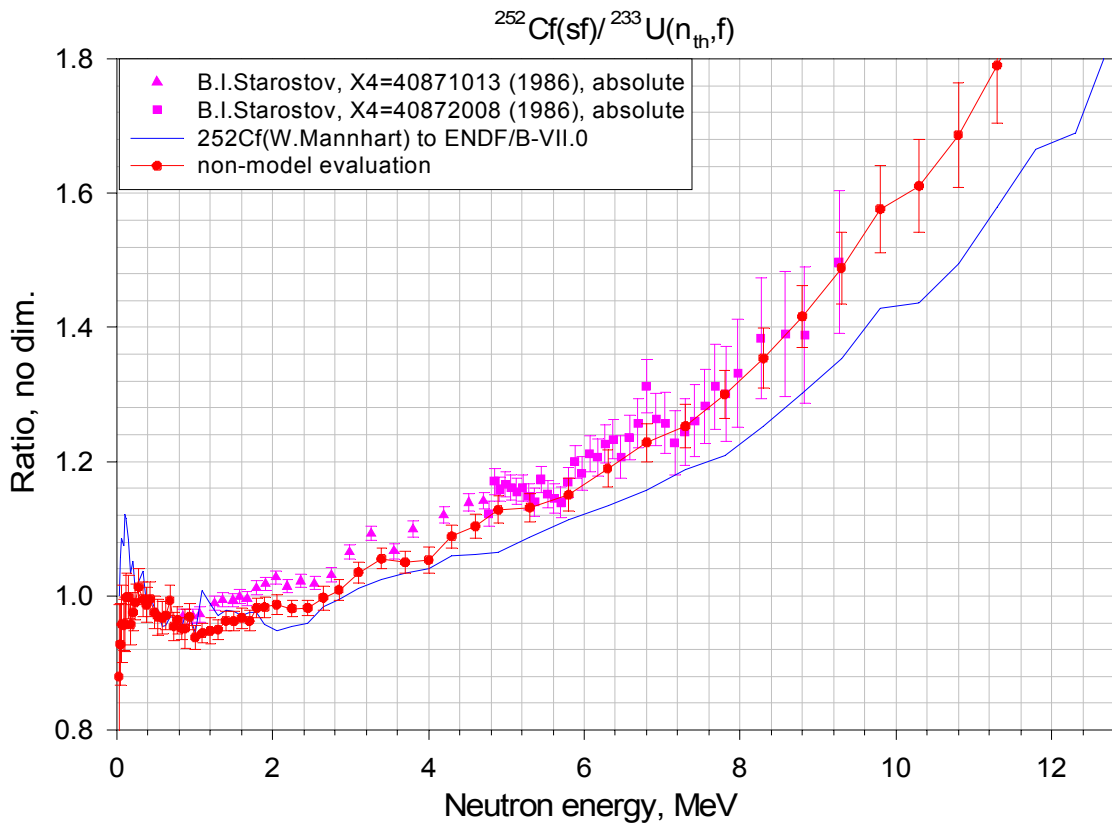


Fig. 50. Comparison of the results of measurements of absolute ratio of the PFNS spectra $^{252}\text{Cf}(sf)/^{233}\text{U}(n_{th},f)$ in linear and logarithmic scales on neutron energy.

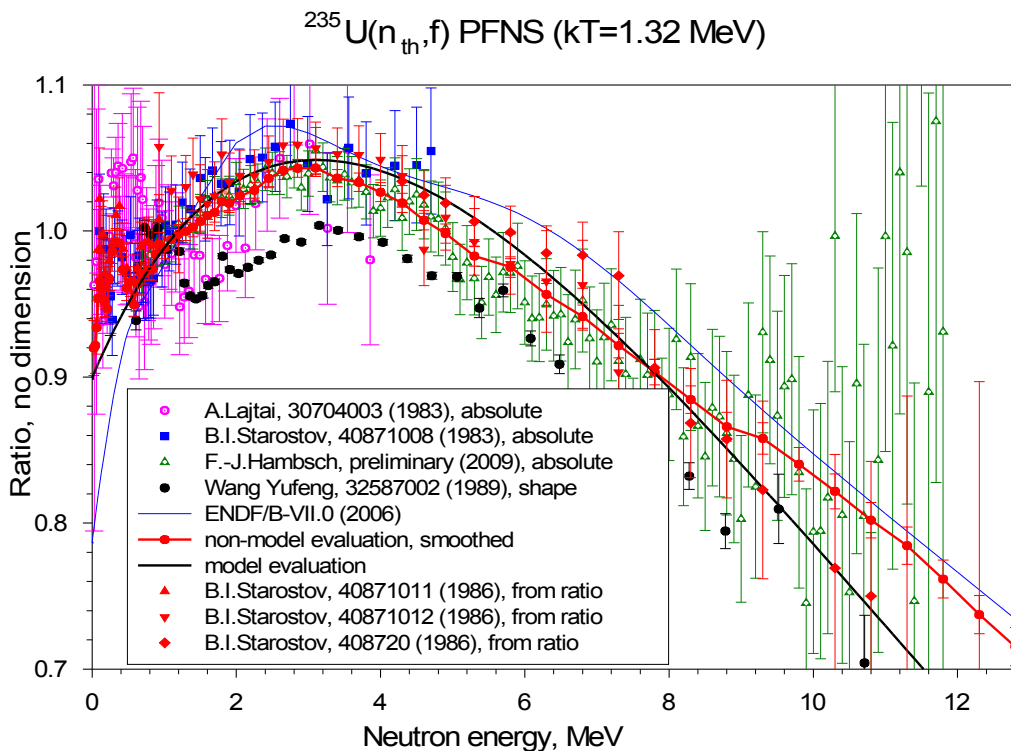
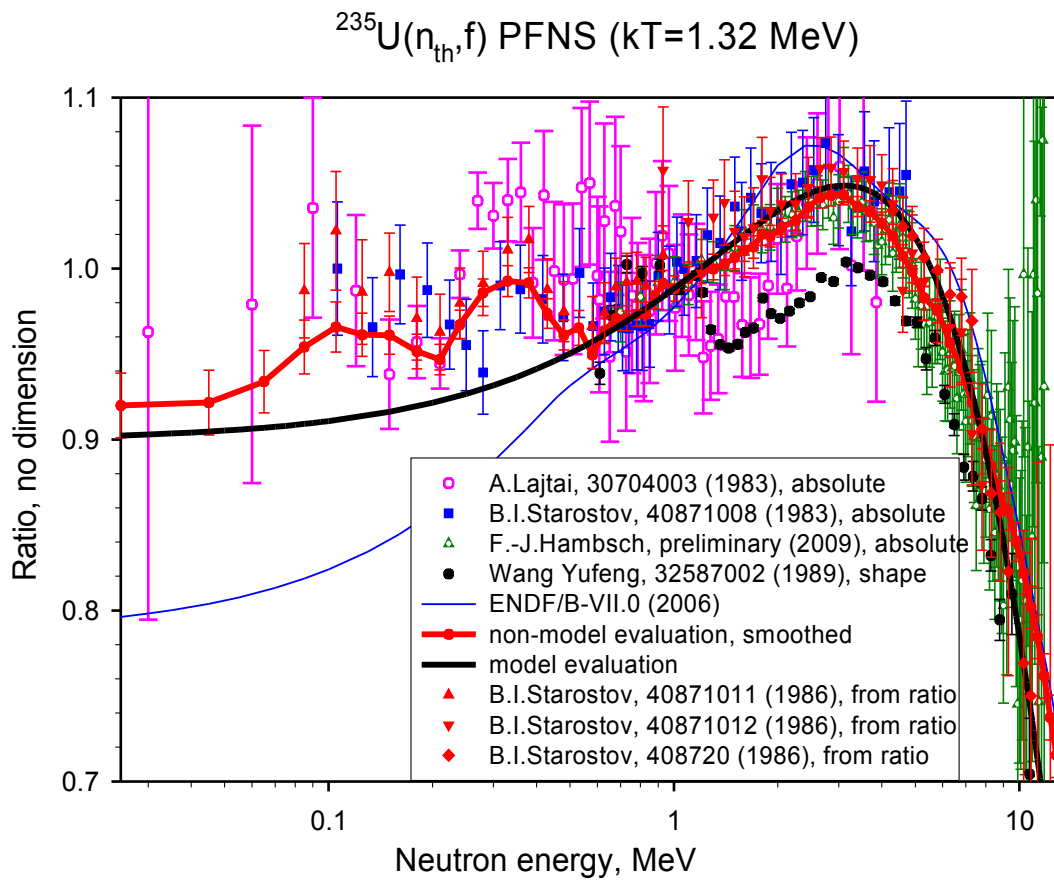


Fig. 51. Comparison of the $^{235}\text{U}(n_{\text{th}},f)$ PFNS in linear and logarithmic scale on the neutron energy. Starostov's (NIAR) data of absolute measurements of ratios were reduced to absolute spectra using new ^{252}Cf simultaneous evaluation. Results of the non-model and model evaluations are shown.

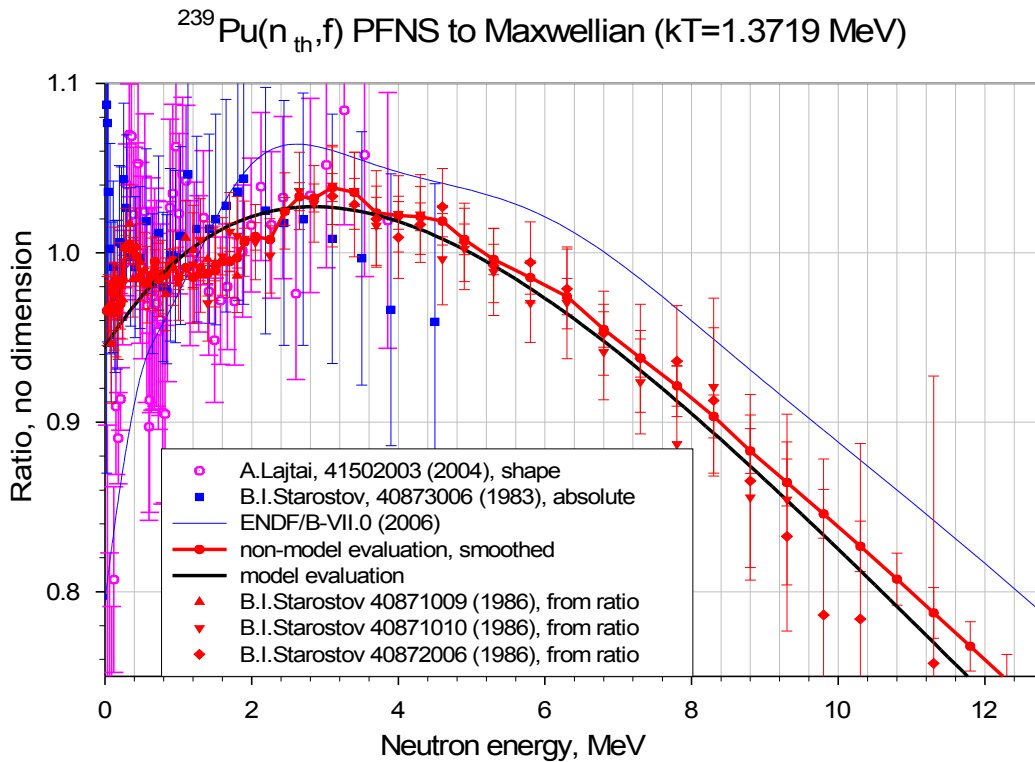
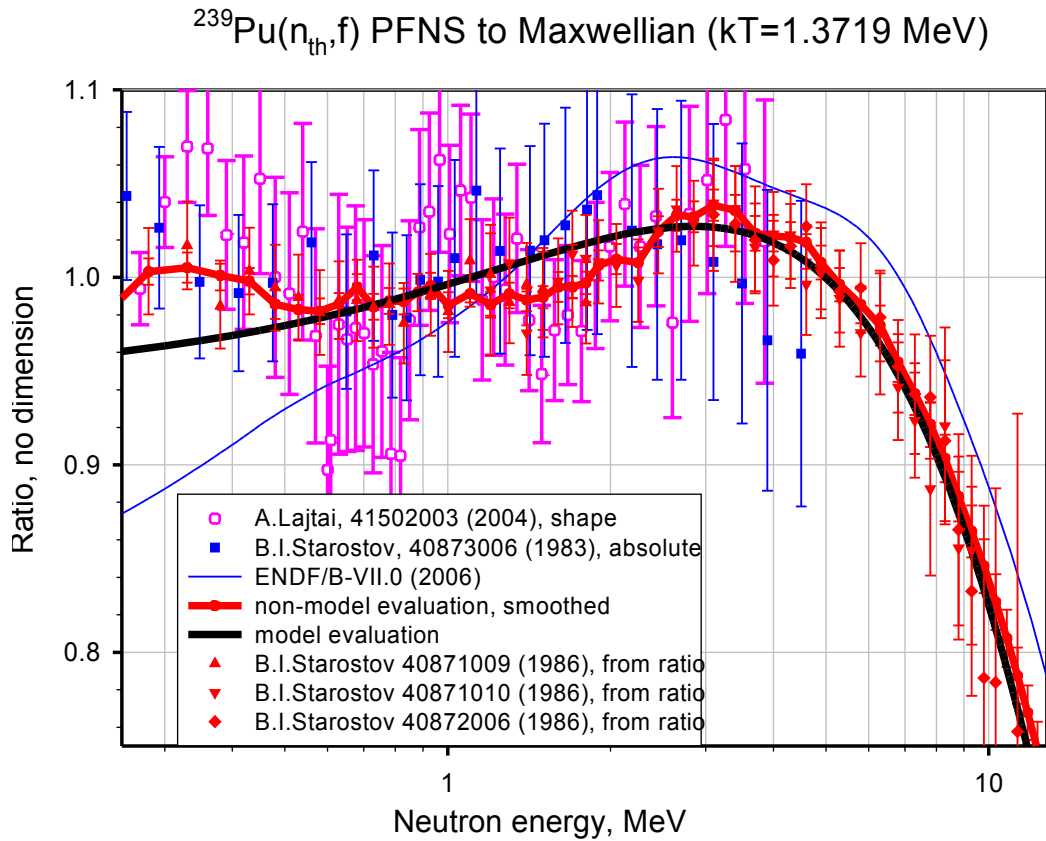
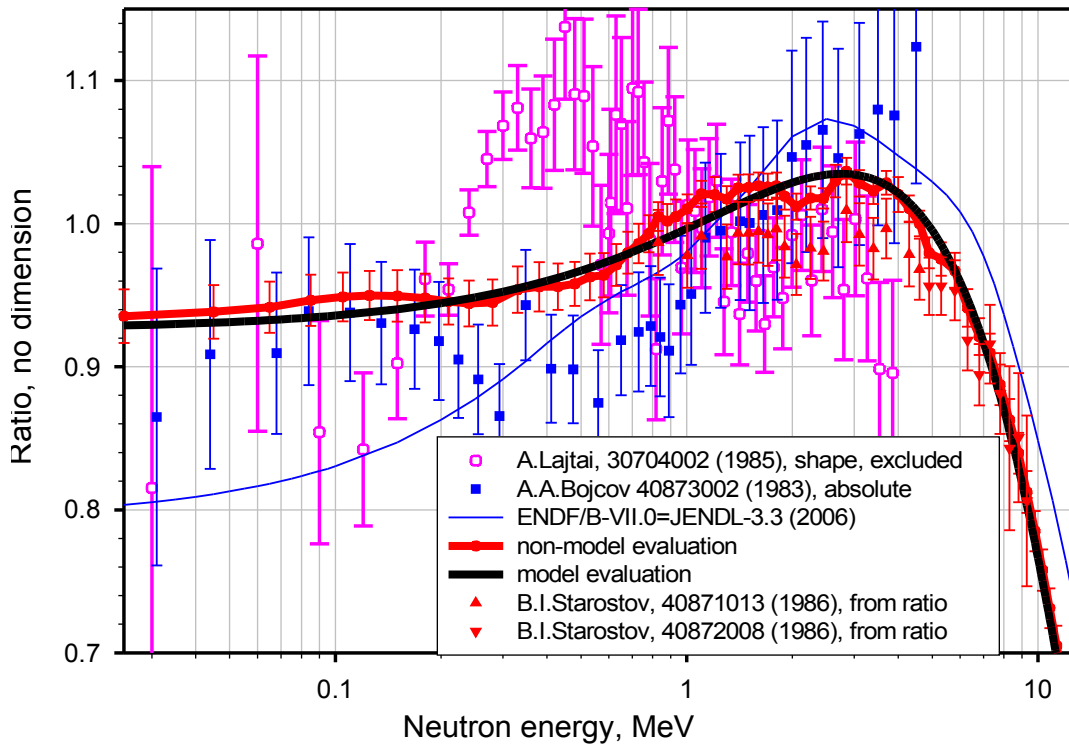


Fig. 52. Comparison of the $^{239}\text{Pu}(n_{\text{th}},f)$ PFNS in linear and logarithmic scale on the neutron energy. Starostov's (NIAR) data of absolute measurements of ratios were reduced to absolute spectra using new ^{252}Cf simultaneous evaluation. Results of the non-model and model evaluations are shown.

$^{233}\text{U}(n_{\text{th}},f)$ PFNS to Maxwellian ($kT=1.34221$ MeV)



$^{233}\text{U}(n_{\text{th}},f)$ PFNS to Maxwellian ($kT=1.34221$ MeV)

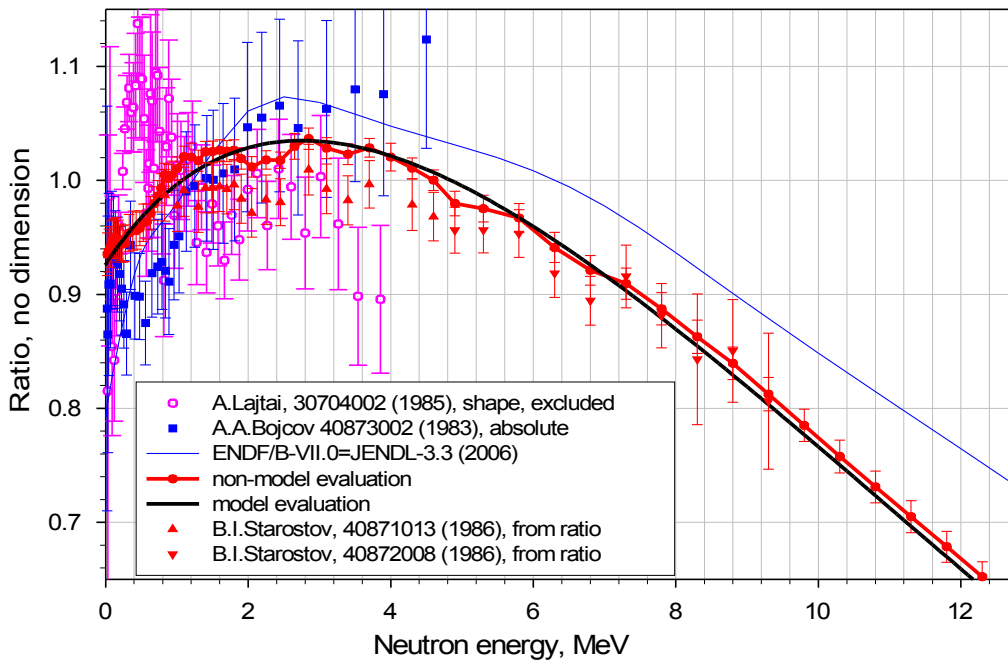


Fig. 53. Comparison of the $^{233}\text{U}(n_{\text{th}},f)$ PFNS in linear and logarithmic scale on the neutron energy. Starostov's (NIIAR) data of absolute measurements of ratios were reduced to absolute spectra using new ^{252}Cf simultaneous evaluation. Results of the non-model and model evaluations are shown.

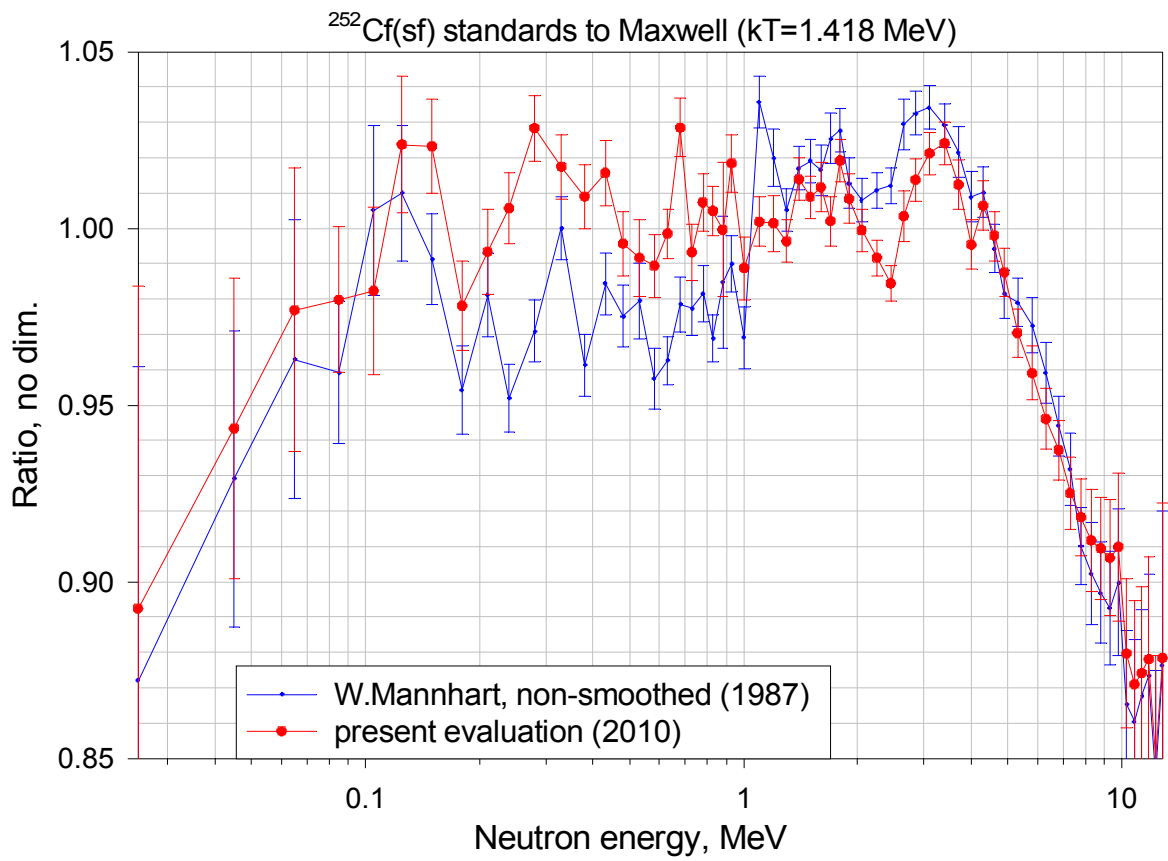


Fig. 54. Comparison of new (combined) and old (based only at Cf spectrum measurements) evaluations of PFNS for $^{252}\text{Cf(sf)}$.

Lecture 2. Covariance matrices of uncertainties of experimental and evaluated data

Covariance matrix of uncertainties obtained in non-model and model fits of the same experimental data and Peelle's effect

In the model fit, the additional elements going in the equation of the least-squares fit of the data are the model parameters and the sensitivity coefficients — partial derivatives of the model function on the given parameter. In the non-model fit, where the parameters of the fit are the own values of the evaluated function in the nodes on the energy, the sensitivity coefficients are equal to 1. The number of parameters in the model fit is usually substantially less than the number of energy nodes where data are evaluated. Model determines the form of the function used for a fit of the data. Its use leads to substantial reduction of the number of parameters (data) needed for presentation of the evaluated values and including of the evaluated model parameters and covariance matrix of their uncertainties. Covariance matrix of uncertainties of the data determined in the nodes on the energy, with number of the nodes exceeding the number of parameters should be a semi-positive definite matrix with a number of eigenvalues equal to the number of parameters. Large advantage of the use of the model is that evaluated function (data) and corresponding to them the covariance matrix of their uncertainties can be constructed for any energy nodes. Serious drawback of using of the models is that ideal (true) models are absent in the nuclear physics, and use of any model for the data fit limits the shape of the fitting function. One of the known ideal models limited in some narrow energy interval is the $1/v$ dependence of capture or fission cross section near the thermal point (0.0253 eV) if the resonances are rather far from this interval. Wolfgang Poenitz gave the names «all world believe» to these type dependence of data included in the GMA data base.

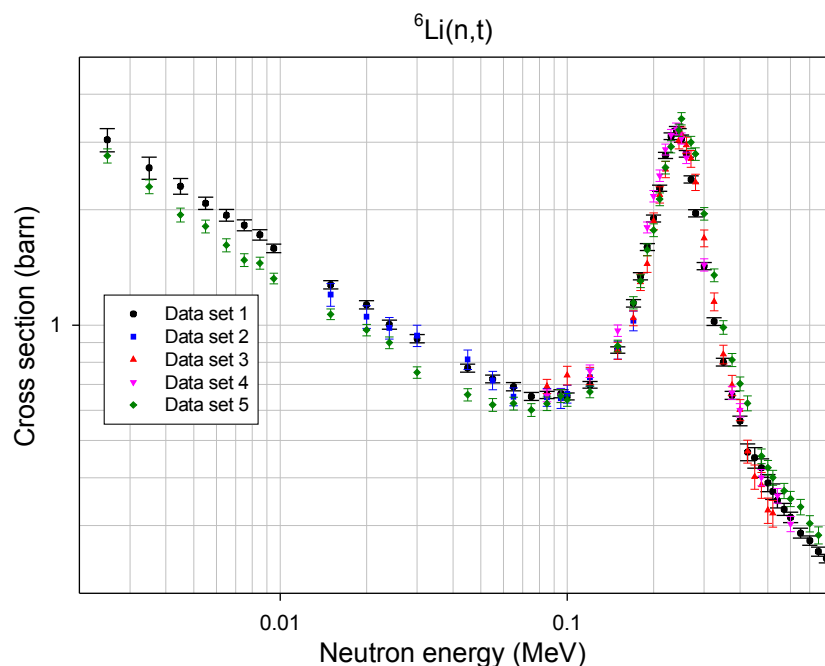


Fig. 55. 5 sets of ${}^6\text{Li}(n,t)$ experimental data selected for implementing of different tests.

Comparison of the results of model and non-model least-squares fits of the same data was done on example of ${}^6\text{Li}(n,t)$ reaction. 5 sets of data used for this were taken from the GMA database (same data are in EXFOR data base). According to the uncertainties assigned by the authors, the covariance matrices of these experimental data sets were constructed. Data are rather discrepant, have strong variations in the fitted energy range, have large LERC components of the uncertainties. Result of the fit done in the model approach (PADE2 - mathematical model of

rational functions presentation, Box-Cox - mathematical model with variable transformations and polynomial expansion, RAC - R-matrix physical model) and non-model fits with GMA and GLUCS shown in figure 56 demonstrate strong appearance of the Peelle's effect (or PPP - "Peelle Pertinent Puzzle"). For convenience of the comparison all data are shown as a ratio to the GMA fit (same for GLUCS) with use of Chiba-Smith option, which minimizes the Peelle's effect. The Peelle's effect in the description of the experimental data is appeared in the visual bias all fits (ordinary GMA and GLUCS fits, model fit with PADE-2 and R - matrix fit with RAC code) below main bulk of the experimental data (e.g., GMA and GLUCS fit being very consistent goes practically out of the spread of the experimental data. General conclusion is that the PPP is the consequence of the strong reduction of data in the construction of the covariance matrices of the uncertainties of experimental data in conditions of strong variation of function and poorly known (or assigned) components of the uncertainties. Appearance of the PPP, technical means of its exclusion, and implementation of strict approach, which will exclude PPP will be discussed below.

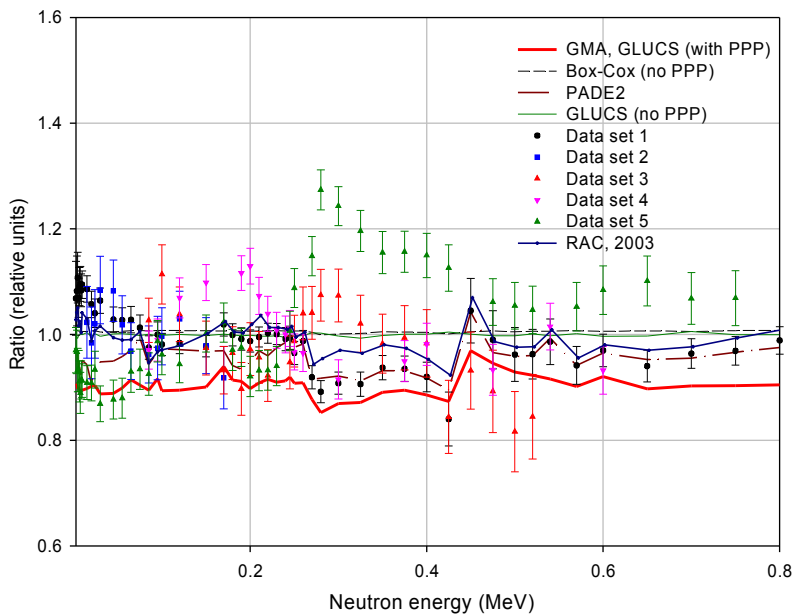


Fig. 56. Results of least-squares fit of experimental data given in Fig. 55 for ${}^6\text{Li}(n,t)$ reaction in different model and non-model approaches. Bias of the evaluations below a main bulk of experimental data is the appearance of the PPP effect.

Comparison of the uncertainties obtained in the model and non-model fits of the same experimental data shows, that their covariance as well as correlation matrices differ substantially. Per-cent errors (or variances — diagonal elements of covariance matrices of the uncertainties) are usually substantially low in the model fit than in the non-model, and off-diagonal elements, or covariances near the diagonal are higher in the model than in non-model fits. The off-diagonal elements in the model and non-model least-squares fits may have negative values, describing the anti-correlations between uncertainties in different data points. The row (column) of the covariance matrix of the uncertainties which obtained in the fit of ${}^6\text{Li}(n,t)$ with use of the model code GMA and non-model codes RAC and PADE2 is shown in Fig. 57. The row (column) includes the variance at 0.2 MeV. As we see, the variance in the non-model code GMA is very different from neighboring covariances. There are no such distinctions in the model fit. This can be explained by influence of strong intrinsic correlations put by the model in the fit of data. Because the rational analytical PADE2 model on the form is close to the R-matrix physical model (both models have poles and smooth components), the fits obtained in these models are

close. Model fits reduce substantially the percent uncertainties in comparison with the non-model least-squares fit.

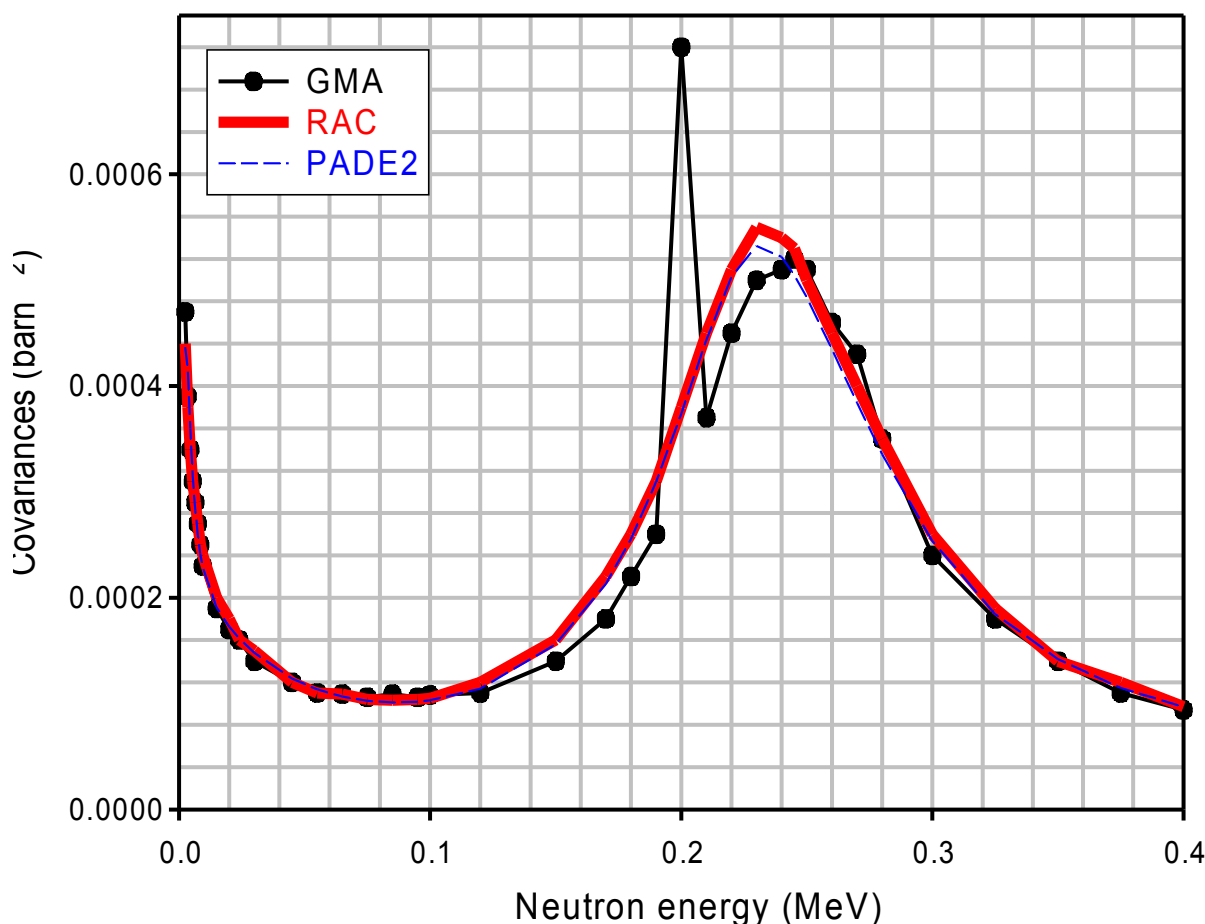


Fig. 57. Comparison of the row (column) of covariance matrix of uncertainties, which includes the variance for 0.2 MeV point and obtained in the model and non-model fits for ${}^6\text{Li}(n,t)$ reaction.

Per-cent error in the fit of the ${}^6\text{Li}(n,t)$ cross section at the full set of data used in the simultaneous evaluation of the standards is shown in the Fig. 58. As we see the non-model fit with GMA gives the largest evaluation of uncertainties, which is rather consistent with the experts estimation of the uncertainties, reachable at the modern measurements of ${}^6\text{Li}(n,t)$ cross section. But in GMA evaluation, beside (n,t) cross section, precision measurements of total and elastic scattering cross sections with account of the relations between total and partial cross sections were used. This explains the higher accuracy of the (n,t) cross section evaluation in the energy range from 100 to 800 keV comparing with the expert estimation based completely at the limitations of modern technique of (n,t) cross section measurements in this energy range. Lowest uncertainty is obtained in the R-matrix fit with EDA code; the fit is based at the ideology, that all experimental data have free normalization, which is chosen for each data set by best consistency with natural physical constraints by R-matrix theory, considered as a true theory for given nuclei and considered energies. Uncertainties of all experimental data in this case are considered as statistical. Because the number of data, especially for inverse channels with angular distributions of charged particles can be very large, the uncertainty of the evaluated parameters, and correspondingly of the cross sections, due to strong reduction of the uncertainty of statistical type can be very low (e.g 0.045% for ${}^6\text{Li}(n,t)$ or 0.01% for ${}^1\text{H}(n,n)$ in thermal point). Another

ideology is used by R-matrix code RAC, which accounts all major components of the uncertainties of the experimental data. Because of this, the uncertainties obtained in RAC fit are substantially larger.

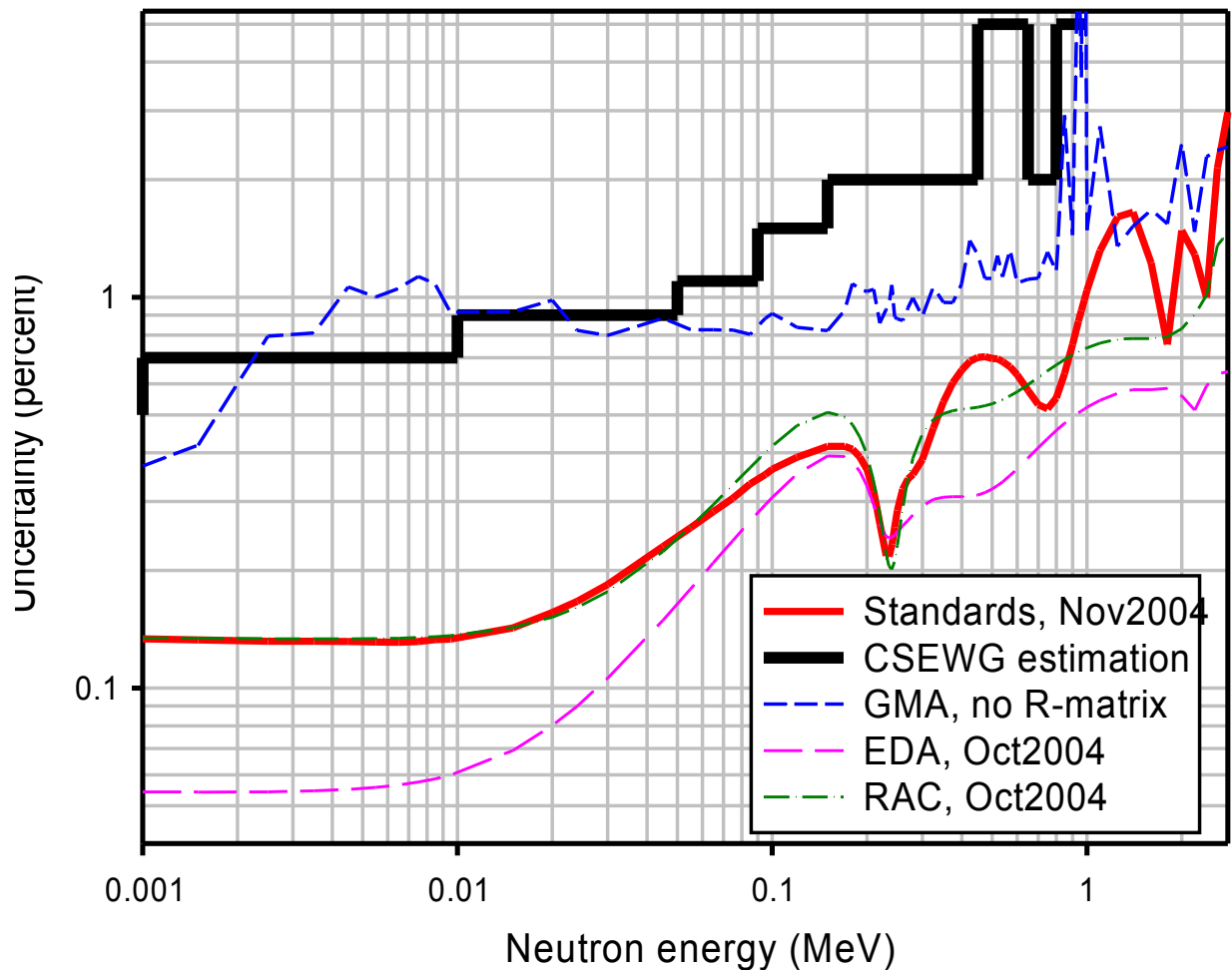


Fig. 58. Comparison of the uncertainties (per-cent errors) of the model and non-model evaluations of the ${}^6\text{Li}(n,t)$ standard cross section with an estimation of the experts (CSEWG) and evaluation recommended for new standards (2004).

In conclusion, we can say that the covariance and correlation matrices of the data obtained in the model or non-model evaluations are very different. As a rule, the per-cent uncertainties in the non-model least-squares fits are substantially higher than in the model fit. As it will be shown below, uncertainties of many applied quantities obtained by the averaging of data evaluated in different model or non-model approaches on different function (reactor spectra, etc.) are very close and can only slightly depend from the type of the model used in the evaluation of the data.

Peelle's (PPP) effect and minimization of its influence at the bias of the evaluation

As it was shown above (see Fig. 56), PPP leads to the bias of the evaluation. The reason of the PPP lays in construction of the «unrealistic» covariance matrices of the uncertainties of the experimental data in cases of limited information about the components of the uncertainties of the data and their correlative properties. Taking two variables, S. Chiba and D. Smith had shown that if V_{11} and V_{22} are the diagonal elements of the covariance matrix of the uncertainties of the experimental data, V_{12} is an off-diagonal element and $V_{11} < V_{22}$, then in case of $|V_{12}| < V_{11}$ the

PPP is absent. The practice had shown that the same is true in case of multivariate functions, when $|V_{ij}| < V_{ii}$, for $V_{ii} < V_{jj}$, but this requires the proof.

The PPP is fully absent, if the uncertainties of the experimental data have pure statistical nature and the covariance matrices of the relative uncertainties are used in the fit, or absolute covariance matrices obtained as a product of the relative covariance matrices of uncertainties at «true» value (or posterior evaluation) are used in the least-squares fit. In case if covariance matrices have rather strong LERC component of the uncertainties, the PPP effect will be substantially suppressed, if in the fit the absolute covariance matrices of the uncertainty of experimental data are obtained from relative covariance matrices and posterior evaluation of data («true values»). Because the posterior evaluation up to the moment of the finishing of the evaluation is not known, then, the iteration procedure can be used, where at the first step the prior evaluation is used instead of posterior and then the least-squares fit is repeated with the replacement at each step the old posterior evaluation at the new one up to the convergence. In all cases only two - three iterations are needed before the prior and posterior evaluations are practically coincided. This technical method of the PPP exclusion was proposed by S. Chiba and A. Smith and implemented in the GMA and GLUCS codes.

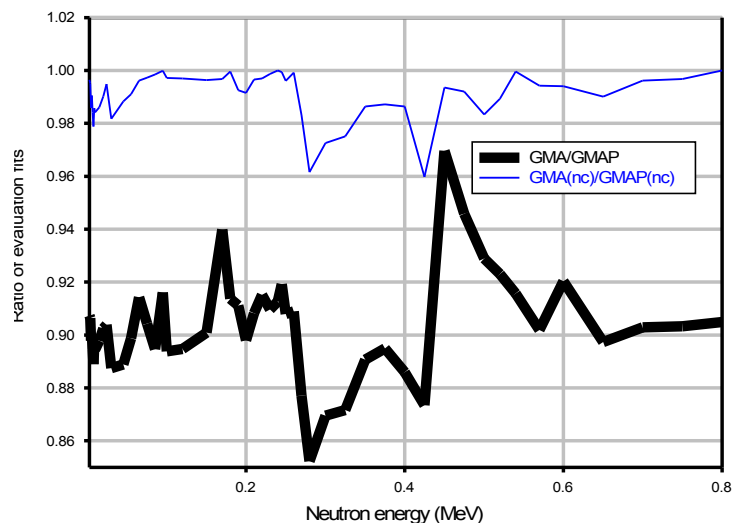


Fig. 59. Evaluation bias due to the PPP effect. Thin line shows the mini-PPP effect, thick line — combined contribution of mini- and maxi-PPP.

PPP effects contains two components leading to the bias of the evaluation. One component is called as mini-PPP, and is simply explained that even for the equal per-cent statistical uncertainties of two sets of data, the larger weight in the evaluation will be from the data having lower values, because they will contribute in the evaluation with a weight inverse to the square of their absolute uncertainties. At the Fig. 59 the ratio of the evaluations for ${}^6\text{Li}(n,t)$ in the approximation when all cross-energy correlations were set to zero but in one case the absolute uncertainty was taken as it was given by the authors (GMA(nc) evaluation) but in other case as the product of relative uncertainty given by the authors at the posterior evaluation (GMAP(nc) evaluation). Deviation of the ratio of the first to the second evaluation from the unit demonstrates the contribution of the mini-PPP effect. Full effect of PPP includes beside the mini-PPP also the maxi-PPP, for which the assigned unjust correlations are responsible. Thick line at the Fig. 59 shows the sum of min- and maxi-PPP, and obtained as ratio the results of usual least-squares fit of the experimental data to the fit where Chiba-Smith technical fix was used. As we see the

effect can be very substantial and should be accounted even if the data are not discrepant and cross-energy correlations in the data sets are small.

There are some other technical approaches minimizing the influence of the PPP effect, namely using of Box-Cox or more simple logarithmic transformation of the data, transforming the data to more linear form. These approaches are described in the details and widely used in the practice of the data evaluation. The biases of the evaluated data obtained in the least-squares fit with use of different technical approaches of the PPP reducing are compared at the Fig. 60. All results are shown as ratios to the fit obtained with a Chiba-Smith fix. As we see the spread in evaluated values using different methods is in the limit of 0.5 % considering that the initial bias due to the PPP was at the level of 10 %.

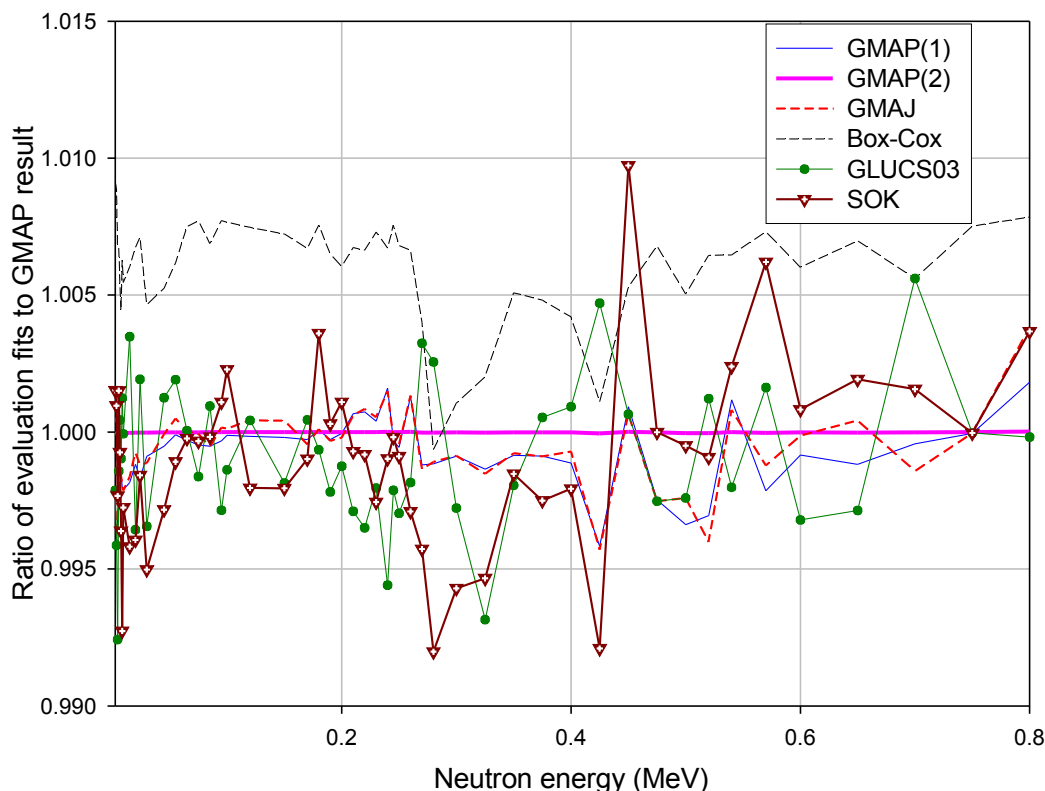


Fig. 60. Ratio of ${}^6\text{Li}(n,t)$ evaluations obtained with the use of different technical approaches of the PPP exclusion: GMAP(1) and GMAP(2) — Chiba-Smith method for 1 and 2 iterations; GMAJ — GMA code rewritten by S. Chiba with 1 iteration; Box-Cox — use of Box-Cox transformation; GLUCS03 – GLUCS version with Chiba-Smith method; SOK – use of logarithm data transformation.

As it was shown by Nancy Larson, that the “true”, unbiased evaluation can be obtained only if use the explicit method of construction of the covariance matrix of the uncertainties of the experimental data — method of propagation of the uncertainties starting from the primarily-measured quantities, which all have only statistical type of uncertainties. It is known that the PPP effect is absent if fitted data and their combinations have only statistical uncertainties, the absolute values of which should be presented as their relative uncertainties from «true» values. Then for construction of the covariance matrices of the uncertainties of the experimental data the only primarily measured quantities should be used (e.g. number of counts per channel for effect and background, similar quantities for measurement of the detector efficiency, etc.) and functions of their reduction to the values used in the evaluations (absolute cross sections, ratios of the cross sections). By this the model of the reduction of the primarily measured quantities, which depends

from the method of the measurements, used detectors and introduced corrections. The model can be strongly varied from experiment to the experiment. Basing at the propagation uncertainty method the relative covariance matrix for given experimental data set can be obtained. It can be transformed in the absolute covariance matrix of the uncertainties if use «true value». Because «true value» (or some posterior evaluation as the approximation to the true value) is not known prior to the evaluation, as true value some prior evaluation is taken with a following iteration procedure, which adjust the absolute uncertainties of the data relative the final posterior evaluation of the data. This approach is most strict and excludes completely the PPP effect in the following fit. To large extent, this approach was implemented by Nancy Larson in her code SAMMY, based on Bayesian search of the resonance parameters and fit of the cross sections in the resolved resonance region. Primary data presented the registered neutrons, gammas and fission fragments in the time of flight method (detector counts per channel). Unfortunately these data and functions of reduction are not always available, what limits the use of this method for construction of the covariance matrices of the uncertainties of the experimental data free from PPP effect in their least-squares fit.

Effect of small uncertainties of the evaluated data. Reasons leading to the small uncertainties

Uncertainties of the evaluated data are often compared on the per-cent error (uncertainty) of the data. This is very incomplete and often misleading comparison, because the full uncertainty of the evaluated data is characterized by the covariance matrix, where only the diagonal values have relations to the per-cent uncertainties. As the practice of the evaluation had shown, the per-cent uncertainties of the data evaluated in the model least-squares fits are substantially below the per-cent uncertainties obtained in the non-model fits.

Per-cent uncertainties obtained in non-model (GMA, GLUCS) and different R-matrix model fits (EDA, RAC, SAMMY3.8, SAMMY4) of the same sets of the experimental data of ${}^6\text{Li}(n,t)$ reaction differ substantially (see Fig. 61). Fits with R-matrix codes RAC and EDA are different because RAC uses in the description of the covariance matrices of experimental data two components of the uncertainties: statistical and systematical (or fully correlated) uncertainties, but EDA uses only statistical component with a free normalization of the data. As it was mentioned above, EDA uses R-matrix theory as absolutely strict theory with the strong constraints at the cross sections, which are determined by fundamental constants and conservation laws. SAMMY3.8 — is the result of the fit with the SAMMY code adjusted for the work with the data as it is done in the RAC code and SAMMY4 — under condition of the work with data as in the EDA code. Uncertainties in the energy range below 100 keV between the model and non-model fits are rather different. This is explained by high accuracy of the experimental data in the thermal point (0.0253 eV), which is not shown at the figure, and well-established $1/v$ dependence in the energy range below 10 keV. Per-cent uncertainties in this range in the model fit is substantially below, and correlations between uncertainties in the neighboring points are substantially higher, than in the non-model fit. We may conclude that the intrinsic correlation properties of the model, which couples the parameters and the cross sections (matrix of the sensitivity coefficients) change substantially the covariance matrix of the uncertainty of the evaluated cross sections.

Uncertainties of the evaluated data, obtained with the EDA code, which does not account the systematical uncertainties in the fit of the large number of the experimental data, can be very low. For example, the uncertainty of the integral scattering elastic cross section of neutrons at the hydrogen in the thermal point can be close to 0.01 %, what causes natural doubts in the justification of the method, which gives such small evaluated uncertainties. In case of using RAC R-matrix code which takes into account all components of the uncertainties of the experimental

data and which uses the same basic principles of the R-matrix model we obtain higher (and realistic) estimation of the uncertainties in the thermal point.

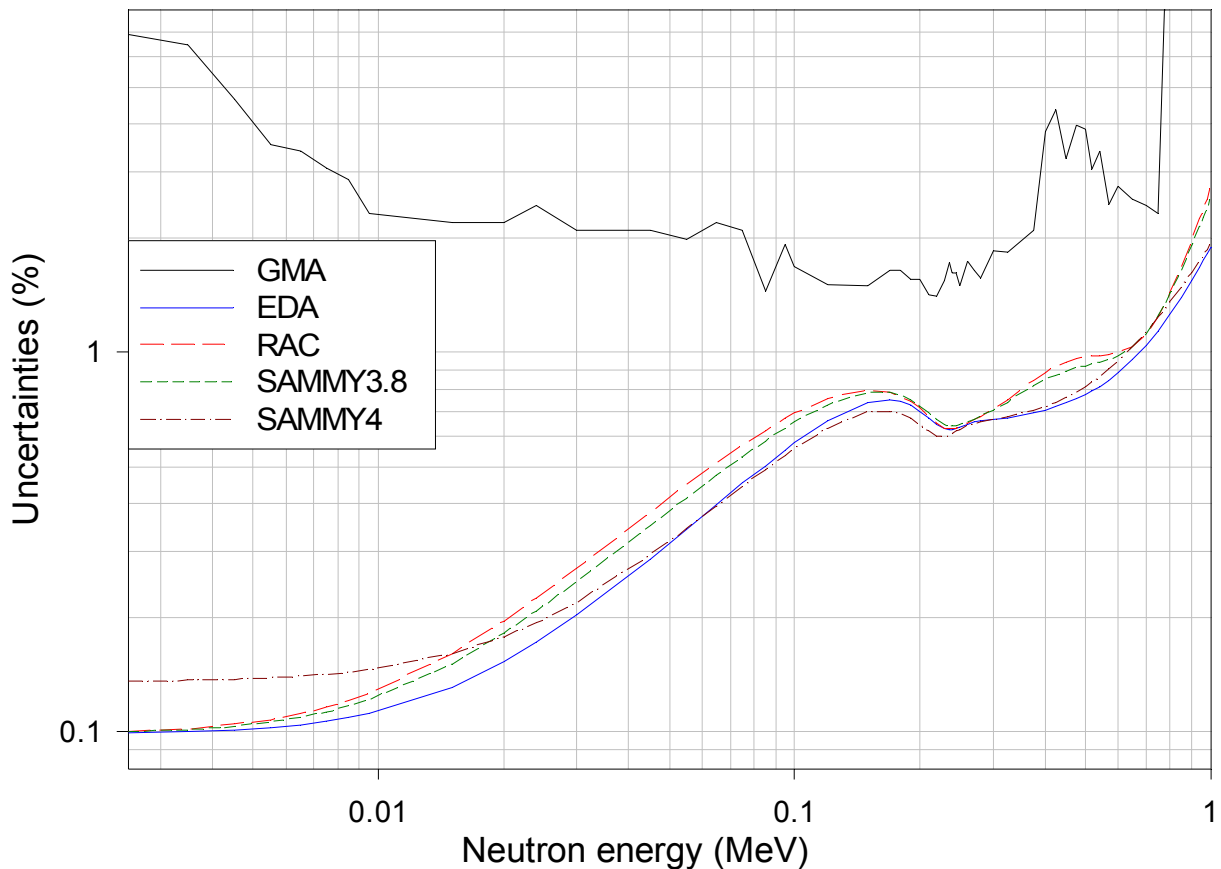


Fig. 61. Per-cent uncertainties of the evaluated data obtained in the non-model and model fits of the same experimental data sets for ${}^6\text{Li}(n,t)$ reaction cross section.

The other reason, leading to the substantial reducing of the uncertainties of the evaluated data is the neglecting by some uncertainties or neglect of the correlations between the components of the uncertainties, which are common for few experimental data sets. This relates, as a rule, to the measurements done in the same laboratory, at the same installation, with the same method, detectors and samples. Generally it is enough even to use the same samples in the measurements in different laboratories with different methods but have large component of uncertainties correlated between two data sets. GMA code allows take into account the correlations between uncertainties in different measurements. Account of such correlations, for example in the evaluation of such important standard as ${}^{235}\text{U}(n,f)$, has a consequence that the minimal per-cent uncertainties even with large account of experimental data sets (186 sets of data with ${}^{235}\text{U}(n,f)$) is never below 0.5 %.

If in the fit of the data, the χ^2 per degree of freedom is larger than 1, important is the determination of the data sets (so-called «outliers») or range of the energies in these data sets, where large discrepancies exist with other data. If it is impossible to understand and exclude the reason of these discrepancies (introduce the correction which were not accounted or use new quantum yields if “old” values were used in the data reduction), then uncertainty of these data should be increased. This will led to some increase of the uncertainties of the evaluated data. The practice of the standards evaluation had shown that the outliers are mostly the data with high uncertainties, and further expanding of their uncertainties does not influence much at the evaluated data and their uncertainties. The search of the outliers is rather difficult procedure,

because for their identification, the knowledge of «true» values is needed. Because the true value “a priori” is not known, the iteration procedure should be organized, when at the first step the realistic prior evaluation can be taken as a true evaluation. Thus, the iteration procedure with replacement of a prior evaluation at the next posterior evaluation is needed as for correction of the outlying data, as well as for exclusion of the PPP effect.

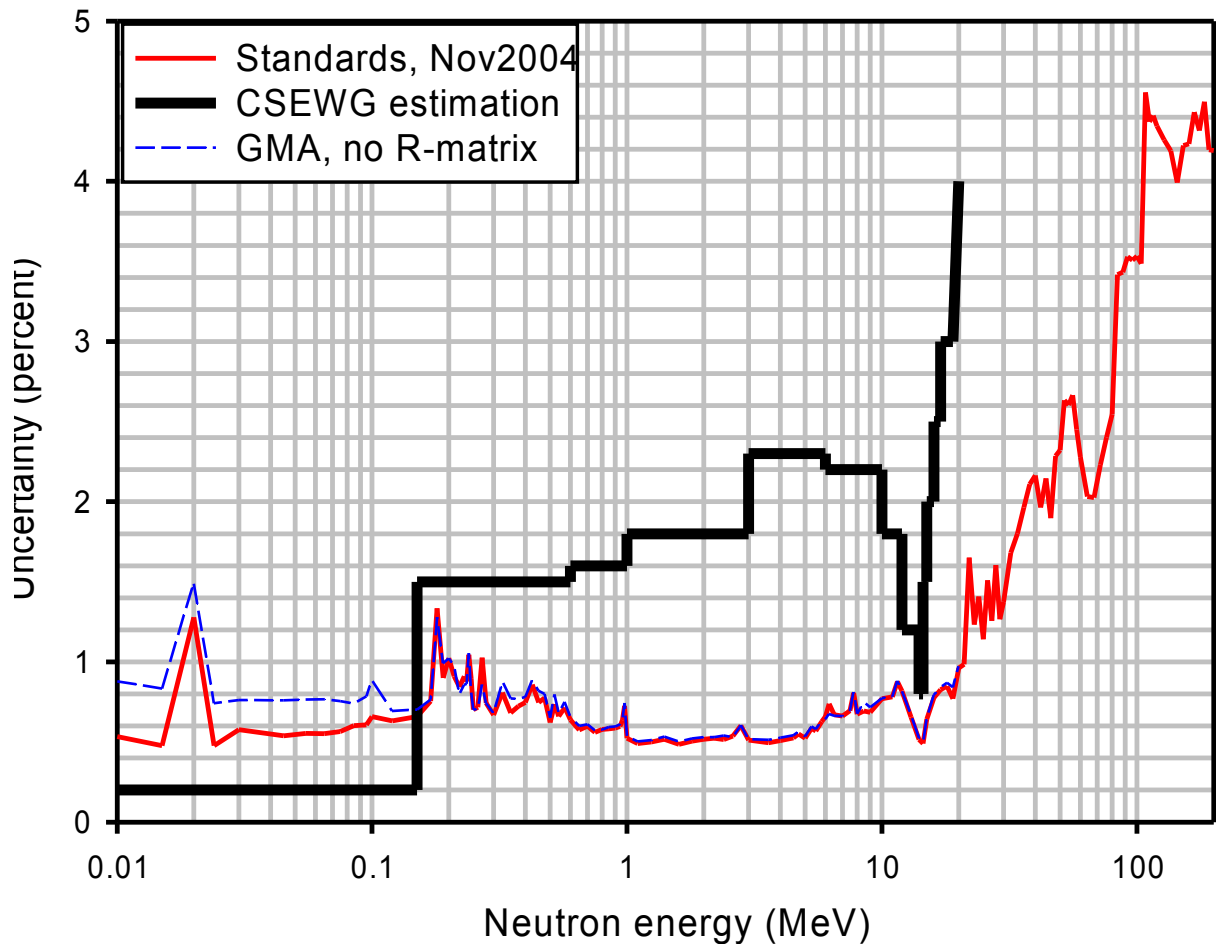


Fig. 62. Comparison of the per-cent uncertainties of the evaluated $^{235}\text{U}(n,f)$ neutron cross section standards with the expert's estimation of the uncertainties which can be achieved in the modern experimental conditions.

Comparison of the per-cent uncertainties obtained in the combined fit of the $^{235}\text{U}(n,f)$ neutron cross section standards with the expert's (1987) estimation of the uncertainties, which can be achieved using modern (1987) technique of the experiment is shown in Fig. 62. The experts had not prepared their estimations of the covariance matrices of the uncertainties, thus their uncertainties should be treated as statistical (fully correlated in each group). The reasons, why the uncertainty of the evaluated data in the energy range between 150 keV to 14 MeV are substantially lower than the expert estimation, is because in the evaluation 186 experimental data sets presenting 16 types of the data, which differ by the methods, detectors, types of used standards, including high-precision absolute measurements (based on associated particles method or hydrogen scattering standard) were used. Covariance matrix of the GMA combined evaluation contains rather large off-diagonal elements, which in case of calculations of some integral parameters on the wide energy spectrum give realistic estimation of the uncertainty of these parameters; as opposed to this, the uncertainty of integral parameters calculated with the expert's estimated per-cent uncertainties can be very low for flat wide spectra of the installations.

Experimental data can be measured with the use of different methods. Each method of measurements may contain some systematic errors, corrections at which were not introduced or uncertainties related to them were not evaluated. We may consider them as hidden (or unrecognized) systematical uncertainties. For revealing of these systematical uncertainties it is important to have a wide spectrum of measurements done with different methods or make new measurements which could be based at new method. Evgeny Gai had developed the approach when in conditions of the sufficient number of the experimental data, additional (hidden) systematical component of the uncertainty in some energy interval for each data set was assigned using bias between the averaged data in this interval relative the arithmetical-averaged value for all data of this interval. The use of this approach gives some information about possible non-accounted systematical uncertainty of each data set and increases the per-cent uncertainty in 1.5 — 2 times comparing with the approaches, where the conception of hidden systematical uncertainty of different methods had not been used.

It is needed to mention, that although the large reduction of the per-cent uncertainty of the data evaluated in the model approaches in comparison with the non-model is a visible effect, it is to some extent also imaginary effect, because in the evaluation of the uncertainty of most functionals calculated with these experimental data, the full covariance matrix of the data uncertainties is used, and not only the per-cent uncertainties in the nodes on the energy, where data are evaluated.

Comparison of the covariance matrices of the uncertainties evaluated in the model and non-model fits and invariants of the uncertainties

As we mentioned above, covariance matrices of the uncertainties of the evaluated data obtained in the model and non-model fits of the same experimental data are substantially different matrices. This causes serious problems in comparison of the uncertainties (it is impossible to compare large number of the matrix elements one to one and came to some conclusion). In many cases, in the comparison of the uncertainties, only the diagonal elements of the matrices, or per-cent uncertainties are taken into account. Such comparison is not complete and representative, and can lead to the wrong conclusion about accuracy of the data. The use of the model introduces substantial correlations and anti-correlations in the covariance matrix of uncertainty of the evaluated data. As a rule, the per-cent uncertainties obtained in the model fits are much lower than obtained in the non-model fits.

The practice of the evaluation had show, that the value, which is conserved approximately and has a weak dependence from the type of the fit (model or non-model) is the sum of all elements of the evaluated covariance matrices of the uncertainties taken in the same nodes. Also with some approximations, the uncertainties of some functional forms, obtained from the data and covariance matrices of the uncertainties evaluated in a wide energy range using model and non-model fits of the same experimental data are conserved. Because of these observations, the hypothesis was formulated [13]: *«at model and non-model fits of the same sets of the experimental data by least-squares method, the sums of the elements of the covariance matrices of the uncertainties of the evaluated data obtained in these fits will be so close to each other, up to what degree such fits are close to each other».*

Results of the fit of 5 experimental data sets for ${}^6\text{Li}(n,t)$ reaction at 51 nodes in the energy interval from 2.5 keV to 800 keV are given in the Table 6. Non-model codes GLUCS, GMA and R-matrix code RAC were used in the fit. Covariance matrices of the experimental data include SERC and LERC components of the uncertainties. R- matrix code EDA cannot be used because it accounts only statistical components of the uncertainties. Because for unequivocal description of the data with the R-matrix model the additional (to ${}^6\text{Li}(n,t)$) data are required, they were

introduced as non-informative data (data with large uncertainties, which do not influence at the evaluation of the uncertainty of the ${}^6\text{Li}(n,t)$ cross section).

As we see from Table 6, the cross sections evaluated with GMA and GLUCS are in agreement with accuracy up to tens parts of the per-cent, but the model fit deviates at some energies up to 10 %. Per-cent uncertainty of the non-model fit is at 1.5 – 2 times higher than in the model fit.

Table 6. Comparison of the model and non-model fits of 5 experimental data sets for ${}^6\text{Li}(n,t)$ reaction.

Energy, MeV	Cross section (central values), b			Error, %		
	GLUCS Bayesian non-model fit	GMA general least squares non-model fit	RAC R-matrix model fit	GLUCS Bayesian non-model fit	GMA general least squares non-model fit	RAC R-matrix model fit
0.2500E-02	2.5643E+00	2.56791130	0.265435E+01	3.4736E+00	3.4	1.4952
0.3500E-02	2.1340E+00	2.13894272	0.224569E+01	3.2550E+00	3.2	1.3900
0.4500E-02	1.8435E+00	1.85487058	0.198312E+01	3.0100E+00	3.0	1.3163
0.5500E-02	1.7385E+00	1.73921302	0.179651E+01	2.5948E+00	2.6	1.2631
0.6500E-02	1.5777E+00	1.57732333	0.165529E+01	2.5518E+00	2.5	1.2244
0.7500E-02	1.4669E+00	1.46900573	0.154373E+01	2.4718E+00	2.5	1.1960
0.8500E-02	1.4182E+00	1.41379212	0.145280E+01	2.2237E+00	2.2	1.1754
0.9500E-02	1.2888E+00	1.28802753	0.137692E+01	1.8064E+00	1.8	1.1606
0.1500E-01	1.0487E+00	1.04513353	0.110908E+01	1.7278E+00	1.7	1.1330
0.2000E-01	9.5192E-01	0.95499096	0.972498E+00	1.8265E+00	1.8	1.1359
0.2400E-01	8.6783E-01	0.86615244	0.897389E+00	1.9348E+00	1.9	1.1403
0.3000E-01	7.6349E-01	0.76628620	0.816803E+00	1.7740E+00	1.8	1.1429
0.4500E-01	6.6971E-01	0.66950549	0.701441E+00	1.8026E+00	1.8	1.1279
0.5500E-01	6.3158E-01	0.63043012	0.659942E+00	1.7502E+00	1.8	1.1120
0.6500E-01	6.0471E-01	0.60438930	0.634664E+00	1.8674E+00	1.9	1.0988
0.7500E-01	5.7693E-01	0.57853288	0.621291E+00	1.9369E+00	1.9	1.0907
0.8500E-01	6.0873E-01	0.60810755	0.617734E+00	1.4020E+00	1.4	1.0873
0.9500E-01	5.9780E-01	0.59926541	0.623171E+00	1.7722E+00	1.8	1.0869
0.1000E+00	5.9648E-01	0.59749230	0.629247E+00	1.5888E+00	1.6	1.0872
0.1200E+00	6.3976E-01	0.64001517	0.678214E+00	1.4318E+00	1.4	1.0877
0.1500E+00	7.9289E-01	0.79463003	0.854758E+00	1.4012E+00	1.4	1.0836
0.1700E+00	1.0061E+00	1.00507612	0.109228E+01	1.5597E+00	1.6	1.0828
0.1800E+00	1.2084E+00	1.20947152	0.127076E+01	1.6308E+00	1.6	1.0826
0.1900E+00	1.4454E+00	1.44870074	0.150399E+01	1.5343E+00	1.5	1.0816
0.2000E+00	1.7253E+00	1.72745634	0.180166E+01	1.5556E+00	1.6	1.0802
0.2100E+00	2.0577E+00	2.06036584	0.216218E+01	1.3899E+00	1.4	1.0810
0.2200E+00	2.4852E+00	2.49007621	0.255463E+01	1.3842E+00	1.4	1.0861
0.2300E+00	2.8005E+00	2.80415714	0.290012E+01	1.4850E+00	1.5	1.0930
0.2400E+00	2.9316E+00	2.94171942	0.308564E+01	1.7320E+00	1.8	1.0950
0.2450E+00	2.8906E+00	2.89460753	0.309124E+01	1.5753E+00	1.6	1.0938
0.2500E+00	2.8530E+00	2.85914450	0.303681E+01	1.5706E+00	1.6	1.0925
0.2600E+00	2.5546E+00	2.55676583	0.278391E+01	1.5635E+00	1.5	1.0956
0.2700E+00	2.3155E+00	2.31343201	0.242963E+01	1.6837E+00	1.7	1.1086
0.2800E+00	1.9120E+00	1.90770162	0.206822E+01	1.6422E+00	1.6	1.1259
0.3000E+00	1.3738E+00	1.37898444	0.148622E+01	1.5593E+00	1.6	1.1524
0.3250E+00	9.8769E-01	0.99184917	0.103940E+01	1.7859E+00	1.8	1.1734
0.3500E+00	7.5831E-01	0.75962702	0.785950E+00	1.7949E+00	1.8	1.2007
0.3750E+00	6.2623E-01	0.62617165	0.633946E+00	1.7922E+00	1.8	1.2349
0.4000E+00	5.4585E-01	0.54580942	0.536660E+00	2.0282E+00	2.0	1.2666
0.4250E+00	4.8323E-01	0.48092828	0.470728E+00	2.9850E+00	3.0	1.2897
0.4500E+00	3.8710E-01	0.38657206	0.423875E+00	4.7772E+00	4.8	1.3035
0.4750E+00	3.8596E-01	0.38682004	0.389265E+00	2.7247E+00	2.7	1.3113
0.5000E+00	3.5704E-01	0.35763385	0.362873E+00	3.0459E+00	3.0	1.3180
0.5200E+00	3.4137E-01	0.34160385	0.345974E+00	3.0316E+00	3.0	1.3256
0.5400E+00	3.2214E-01	0.32279109	0.331882E+00	3.2962E+00	3.3	1.3368
0.5700E+00	3.1541E-01	0.31529003	0.314719E+00	2.8556E+00	2.9	1.3611
0.6000E+00	2.9205E-01	0.29302733	0.301110E+00	2.3312E+00	2.4	1.3905
0.6500E+00	2.7146E-01	0.27220681	0.283922E+00	2.5621E+00	2.5	1.4259
0.7000E+00	2.5607E-01	0.25551707	0.271434E+00	2.4689E+00	2.4	1.4123
0.7500E+00	2.3794E-01	0.23822164	0.262131E+00	2.4283E+00	2.4	1.4248
0.8000E+00	2.2406E-01	0.22433707	0.255110E+00	2.5081E+00	2.4	1.8872

Table 7. Covariances of the evaluated data for the 1-st and 25-th row (column) of the covariance matrices of the data evaluated in the model (RAC) and non-model (GMA) approaches.

Point #	Point #1		Point#25	
	GMA	RAC	GMA	RAC
1	0.00775	0.00158	0.00047	0.00044
2	0.00076	0.00123	0.00039	0.00038
3	0.00064	0.00102	0.00034	0.00034
4	0.00051	0.00086	0.00031	0.00031
5	0.00050	0.00076	0.00029	0.00029
6	0.00048	0.00067	0.00027	0.00027
7	0.00042	0.00060	0.00025	0.00025
8	0.00038	0.00055	0.00023	0.00024
9	0.00032	0.00036	0.00019	0.00020
10	0.00028	0.00027	0.00017	0.00018
11	0.00025	0.00023	0.00016	0.00016
12	0.00022	0.00019	0.00014	0.00015
13	0.00020	0.00015	0.00012	0.00012
14	0.00018	0.00014	0.00011	0.00011
15	0.00017	0.00014	0.000109	0.000109
16	0.00017	0.00015	0.000106	0.000104
17	0.00016	0.00015	0.000109	0.000103
18	0.00016	0.00016	0.000106	0.000104
19	0.00017	0.00017	0.000108	0.000105
20	0.00018	0.00019	0.00011	0.00012
21	0.00022	0.00024	0.00014	0.00016
22	0.00028	0.00029	0.00018	0.00022
23	0.00033	0.00032	0.00022	0.00026
24	0.00039	0.00038	0.00026	0.00031
25	0.00047	0.00044	0.00072	0.00038
26	0.00056	0.00053	0.00037	0.00045
27	0.00067	0.00064	0.00045	0.00051
28	0.00075	0.00074	0.00050	0.00055
29	0.00075	0.00080	0.00051	0.00054
30	0.00076	0.00082	0.00052	0.00053
31	0.00075	0.00080	0.00051	0.00050
32	0.00065	0.00071	0.00046	0.00045
33	0.00064	0.00061	0.00043	0.00040
34	0.00052	0.00051	0.00035	0.00035
35	0.00038	0.00036	0.00024	0.00026
36	0.00027	0.00026	0.00018	0.00019
37	0.00021	0.00021	0.00014	0.00014
38	0.00017	0.00018	0.00011	0.00012
39	0.00014	0.00015	0.000094	0.000097
40	0.00014	0.00014	0.000089	0.000083
41	0.000098	0.00012	0.000070	0.000073
42	0.000102	0.00012	0.000065	0.000066
43	0.000106	0.000104	0.000065	0.000061
44	0.000100	0.000098	0.000061	0.000059
45	0.000075	0.000092	0.000052	0.000057
46	0.000087	0.000083	0.000058	0.000054
47	0.000079	0.000076	0.000050	0.000052
48	0.000079	0.000068	0.000050	0.000050
49	0.000071	0.000064	0.000047	0.000048
50	0.000065	0.000064	0.000043	0.000045
51	0.000063	0.000067	0.000041	0.000041
Sum	0.023875	0.019656	0.011163	0.011191
Ratio, model to Non-model	0.82		1.002	

Comparison of the covariances (in the units of barn²) for 1-st and 25-th row (column) of the covariance matrices of the uncertainties are shown in Table 7. There are visible differences in the covariances at the diagonal or close to the diagonal. However, if we will sum up the elements of the matrices along the row (column), then the differences in the sums will be small, and total sums of all elements of covariance matrices differ at few percents.

The existence of such conserving quantity independent from the fit (invariant) could mean, that the uncertainties of the integral characteristics calculated with the data evaluated in different model and non-model fits may have non-substantial difference, although the covariance matrices of the uncertainties of these evaluations can look differently. ***This invariant can be called as universal measure of the data uncertainties.***

It is well known the invariant for covariance matrix of the spectrum (or any other function), if constraint is set up, that integral under evaluated spectrum (function) is precisely equal to the predetermined value (e.g., spectrum should be normalized at 1), then the sum of all elements of covariance matrix should be equal to 0. In this case, the sum of all elements of covariance matrix along any row or column also should be equal 0.

Studies done by Evgeny Gai on the search of invariants of covariance matrices of the uncertainties revealed few forms with covariance matrices of the uncertainties, which are strict invariants [14].

If \mathbf{R} is covariance matrix of uncertainties of experimental data, \mathbf{G} is matrix of the coefficients of the sensitivity (partial derivatives from the model function on parameters), T and -1 indexes mean transposing and inversion of the matrix, then the least-squares method gives the covariance matrix of the evaluated parameters \mathbf{W} :

$$\mathbf{W}=(\mathbf{G}^T\mathbf{R}^{-1}\mathbf{G})^{-1}$$

Covariance matrix \mathbf{V} of the evaluated uncertainties in the nodes, where the experimental data are given can be written as:

$$\mathbf{V}=\mathbf{G}^T\mathbf{W}\mathbf{G}$$

From here, spur (Sp) of the product of the matrices \mathbf{R}^{-1} and \mathbf{V} does not depend from the used model and quality of the fit determined by the χ^2 criterion and equals to the number of the model parameters M :

$$Sp\mathbf{R}^{-1}\mathbf{V}=\sum_{i,k} R_{i,k}^{-1}V_{k,i} = \sum_{i,k} \sum_{\alpha,\beta} R_{i,k}^{-1}G_{\alpha,i}^T W_{\alpha,\beta}^{-1} G_{\beta,k} = \sum_{\alpha,\beta} W_{\alpha,\beta} W_{\alpha,\beta}^{-1} = M$$

This relation is also carried out for matrices of the relative covariances \mathbf{r} and \mathbf{v} :

$$Sp\mathbf{r}^{-1}\mathbf{v} = M$$

Using this approach it can be shown, that:

$$\mathbf{V}\mathbf{R}^{-1}\mathbf{V} = \mathbf{V}$$

$$\mathbf{r}^{-1}\mathbf{v} = \mathbf{v}$$

It can be shown also that, the following relations are strictly carried out for the models, which use the polynomial expansion, and only approximately for general non-model fits by the least-squares method of the large number of the data sets:

$$\sum_{k,j} R_{i,k}^{-1}V_{k,j} = I,$$

for any line, and:

$$\sum_{i,k,j} R_{i,k}^{-1}V_{k,j} = N$$

$$Det(\mathbf{V} - \mathbf{R}) = 0,$$

where N is a number of data points (energy nodes) and Det is a determinant of the difference of two matrices given in the parentheses.

In the case of the polynomial models the quality of the fit does not influence at the strict equalities, but this is not so in the general case. All equalities are obtained analytically, basing at the conditions of the necessity and sufficiency of the solutions existing, and tested numerically using the PADE model of the analytical expansion. These relations can be used for the checking of the covariance matrices of the evaluated data obtained in different least-squares fits of the same experimental data.

It was also strictly shown for the evaluations with the model function of the regression type $y(x,p) = p_1 + g(x;p_2, \dots, p_M)$ with p_1 as a parameter of the constant shift, that the uncertainty of the weighted averaged value P_{wa} for evaluated data $y(x_k)$, where averaged values are determined as

$$\bar{y}_{wa} = \frac{\sum_{i,k=1}^N R_{i,k}^{-1} y(x_k)}{\sum_{i,k=1}^N R_{i,k}^{-1}}$$

is a strict invariant, which does not depend from other characteristics of the model and depends only from the covariance matrix of uncertainties of the experimental data:

$$P_{wa} = \langle (\Delta \bar{y}_{wa})^2 \rangle = \frac{\sum_{i,k,l,m} R_{i,k}^{-1} V_{k,l} R_{i,m}^{-1}}{(\sum_{i,k} R_{i,k}^{-1})^2} = \frac{1}{(\sum_{i,k} R_{i,k}^{-1})}$$

Although the strict invariant for covariance matrix of the uncertainties of the evaluated data in case of any model was not found, comparison of the sums of the elements of the covariance matrices of the uncertainties evaluated in different models, or uncertainties of the integral quantities calculated with the evaluations in different models gives more objective picture of the uncertainties comparison, then just comparison of their per-cent uncertainties.

References

1. W.P. Poenitz, The Simultaneous Evaluation of Interrelated Cross-Sections by Generalized Least-Squares and Related Data File Requirements, pp. 426-430 in Proc. Advisory Group Meeting on Nuclear Standard Reference Data, International Atomic Energy Agency, IAEA-TECDOC-335 (1985).
2. D.M. Hetrik, C.Y. Fu, GLUCS: A Generalized Least-Squares Program for Updating Cross Section Evaluations with Correlated Data sets, ORNL/TM-7341 (1980).
3. N.M. Larson, Proof that Bayes and Least Squares Give Exactly Equivalent Results for Arbitrary Numbers of Data Sets (Assuming Linearity), pp. 91-95 in Summary Report of the First Research Coordination Meeting on Improvement of the Standards Cross Sections for Light Elements, INDC(NDS)-438, IAEA, Vienna, Austria, (2003).
4. D.M. Hetrik, C.Y. Fu, GLUCS: A Generalized Least-Squares Program for Updating Cross Section Evaluations with Correlated Data sets, ORNL/TM-7341 (1980).
5. V. Pronyaev, S. Tagesen, H. Vonach, S. Badikov, "Evaluation of the fast neutron cross sections of ^{52}Cr and ^{56}Fe including complete covariance information", Physik Daten 13-8 (1995).
6. L.C. Mihailescu, C. Borcea, A.J. Koning, A.J.M. Plompen, Nucl. Phys., A786, p. 1 (2007).

7. V. Pronyaev, S. Tagesen and H. Vonach, Final Report for Contract ERB 5000 CT 9.5 0068 NET "Evaluation of all important neutron cross sections for ^9Be and evaluation of the secondary neutrons from the interaction of neutrons with ^9Be in the neutron energy range from 10-5 eV - 20 MeV, Report EFF-DOC-552 (1996).
8. T.D. Beynon, B.S. Sim, Ann.Nucl.Energy 15, p. 27 (1988).
9. W.P. Poenitz, S.E. Aumeier, "The Simultaneous Evaluation of the Standards and other Cross Sections of Importance for Technology", ANL/NDM-139, Argonne National Laboratory, USA (1997).
10. International Evaluation of Neutron Cross Section Standards, Report STI/PUB/1291, IAEA (2007).
11. A.D. Carlson, V.G. Pronyaev, D.L. Smith et al., "International Evaluation of Neutron Cross Section Standards", Nucl. Data Sheets, p. 3215 (2009).
12. F. Tovesson and S.E. Hill, Nucl. Sci. Eng., 159, p. 94 (2008).
13. V.G. Pronyaev, A.V. Bytchkova, "Subjective Judgment on Measure of Data Uncertainty", pp. 327-331 in Summary Report of the Second Research Coordination Meeting on Improvement of the Standards Cross Sections for Light Elements, INDC(NDS)-453, IAEA, Vienna, Austria (2004).
14. E. Gai, V. Pronyaev, "Uncertainty Justification of Neutron Cross Section Standards", in Proc. of Int. Conf. on Nucl. Data for Sci. and Technology, April 22-27, 2007, Nice, France, v. 2, p. 1239 (2007).